Istituto Nazionale di Fisica Nucleare

# *Isospin influence on nuclear reaction dynamics at Fermi energies: firsts results on the CHIFAR experiment at LNS and future perspectives about neutron detection*


***PAGANO EMANUELE VINCENZO*[(1)]**

(1) INFN, Laboratori Nazionali del Sud, Catania, Italy


# IMF production and isospin dependence in dynamical fission of projectile-like fragments at 20 and 35 MeV/A

**A little bit of story for the physical case**

**REVERSE experiment with CHIMERA at LNS**

**$^{124}$Sn + $^{64}$Ni neutron rich system**
**and**
**$^{112}$Sn + $^{58}$Ni neutron poor system**

ELSEVIER

Nuclear Physics A734 (2004) 504–511

NUCLEAR PHYSICS A

www.elsevier.com/locate/npe

Fragmentation studies with the CHIMERA detector at LNS in Catania: recent progress

A. Pagano[a], M. Alderighi[b],F. Amorini[c], A. Anzalone[c], N. Arena[a], L. Auditore[d], V. Baran[c], M. Bartolucci[e], I. Berceanu[f], J. Blicharska[g], J. Brzychczyk[h], A. Bonasera[c], B. Borderie[i], R. Bougault[j], M. Bruno[k], G. Cardella[a], S. Cavallaro[c], M.B. Chatterjee[l], A. Chbihi[m], J. Cibor[n], M. Colonna[c], M. D'Agostino[k], R. Dayras[o], E. De Filippo[a], M. Di Toro[c], W. Gawlikowicz[h], E. Geraci[k], F. Giustolisi[c], A. Grzeszczuk[g], P. Guazzoni[e], D. Guinet[p], M. Iacono-Manno[c], S. Kowalski[g], E. La Guidara[c], G. Lanzano'[a], G. Lanzalone[c], N. Le Neindre[i], S. Li[q], S. Lo Nigro[e], C. Maiolino[c], Z. Majka[h], G. Manfredi[e], T. Paduszynski[g], M. Papa[a], M. Petrovici[f], E. Piasecki[r], S. Pirrone[a], R. Planeta[h], G. Politi[a], A. Pop[f], F. Porto[c], M. F. Rivet[i], E. Rosato[s], F. Rizzo[c], S. Russo[e], P. Russotto[c], M. Sassi[e], G. Sechi[b], V.Simion[f], K. Siwek-Wilczynska[r], I. Skwira[r], M. L. Sperduto[c], J.C. Steckmeyer[j], L. Swiderski[r], A. Trifirò[d], M. Trimarchi[d], G. Vannini[k], M. Vigilante[s], J. P. Wieleczko[m], J. Wilczynski[t], H. Wu[q], Z. Xiao[q], L. Zetta[e], W. Zipper[g]

# CHIEMERA
# (Charged Heavy Ion Mass and Energy Resolving Array)

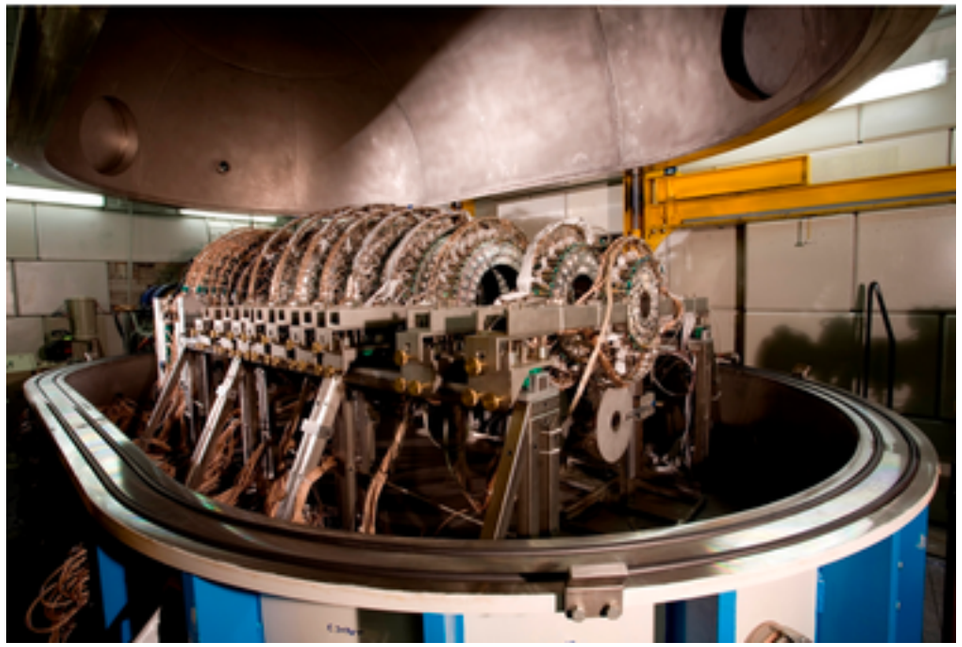

1999 - 2002

688 Si-CsI(Tl) forward Telescopes 1° - 30° (9 rings)

Since 2003

688 Si-CsI(Tl) forward Telescopes 1° - 30° (9 rings)
+
504 Si-CsI(Tl) telescope 30° - 178° (sphere)
=
1192 Si-CsI(Tl) telescope 1° - 178° (98% of 4 )

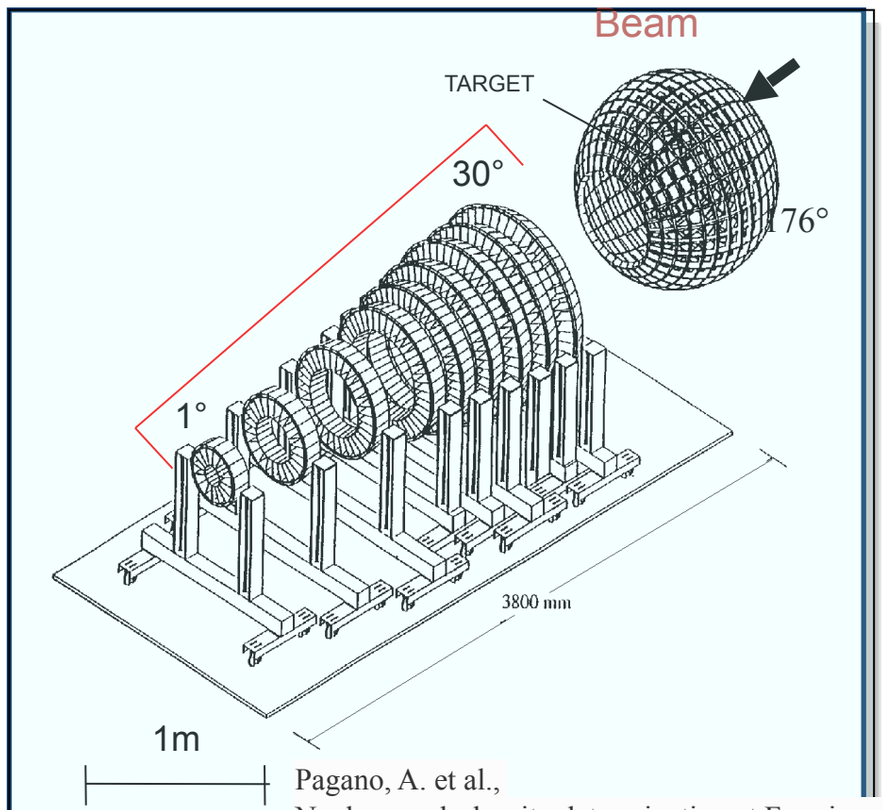


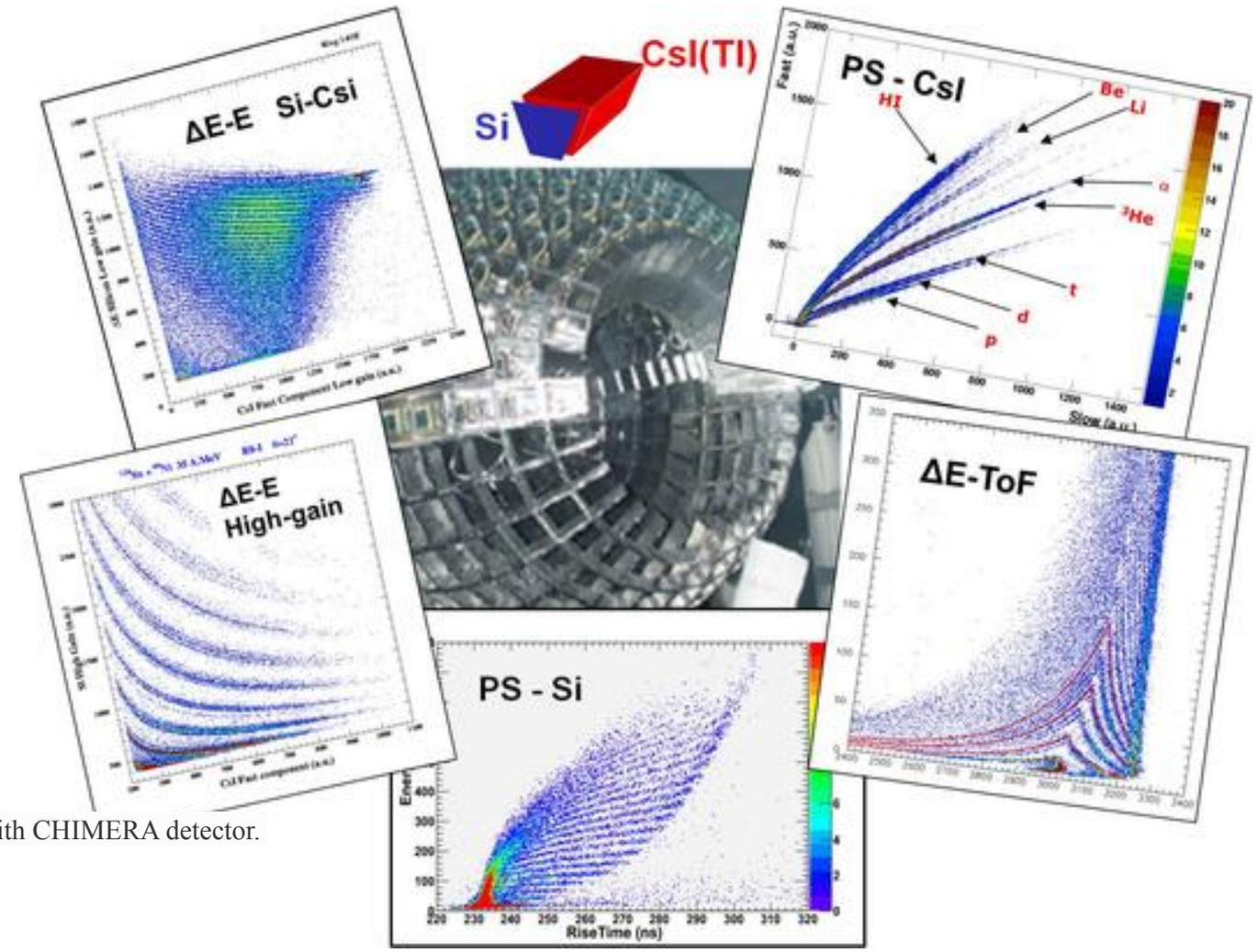


Pagano, A. et al.,
Nuclear neck-density determination at Fermi energy with CHIMERA detector.
*Eur. Phys. J. A* **56**, 102 (2020). And referece therein.
https://doi.org/10.1140/epja/s10050-020-00105-z

# Timescale of IMFs emission in HI reactions

Enrico De Filippo courtesy

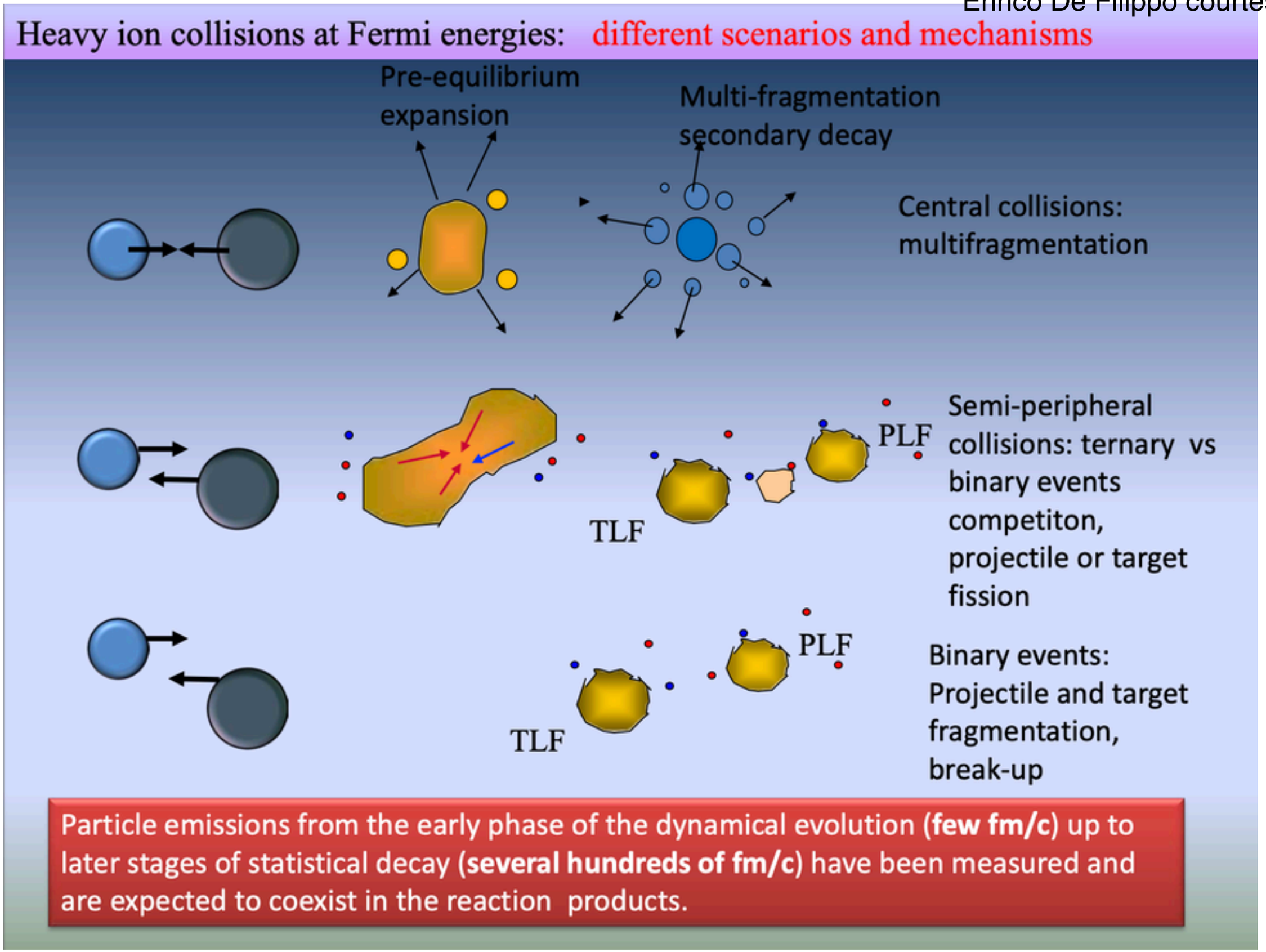

# Timescale of IMFs emission in HI reactions

Enrico De Filippo courtesy

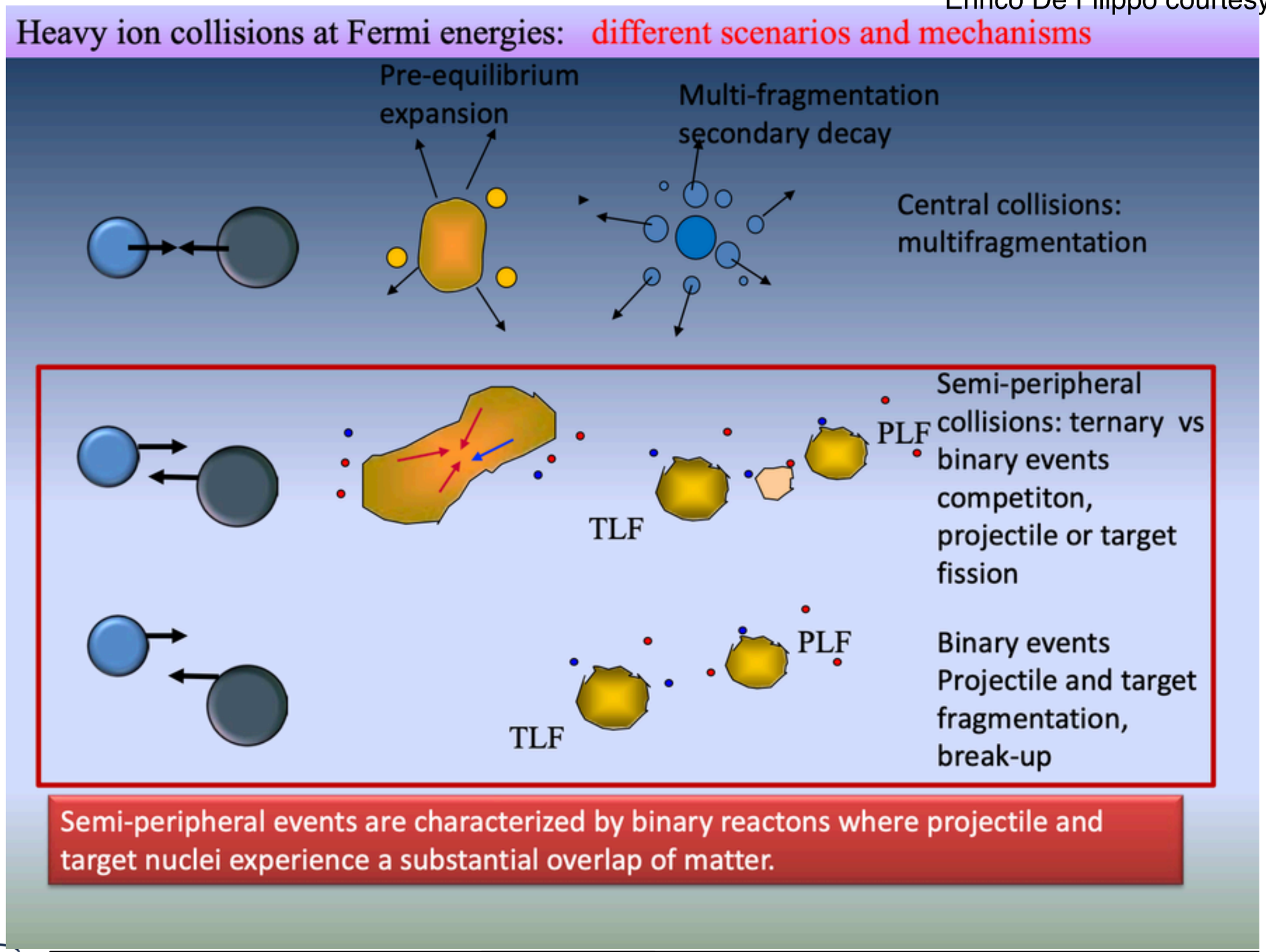

# Isospin transport to the “neck”

**M. Colonna Progress in Part. and Nucl. Phys. 113 (2020) 103775 and reference therein**

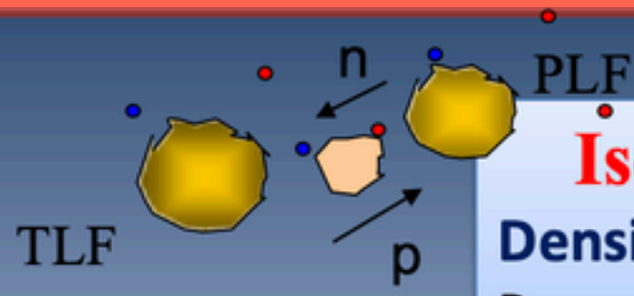


## Isospin drift (fast timescale: around 100 fm/c)

**Density gradient**

Depending on slope of the symmetry energy

Migration of neutrons in low density region

$$j_n - j_p \propto E_{sym}(\rho)\nabla I + \frac{\partial E_{sym}(\rho)}{\partial \rho} I \nabla \rho$$

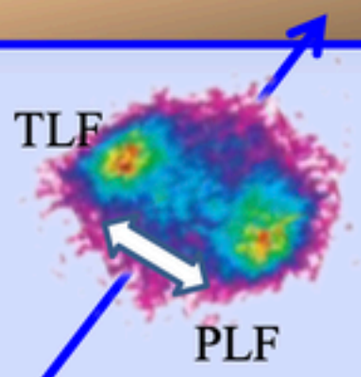


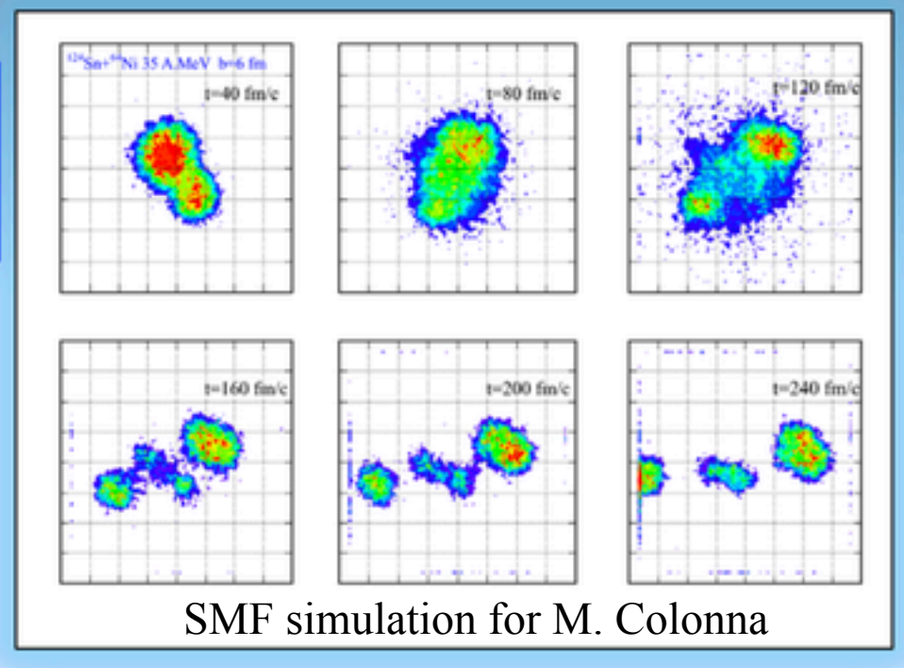


SMF simulation for M. Colonna

## Isospin diffusion

**Isospin gradient** (N/Z asymmetry in the initial system)

Depending on absolute value of the symmetry energy

Isospin equilibration between projectile and target

# What is the "Symmetry Energy" $E_{sym}(\ )$?

We can do a "step back"

# The Equation of State of nuclear matter (EoS)

- The Equation of State of nuclear matter describes a relation between Pressure (P), barion density (ρ), Temperature (T) and **in asymmetric nuclear matter** the isospin asymmetry δ=(N-Z/A). It affects both nuclear physics and astrophysics **from the dynamics of heavy ion collisions to the stability of neutron stars.**

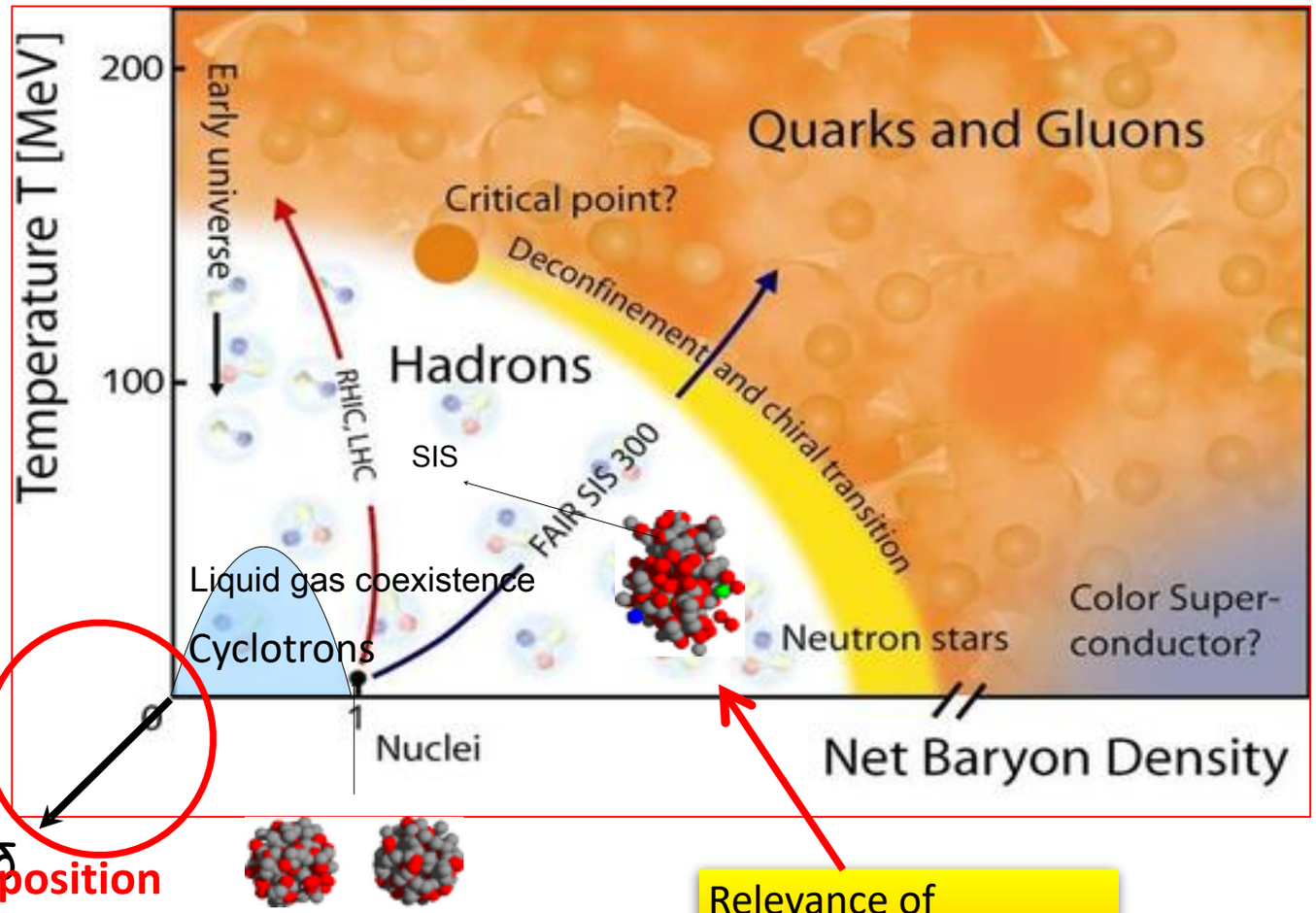


Isospin asymmetry

Relevance of symmetry energy in astrophysical objects

Heavy ion collisions (HIC): Why and how can give information on density dependence of Symmetry term of EOS ?

With HIC large density variations (density gradients) in nuclear matter can be obtained in a short timescale.

# EOS of asymmetric nuclear matter and neutron matter

$$E(\rho,\delta) = E(\rho,\delta=0) + \mathbf{S}(\rho)\delta + \ldots$$

$$\delta = \frac{\rho_n - \rho_p}{\rho_n + \rho_p} = \frac{N-Z}{A}$$

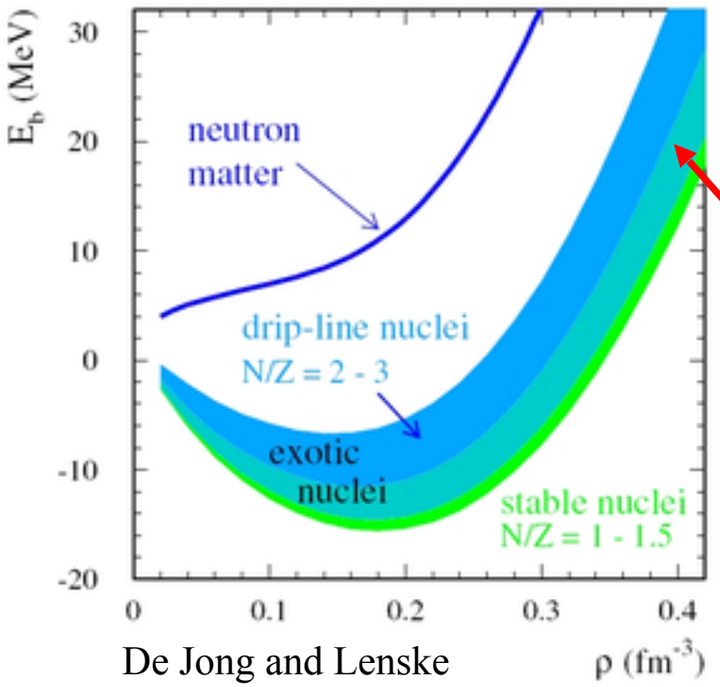


Isospin asymmetry is present in nuclei far from stability valley (drip-line nuclei) and astrophysical objects (like neutron stars), where EOS behaviour determines important properties as the Mass and Radius.

$$E(\rho, T, \delta \neq 0)$$

Asymmetric nuclear matter

The nuclear asymmetry energy describes the increase in energy starting from a symmetric configuration with N=Z toward the extreme limit of neutronic matter

# EOS of asymmetric nuclear matter and neutron matter

## Symmetry energy parametrization: "common" representation

$$E(\rho,\delta) = E(\rho,\delta=0) + \mathbf{S}(\rho)\delta + \ldots$$

$$\delta = \frac{\rho_n - \rho_p}{\rho_n + \rho_p} = \frac{N-Z}{A}$$

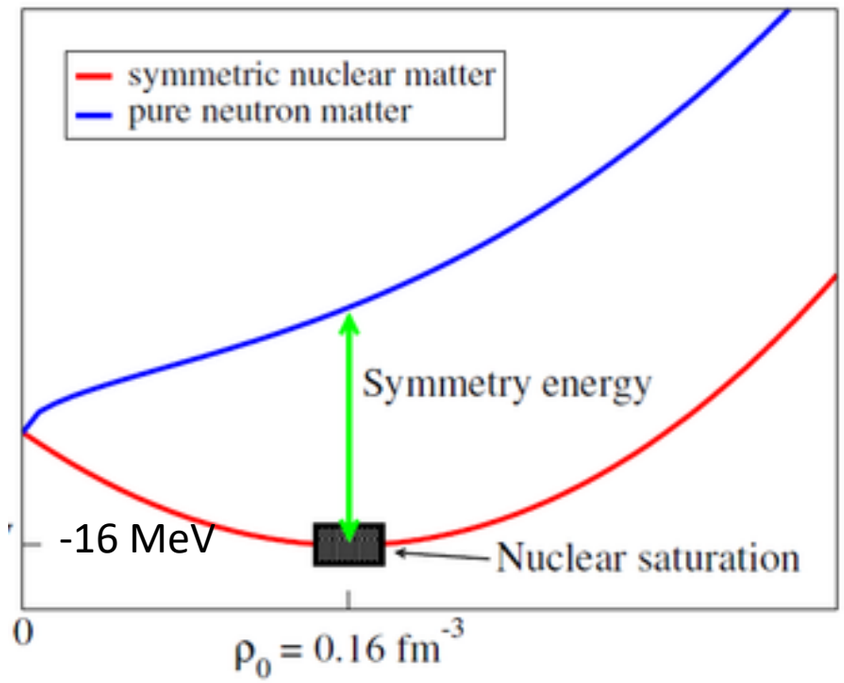


Isospin asymmetry is present in nuclei far from stability valley (drip-line nuclei) and astrophysical objects (like neutron stars), where EOS behaviour determines important properties as the Mass and Radius.

$$E(\rho, T, \delta \neq 0)$$

Asymmetric nuclear matter

The nuclear asymmetry energy describes the increase in energy starting from a symmetric configuration with N=Z toward the extreme limit of neutronic matter

$$E_{sym}(\rho) = E(\rho,\delta=1) - E(\rho,\delta=0)$$

## Second order expansion of symmetry energy around $\rho_0$

$$S(\rho) = S_0 + \frac{L}{3}\left(\frac{\rho-\rho_0}{\rho_0}\right) + \frac{K_{sym}}{18}\left(\frac{\rho-\rho_0}{\rho_0}\right)^2 + \ldots.$$

$S_0 = E_{sym}(\rho_0)$ **Strength**

**The curvature parameter**

$$L = 3\rho_0 \frac{dS(\rho)}{d\rho}$$ **Slope**

$$P_{SYM} = \rho^2 \left(\frac{dS}{d\rho}\right)_{\rho=\rho_0} = \frac{\rho_0}{3} L$$ **Pressure**

$$E_{sym} = E_{sym}^{kin} + E_{sym}^{pot}$$

$$= 12\text{MeV}\cdot(\rho/\rho_0)^{2/3} + 22\text{MeV}\cdot(\rho/\rho_0)^{\gamma}$$

$\gamma<1$ soft, $\gamma>1$ stiff

$L \approx 3S_0\gamma$

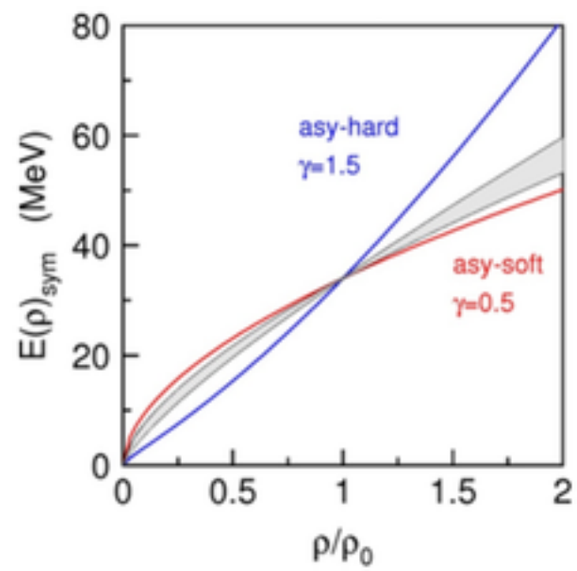

# The key problem: the symmetry energy as a function of the barionic density

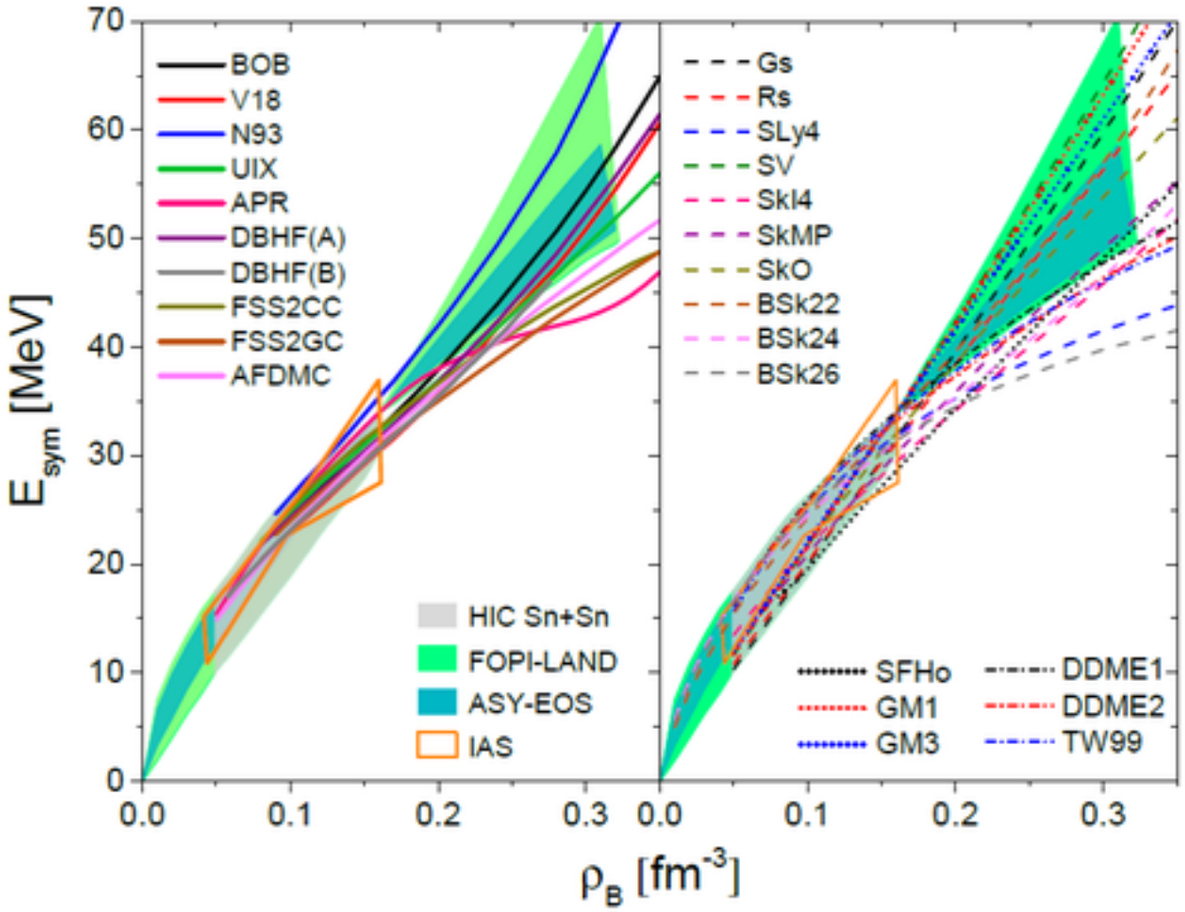


G.F. Burgio et al. (2021): https://doi.org.10.3390/sym13030400

Symmetry energy constrained by neutron and charged particle elliptic flow in ASYEOS experiment at GSI

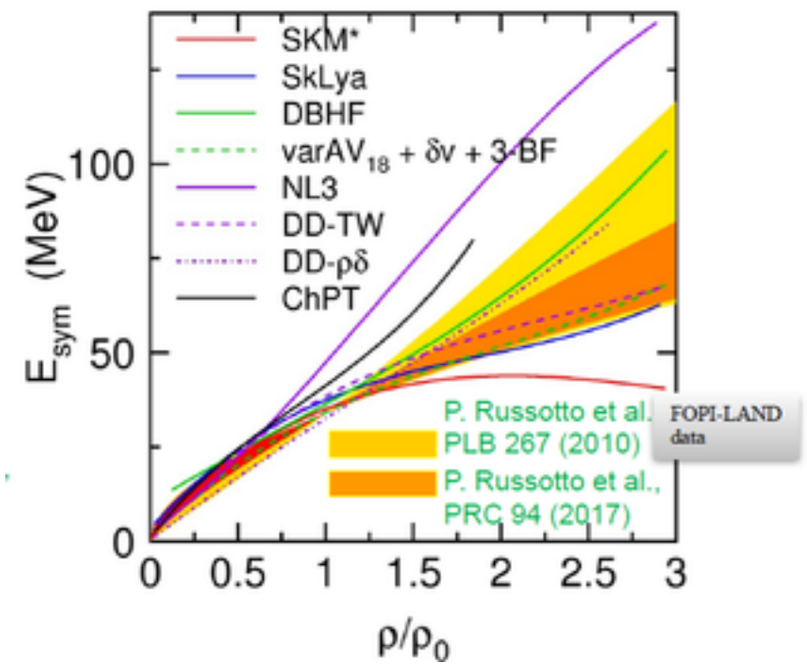


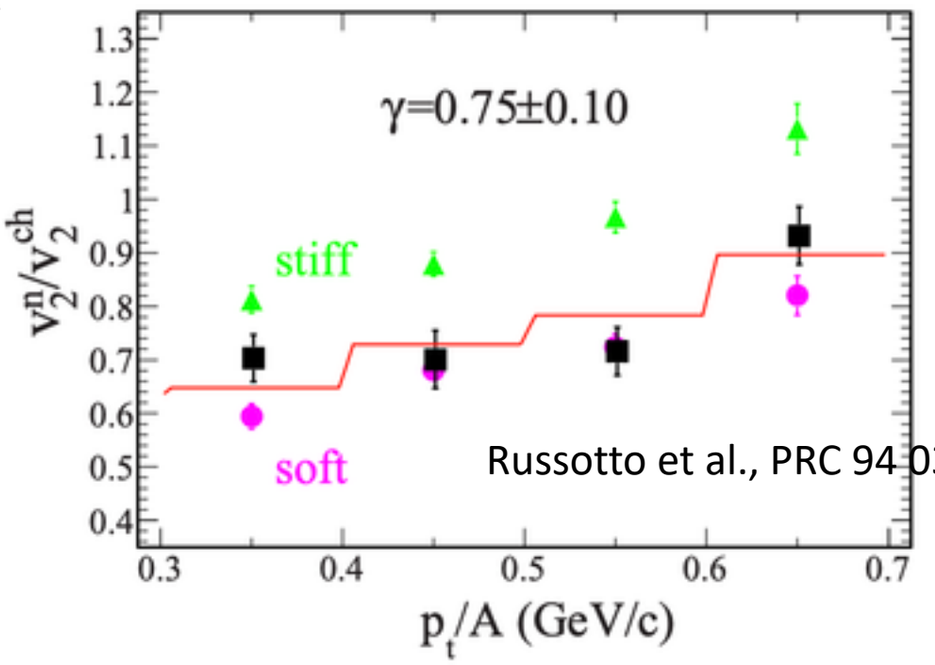


Russotto et al., PRC 94 034608 (2016)

# How to constraints (and Why? ) the density dependence of symmetry energy ?

**ASTROPHYSICS**

- Neutron star structure, composition, size, mass and cooling rate, crust-core transition density
- Pulsars, masses, spin rates
- Supernova explosions
- Stellar nucleosynthesis, r-process

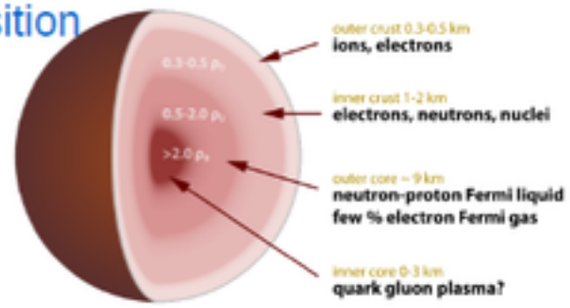


Robert Schulze (Wikipedia)

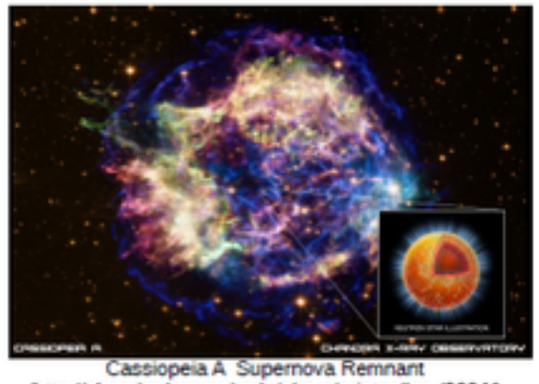

Cassiopeia A Supernova Remnant
(http://chandra.harvard.edu/photo/printgallery/2004/)

Mainly constrained at supra-saturation densities (multi-messanger astronomy)

**STRUCTURE**

- Structure of exotic nuclei (masses, drip lines)
- Neutron skin thickness
- IvGDR, ISGDR
- Pygmy resonances
- Differences between IAS

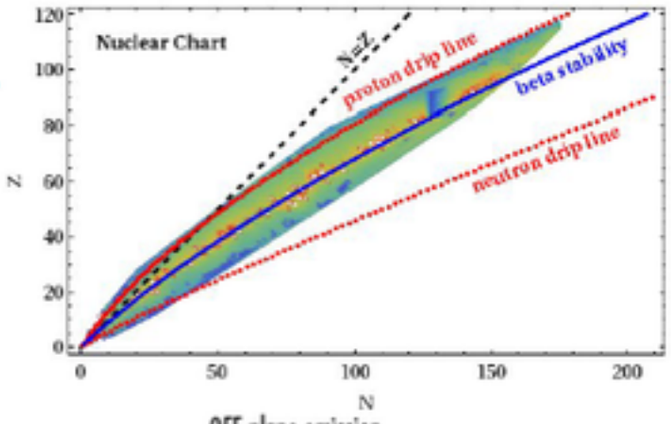


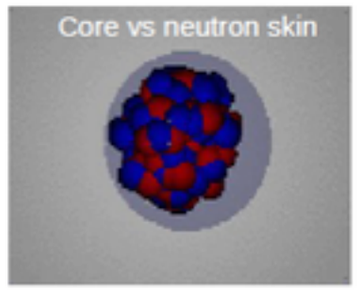


PDR

Only at sub-saturation densities

**REACTIONS**

- Flow patterns in HIC
- Multifragmentation, isoscaling, isospin diffusion, neck emission
- n/p, t/$^3$He, $\pi^-/\pi^+$, $K^+/K^0$ ratios in HIC

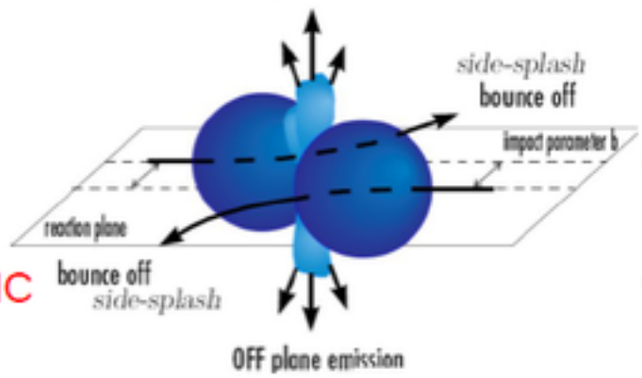


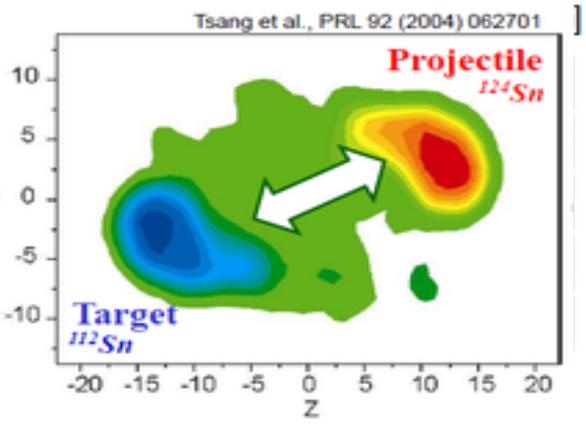


HIC : it is the only way in terrestrial laboratories to access EOS from sub- to supra-saturation densities

# “Multi-messenger Astronomy”

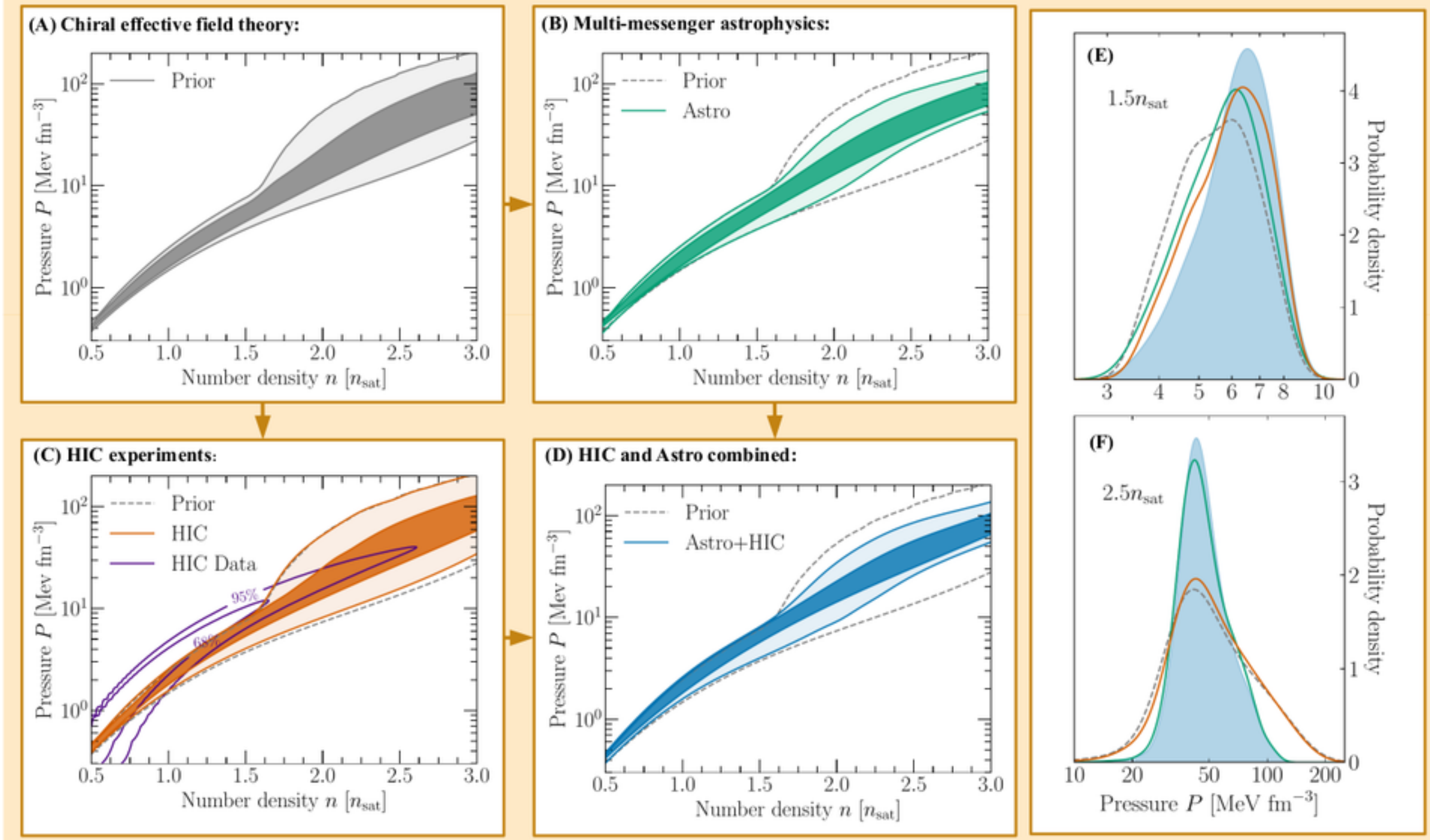


Huth, S., Pang, P.T.H., Tews, I. *et al.* Constraining neutron-star matter with microscopic and macroscopic collisions. *Nature* **606**, 276–280 (2022). https://doi.org/10.1038/s41586-022-04750-w

# The Physics case:
# dynamical vs. statistical production of Intermediate Mass Fragments (IMF).

Enrico De Filippo courtesy

## Dynamical IMF emission in semi-peripheral collisions

1) The "**neck**" emission where light IMFs (Z<≈9) are produced at midrapidity due to the rupture of a piece of nuclear matter a low density ("neck"). This is generally a **FAST** process (<100 fm/c)

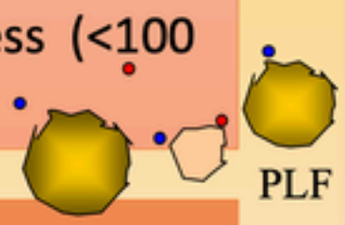


2) Excitation of a primary Projectile-like PLF* (TLF*) followed by its splitting. In case of (non-equilibrated) **dynamical fission** the emission of the **lighter IMF** is preferentially backwards in the PLF reference system **(anisotropy in angular distributions)**

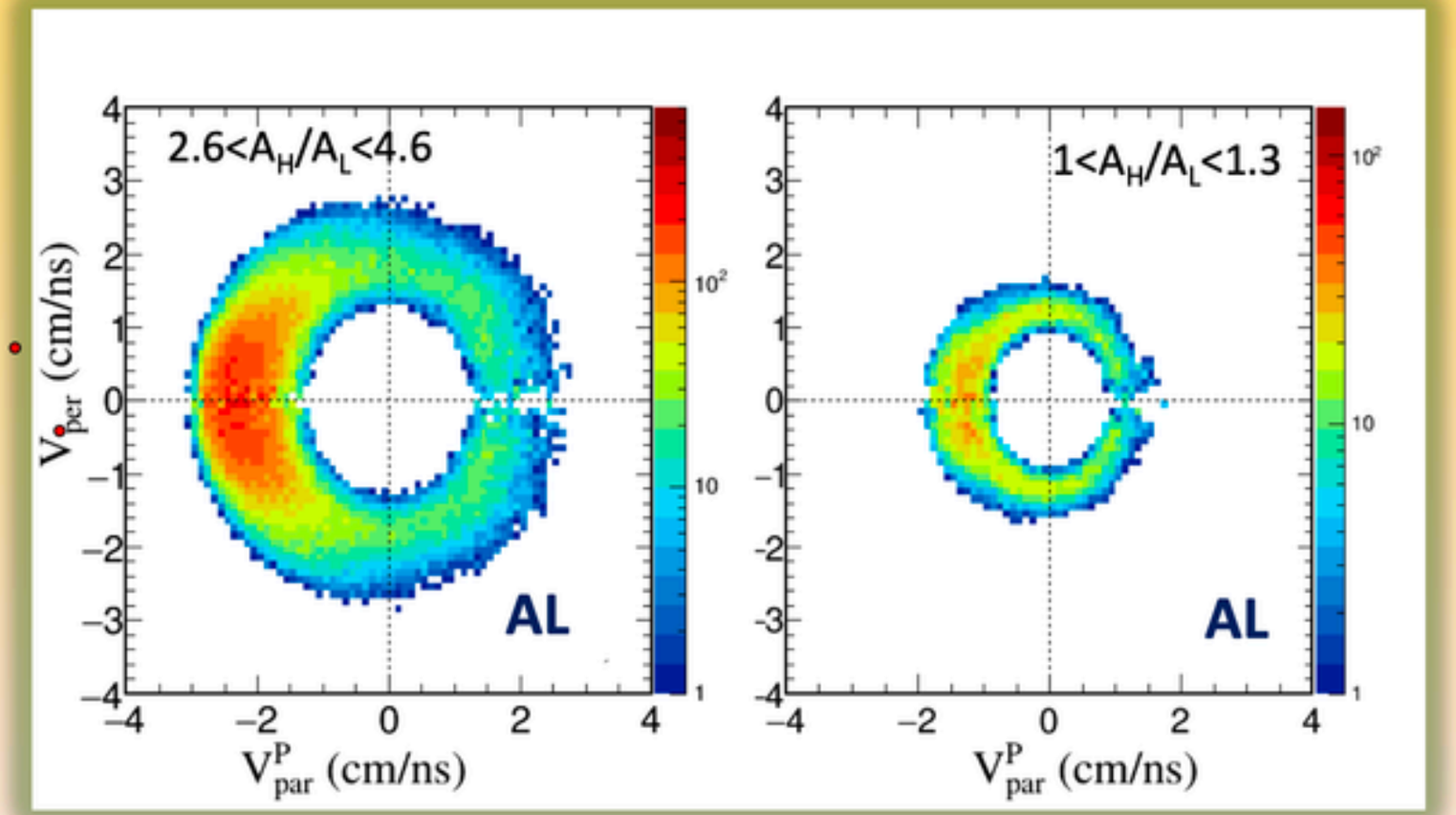


**P. Russotto et al. $^{124}$Xe + $^{64}$Ni @35 A.MeV see: Eur. Phys. Jour. A56, 12 (2020)**

$$j_n - j_p \propto E_{sym}(\rho)\nabla I + \frac{\partial E_{sym}(\rho)}{\partial \rho} I \nabla \rho$$

BLOB simulation P. Napolitali

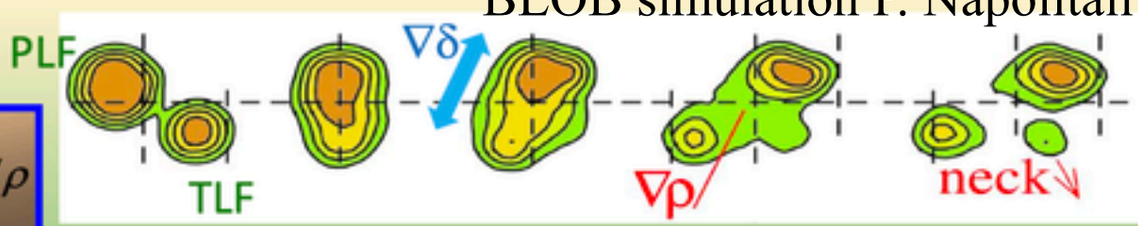

# The Physics case:
# dynamical vs. statistical production of Intermediate Mass Fragments (IMF).

how can we separate dynamical from statistica emission?

1) Wilczynsky plot II

Relative velocities are expressed in units of the velocity corresponding to the Coulomb repulsion energy of a given subsystem according to the Viola systematics (see J. Wilczynsky et al. IJMPE 14 353 and E.d.F. et al. Phys Rev. C71, 044602, 2005).

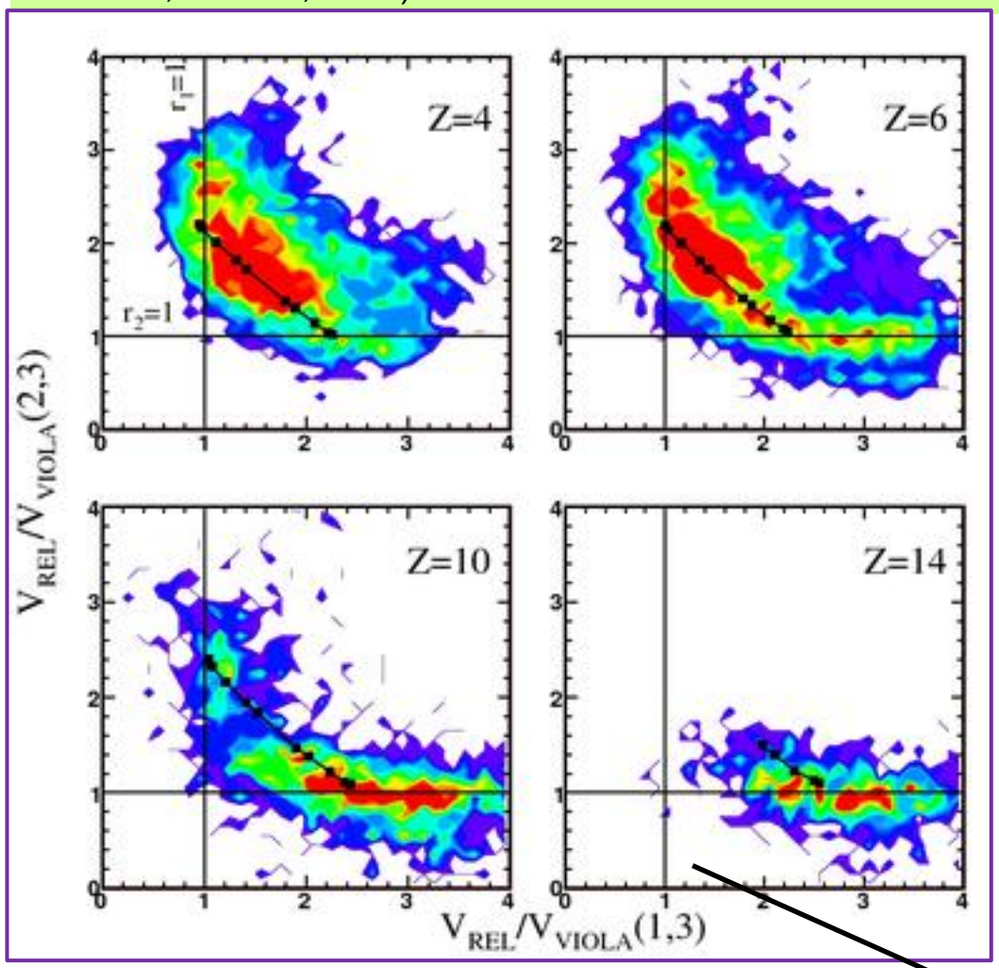


Emission cronology: light fragments are produced earlier (~40 fm/c) than heavier ones (~120 fm/c)

2) Theta proximity angle distribution

$Theta_{prox}$ is the angle between the beam axis (TLF-PLF) and the breakup axis (PLF - IMF)

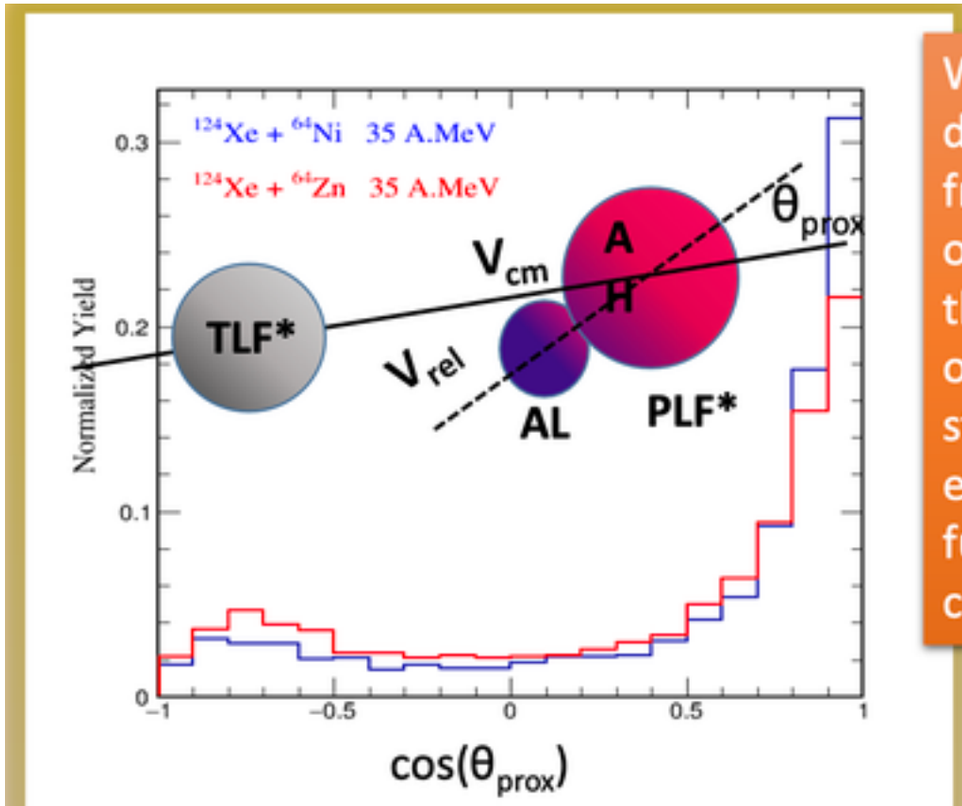


We use angular distribution of fragments in order to estimate the probabilities of dynamical vs. statistical emission as a function of IMFs charge

the value $V_{REL}/V_{VIOLA} = 1$ (pure coulomb repulsion) indicates sequential decay

# REVERSE

One result:

The IMF dynamical emission probability for the PLF fission is enhanced by the increase of both the projectile and the target N/Z content (isospin content)

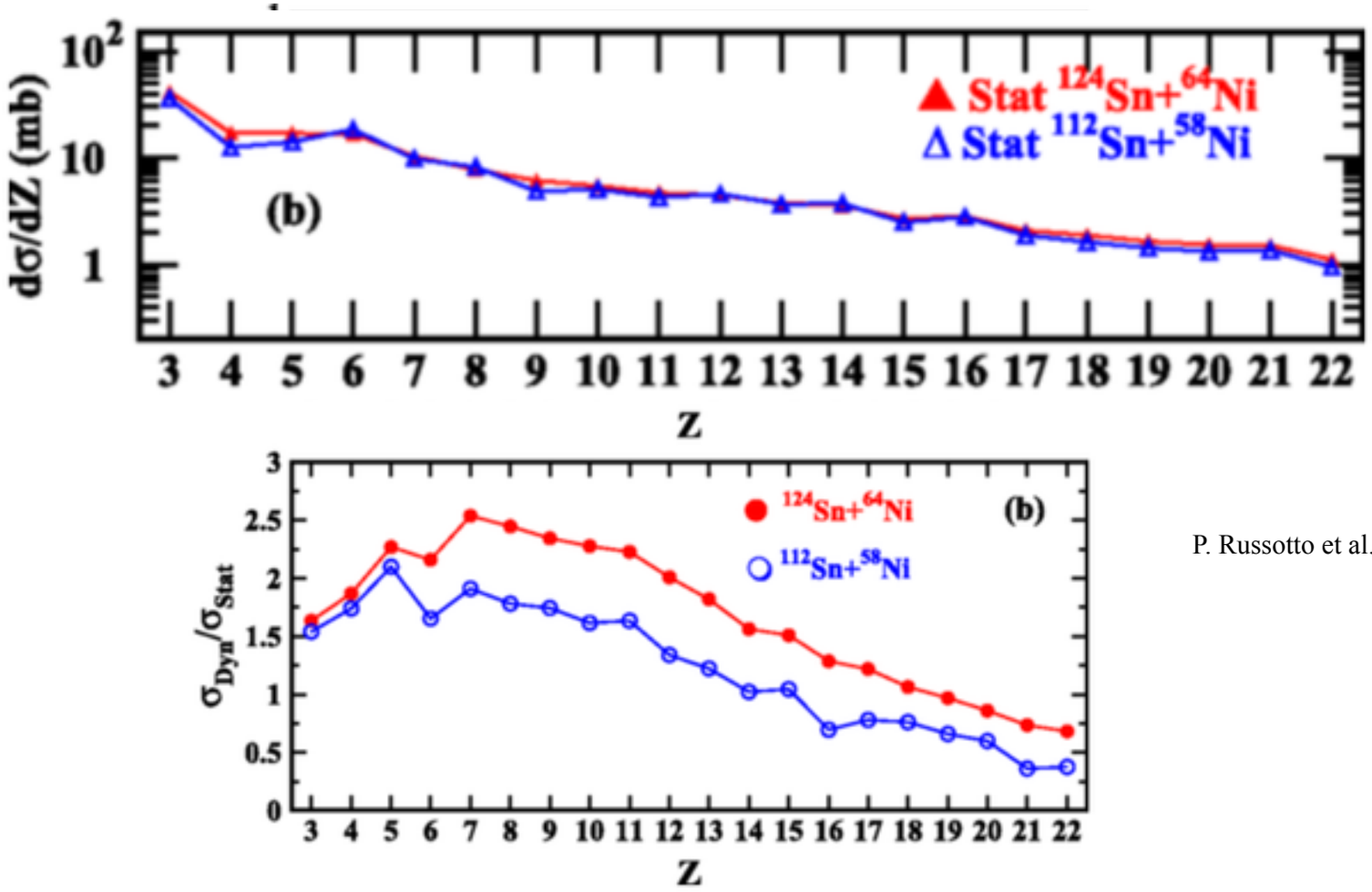


P. Russotto et al., PRC 91 014610 (2015)

But

The two colliding systems of the REVERSE experiment ($^{124}$Sn + $^{64}$Ni and $^{112}$Sn + $^{58}$Ni) have not only different isospin but also different mass (and size)

# INKIISSY

## (INvers KInematic ISobaric SYstem)

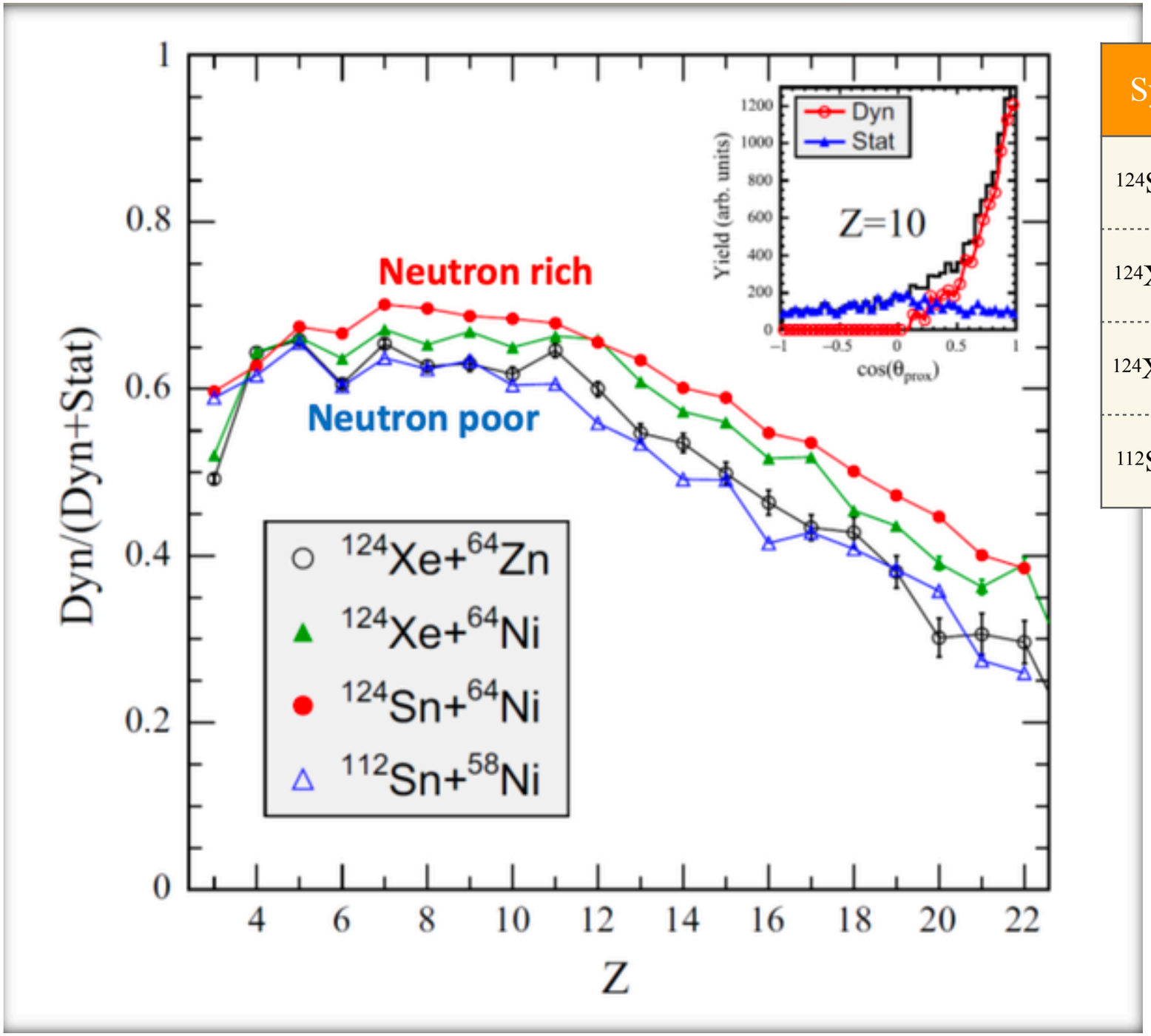


| System | N/Z Projectile | N/Z Target | N/Z Compoud | Experiment |
|---|---|---|---|---|
| $^{124}$Sn+$^{64}$Ni | 1.48 | 1.29 | 1.41 | Reverse |
| $^{124}$Xe+$^{64}$Ni | 1.30 | 1.29 | 1.29 | INKIISSY |
| $^{124}$Xe+$^{64}$Zn | 1.30 | 1.13 | 1.24 | INKIISSY |
| $^{112}$Sn+$^{58}$Ni | 1.24 | 1.07 | 1.18 | Reverse |

Two new systems with same mass of the neutron rich but N/Z similar to the neutron poor ($^{124}$Xe + $^{64}$Ni and $^{124}$Xe + $^{64}$Zn) at the same bombarding energy of 35 AMeV

The Isospin dependence in the dynamical emission is preserved

# CHIFAR Experiment

## (CHIMERA - FARCOS)

We decided to explore nuclear dynamics as a function of the energy
In particolare at lower energy regime: 20AMeV

**CHIFAR experiment**:

Study of the dynamical and statistical PLF break-up @20 MeV/A

**$^{124}$Sn+$^{64}$Ni, $^{112}$Sn+$^{58}$Ni and $^{124}$Xe+$^{64}$Zn at 20 A MeV (November 2019)**

Spokes: E.V. Pagano, E. De Filippo, P. Russotto et al.

**CHIMERA + 10 FARCOS telescopes in a "quasi"- ring configuration**

**FARCOS arranged in a ring structure with 16< <30 polar angle**

**Only 6 analyzed for the present work**

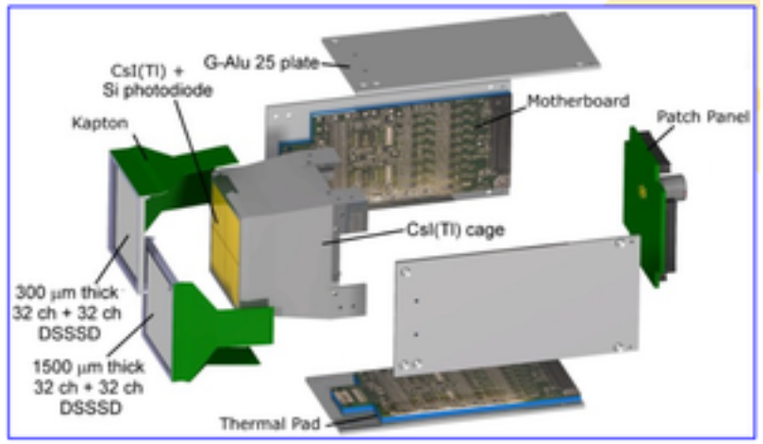


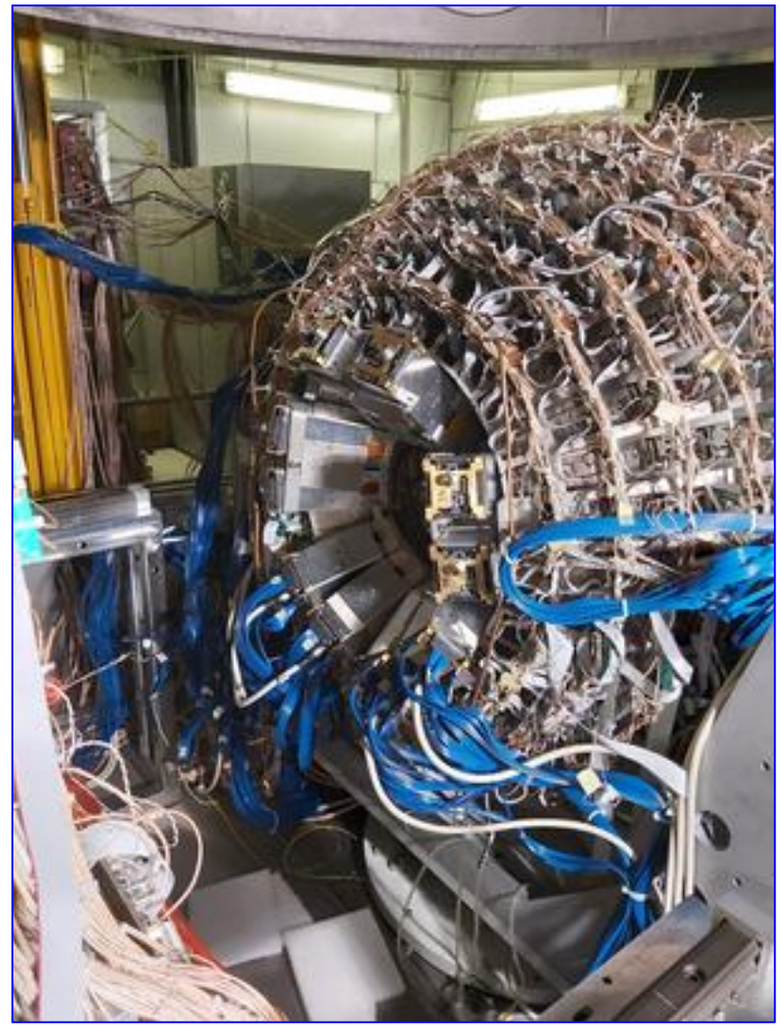

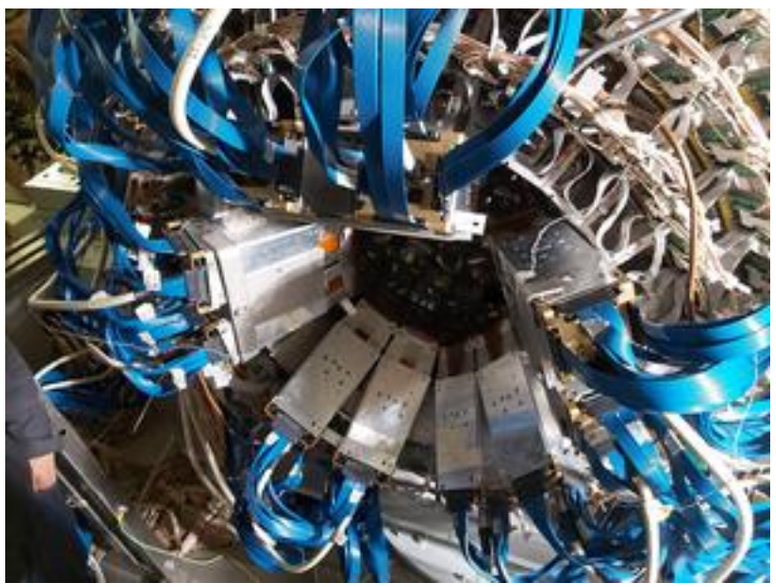

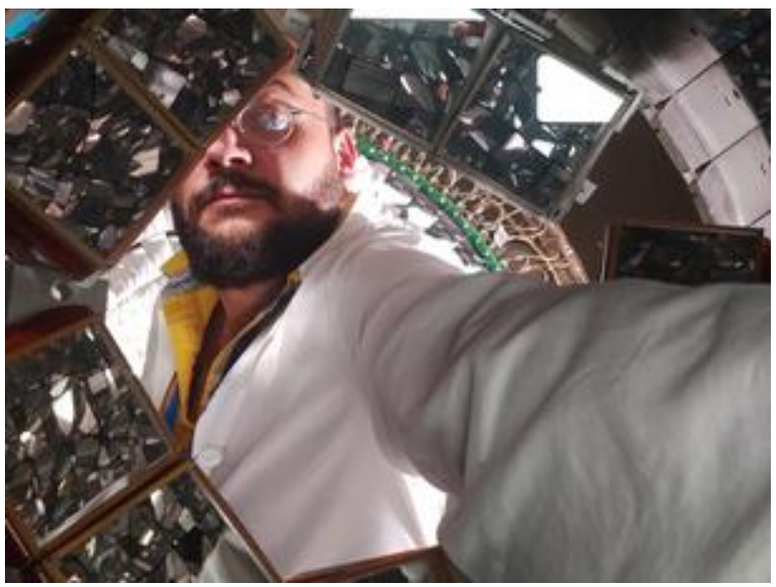

# FARCOS

(Femtoscopy ARray for Correlation and Spectroscopy )

- Based on (62x64x64 mm³) clusters
- 1 square (0.3x64x64 mm³) DSSSD 32+32 strips
- 1 square (1.5x64x64 mm³) DSSSD 32+32 strips
- 4 60x32x32 mm³ CsI(Tl) crystals

**132 Independent electronic channels**

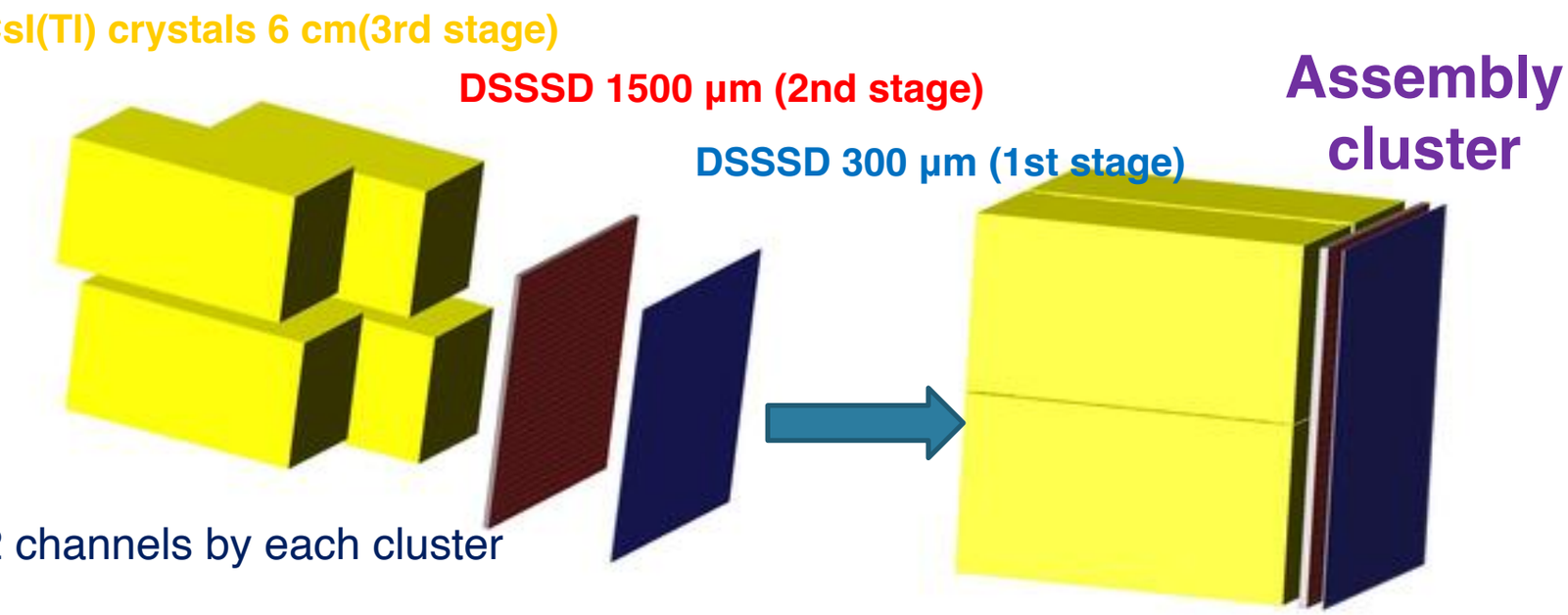


132 channels by each cluster

- **Modular array of telescopes**
- **High energy and angular resolution**
- **ΔE/E discrimination, pulse-shape discrimination and possible TOF discrimination like in 4pi CHIMERA**
- **Digitization (GET Electronics)**
- **DSSSD(Double-Sided Silicon Strip Detector) each with 32 strips, both in vertical and in a horizontal and 4 crystals of CsI(Tl).**
- **Portability and modularity to be coupled to 4π detectors as CHIMERA or magnetic spectrometers**
- **Integrated and reconfigurable electronics**
- **Possibility of updating and upgrades**

# Calibration FARCOS's silicon strips in the CHIFAR EXP

## Technique used: Punch Through

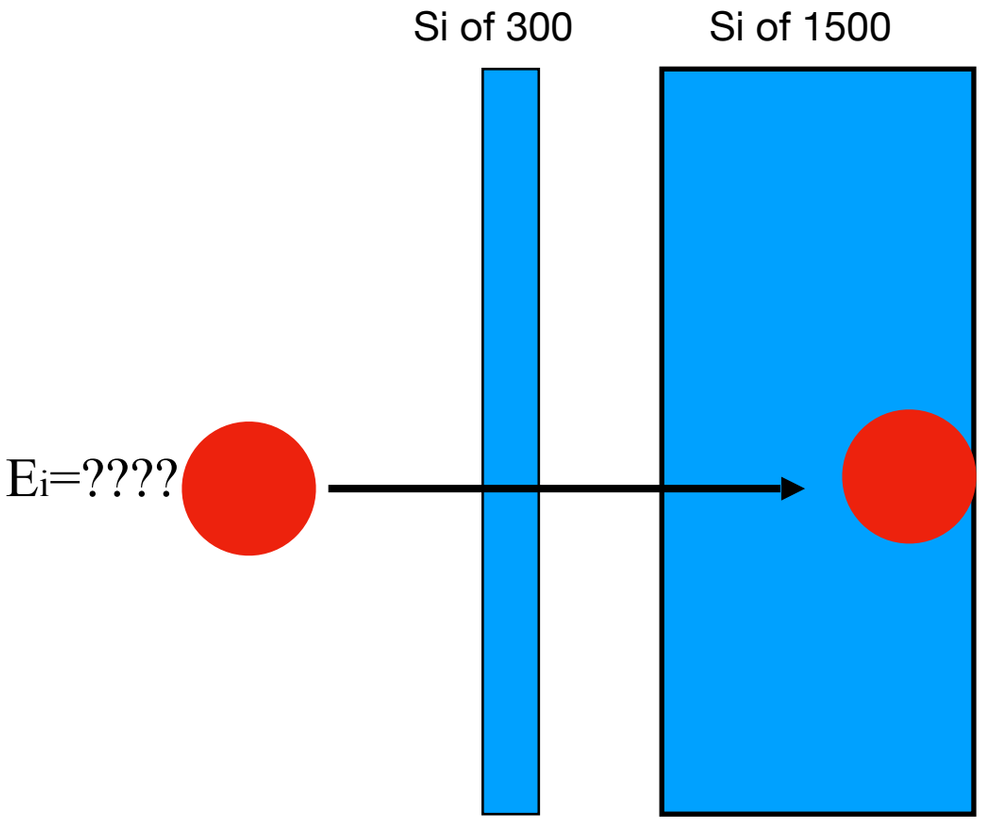


First step in transmission  Second step full stopped

If the partile if arrested in 1800 of Silicon the initial energy $E_i$ is known

Particles used for the calibration and their energies calculated by LISE++*

| Particle | 300 (MeV) | 1500 (MeV) | 1800 (MeV) |
|---|---|---|---|
| $^{7}$Li | 13,57 | 125,38 | 138,95 |
| $^{7}$Be | 18,52 | 172,68 | 191,2 |
| $^{9}$Be | 20,82 | 192,68 | 213,5 |

*http://lise.nscl.msu.edu/lise.html

1

# Calibration FARCOS's silicon strips in the CHIFAR EXP

Telescopes of FARCOS good and calibrated : T1, T5, T7, T8, T9, T10

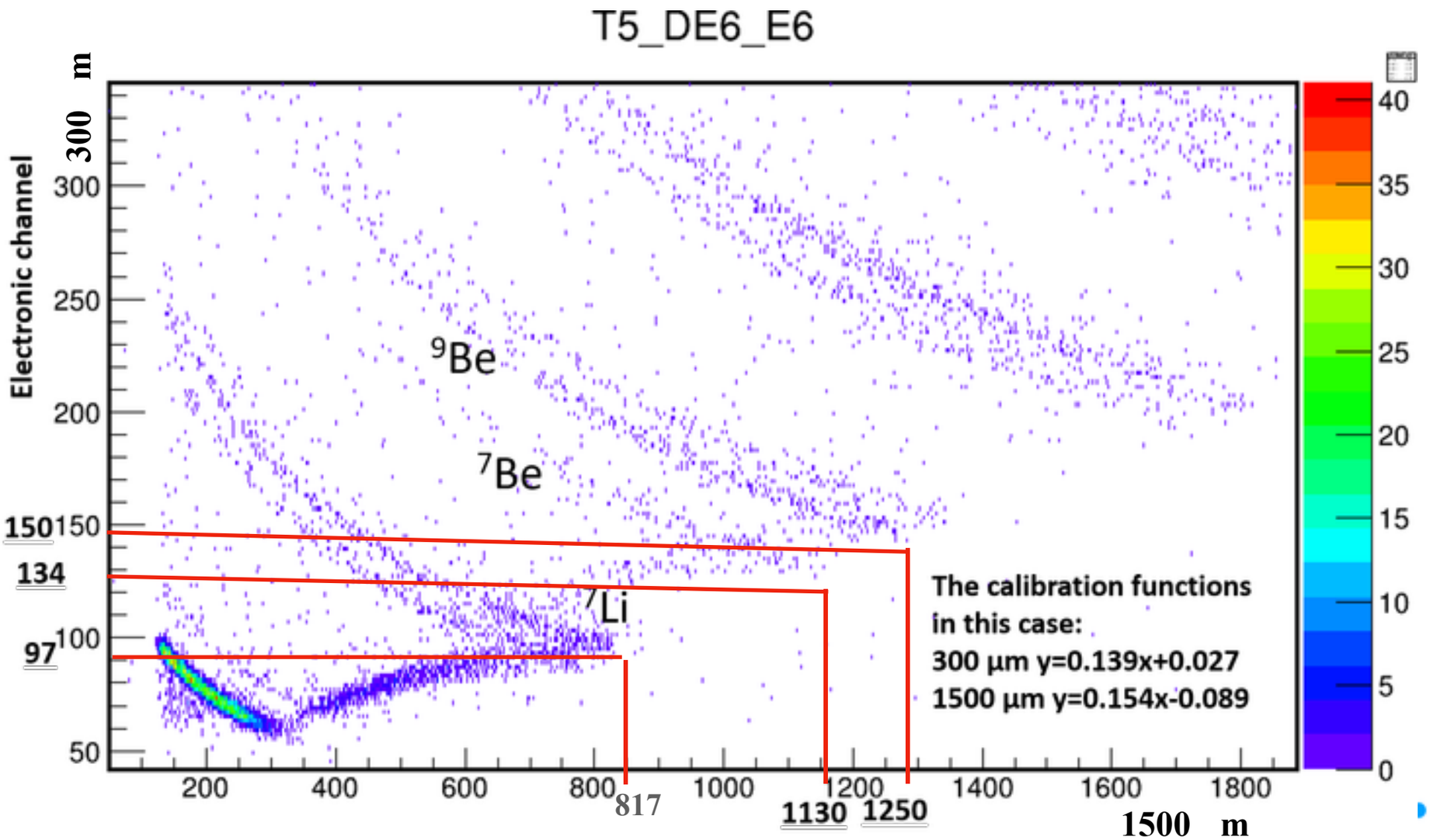


**Fit performing**
**Very good linearity**

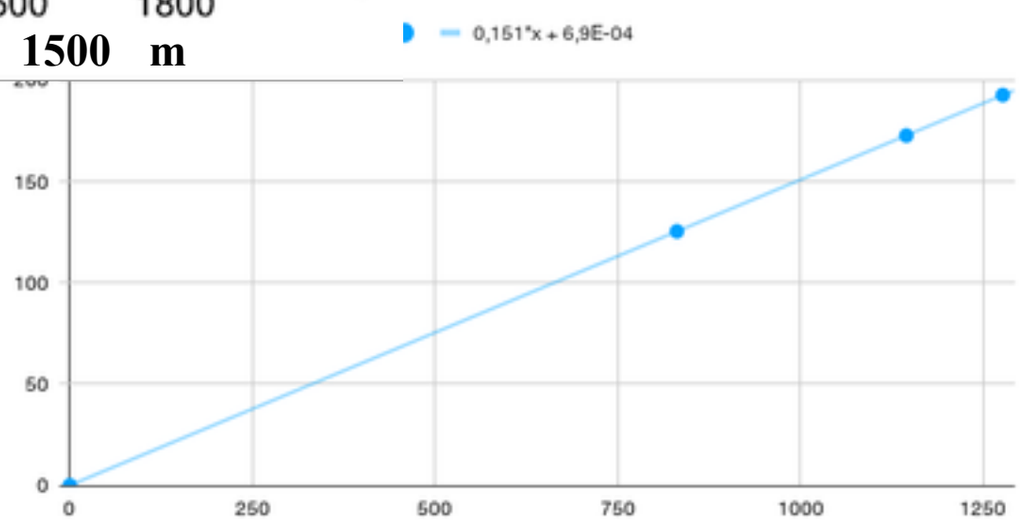


**Electronic channel**

# Calibration FARCOS's silicon strips in the CHIFAR EXP

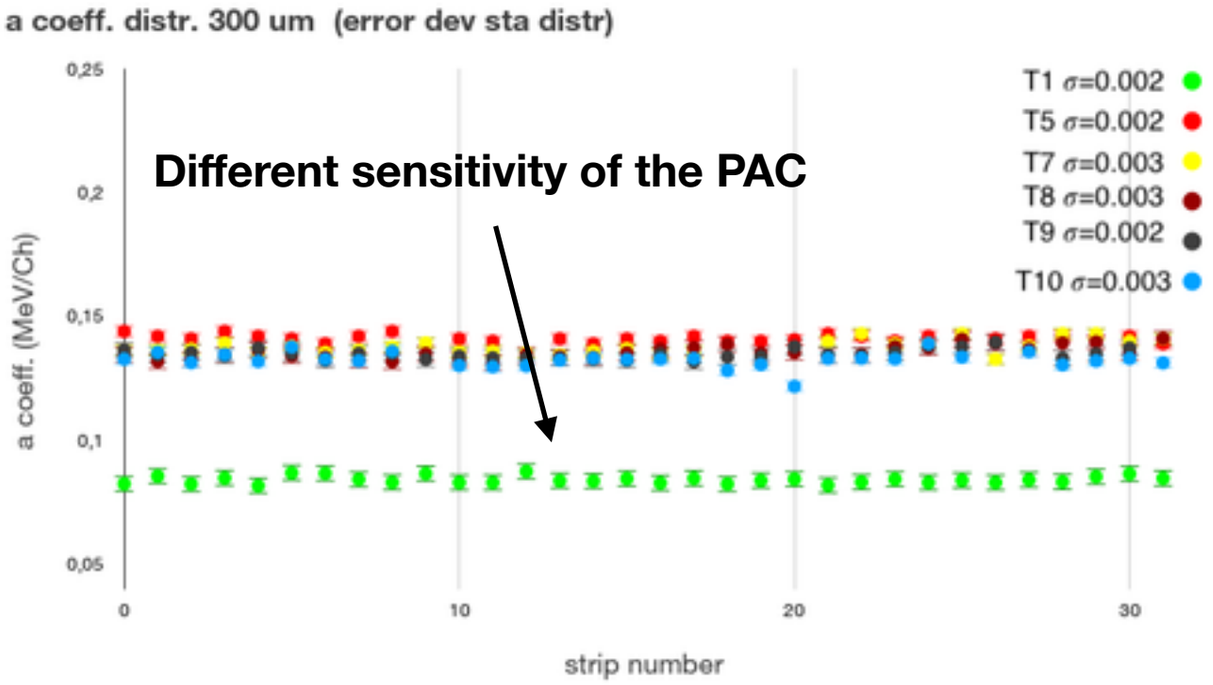


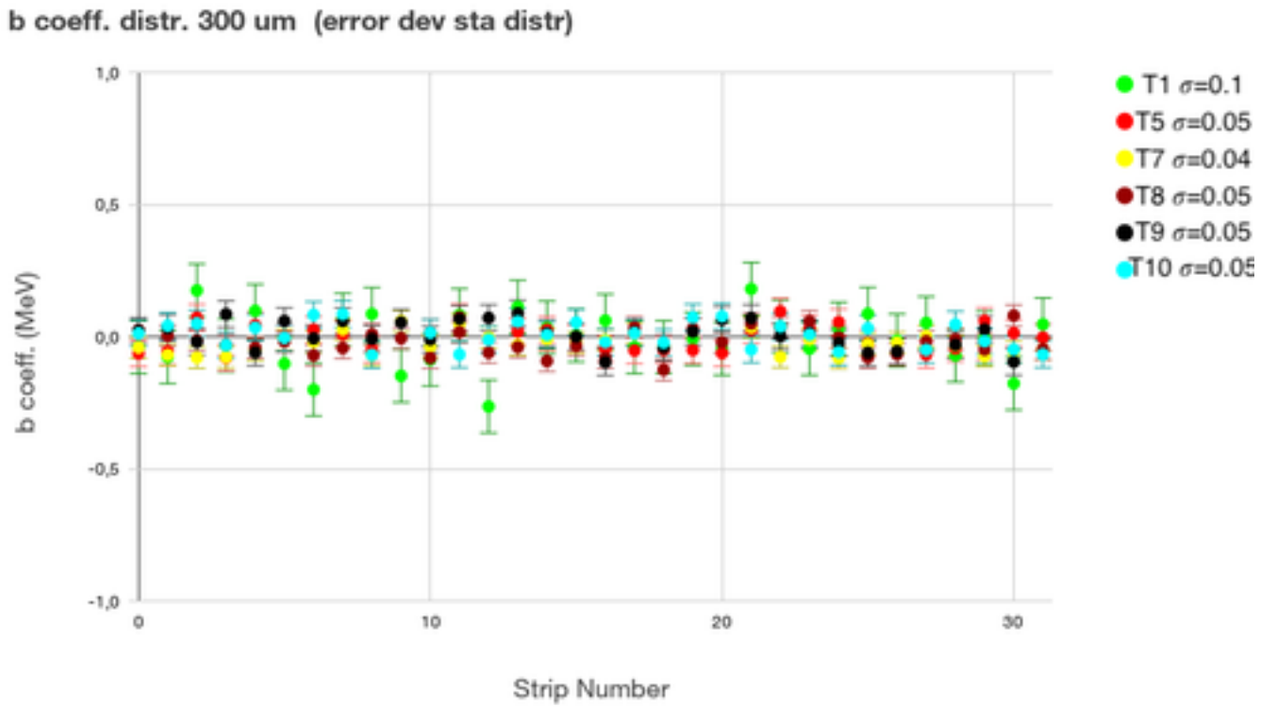


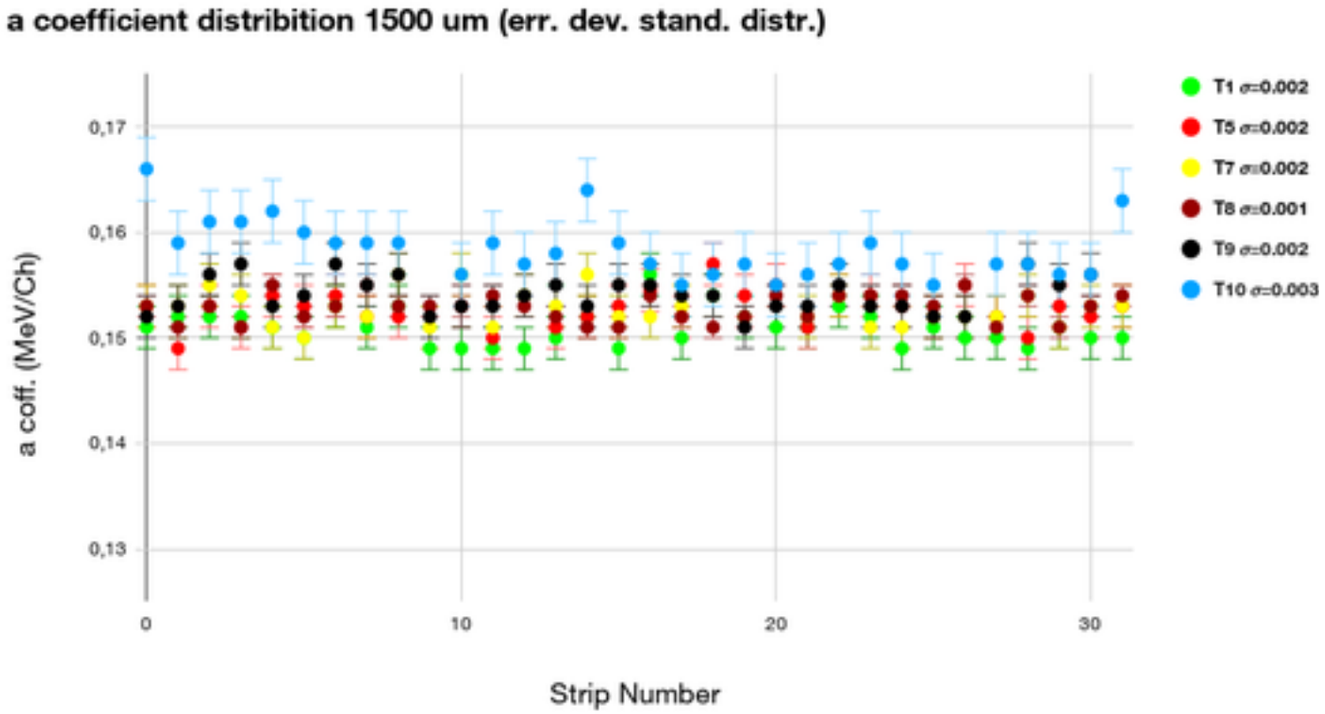


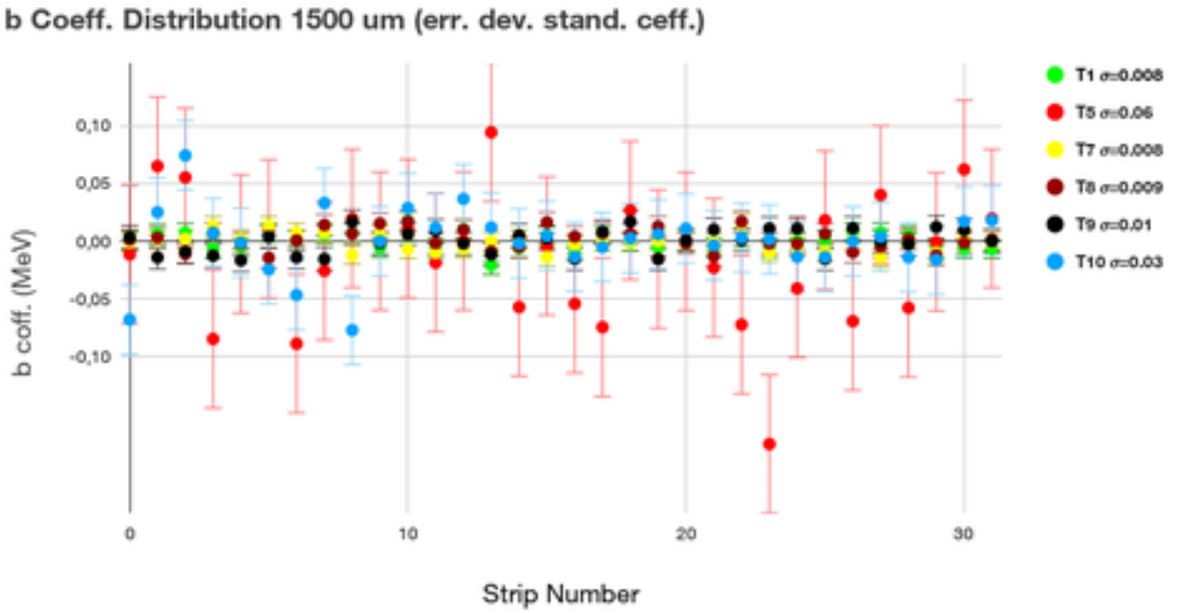

# Calibration FARCOS's silicon strips in the CHIFAR EXP

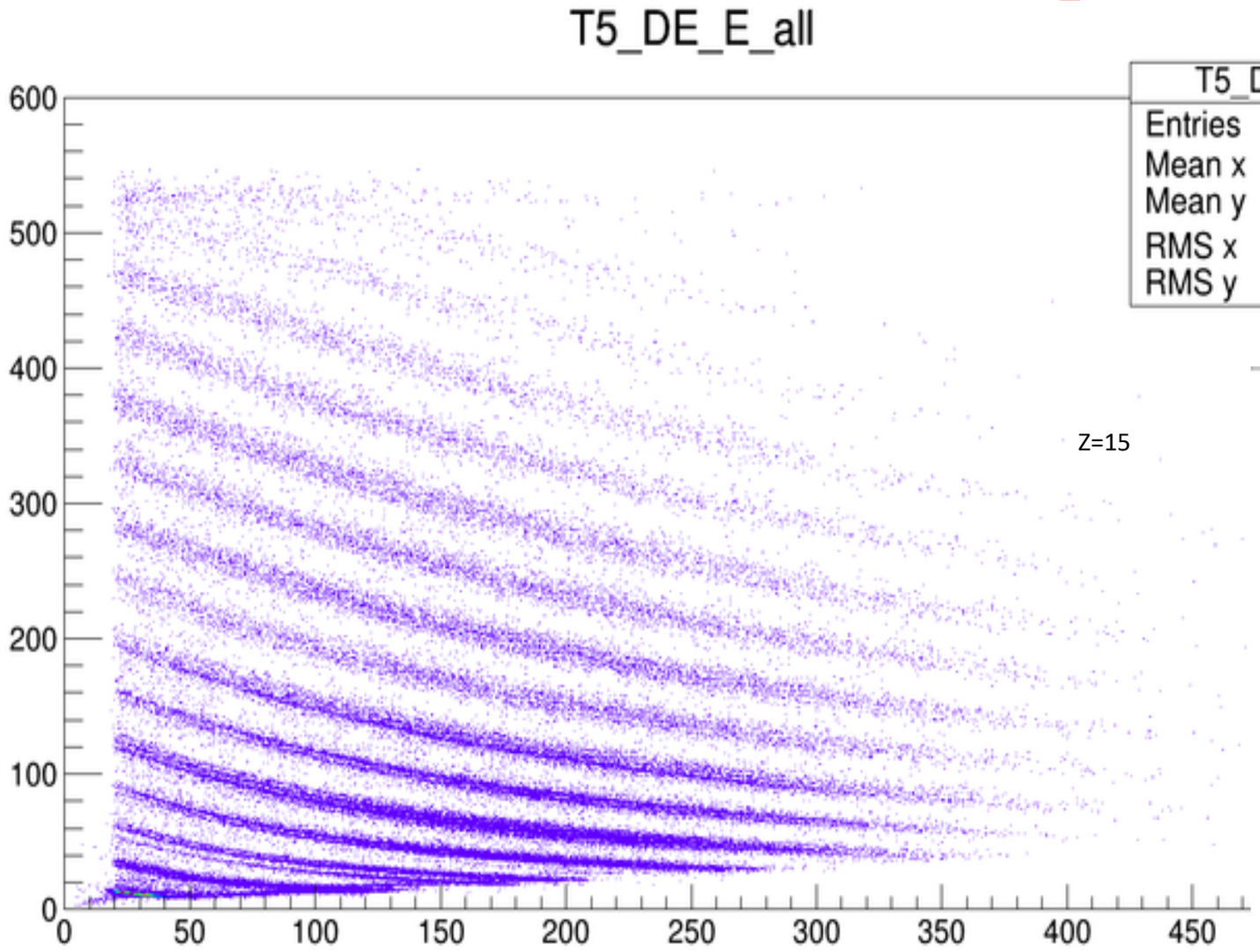


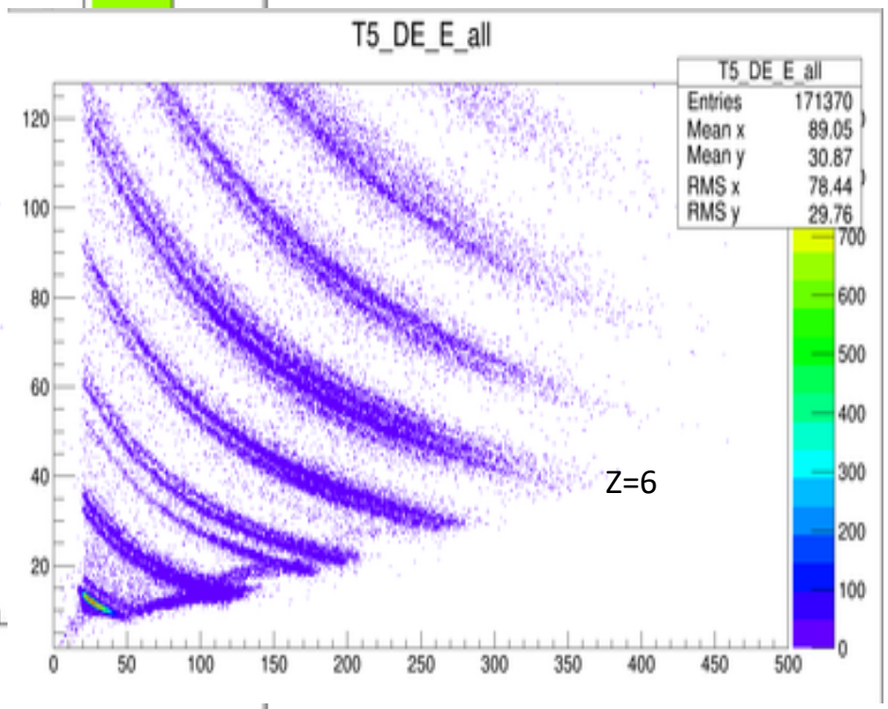


Back side energy calibration

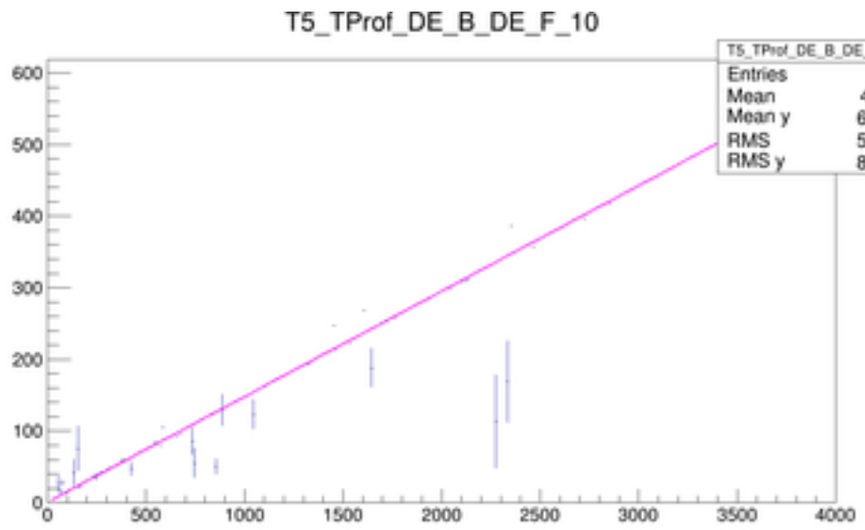


# Pixelation

Experimental constraints to select only "true particles":

- particle multiplicity
  - = 1 for Si−300 µm, front and back;
  - = 1 for Si−1500 µm, front;
  - < 4 for Si−1500 µm, back;
  - = 0 for CsI(Tl)
- $85\%\ \Delta E_{back} < \Delta E_{front} < 115\%\ \Delta E_{back}$
- $N_{strip}$ (300 µm) = $N_{strip}$ (1500 µm) || $N_{strip}$ (300 µm) = $N_{strip}$ (1500 µm) ±1

# Particles identification

## Fit T5 DE-E identification

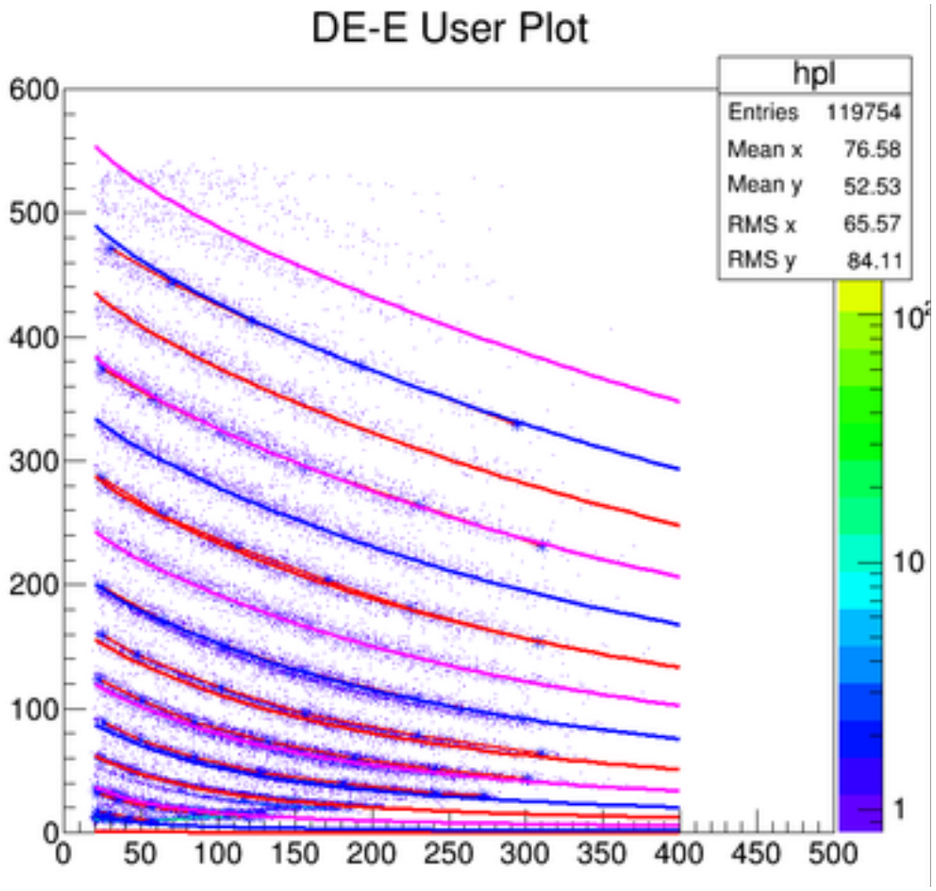


Part of Cristina Zagami's PhD work at UNICT

"neutron poor"
$^{112}Sn+^{58}Ni$
@ 20 AMeV

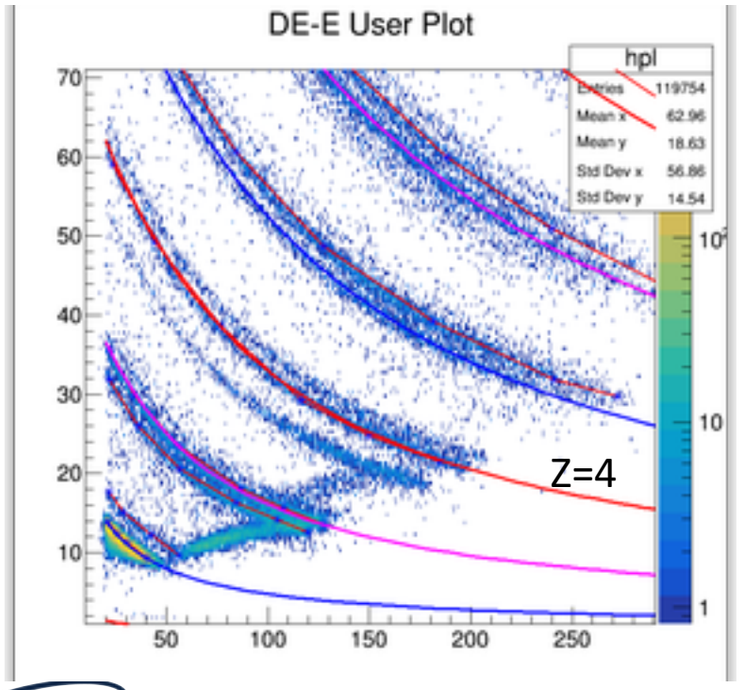


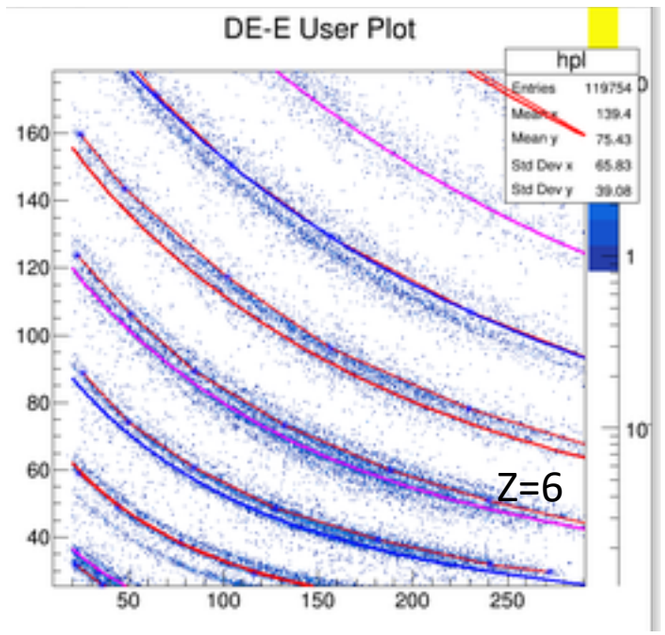


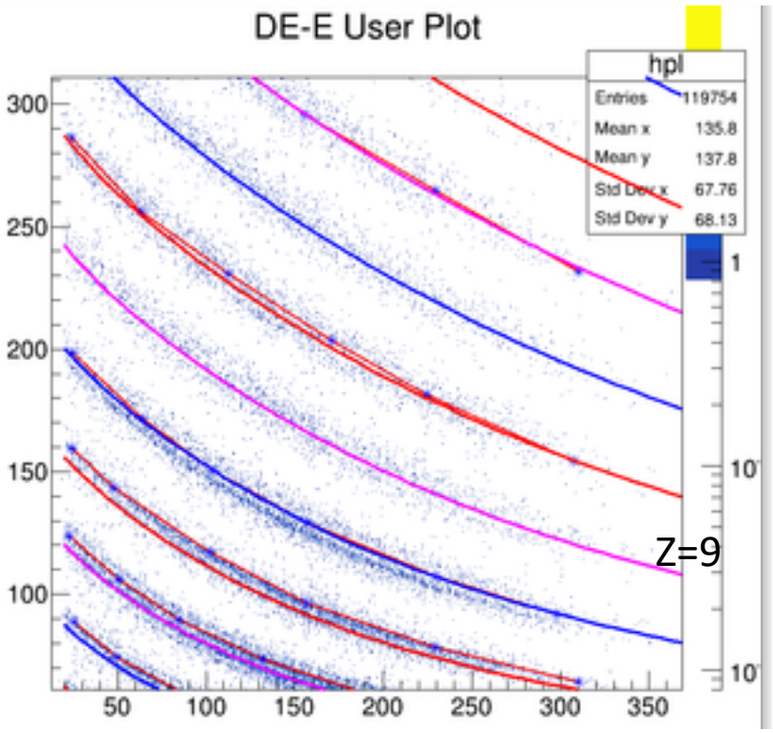

"neutron poor"
$^{112}Sn+^{58}Ni$
@ 20 AMeV

Part of Cristina Zagami's PhD work at UNICT

# Mass spectra: isotopic identification

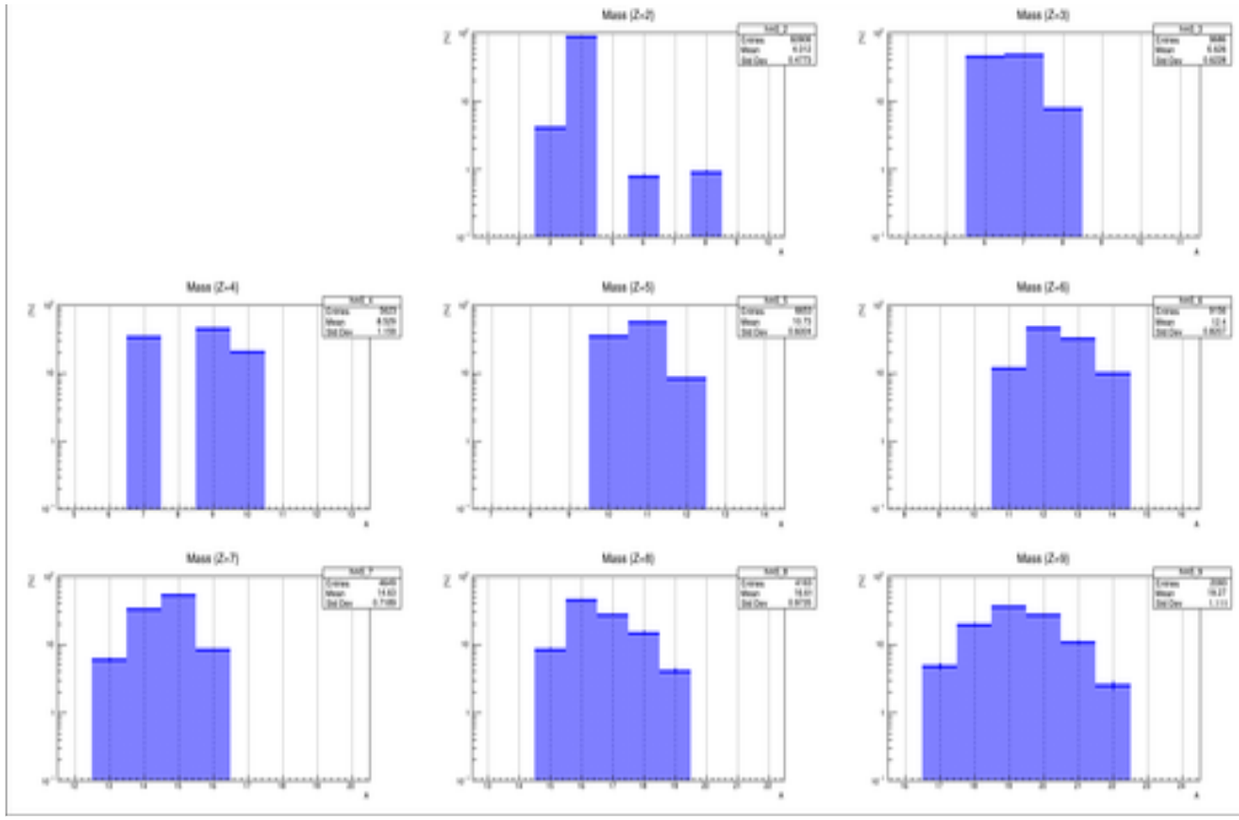


# Charge identification

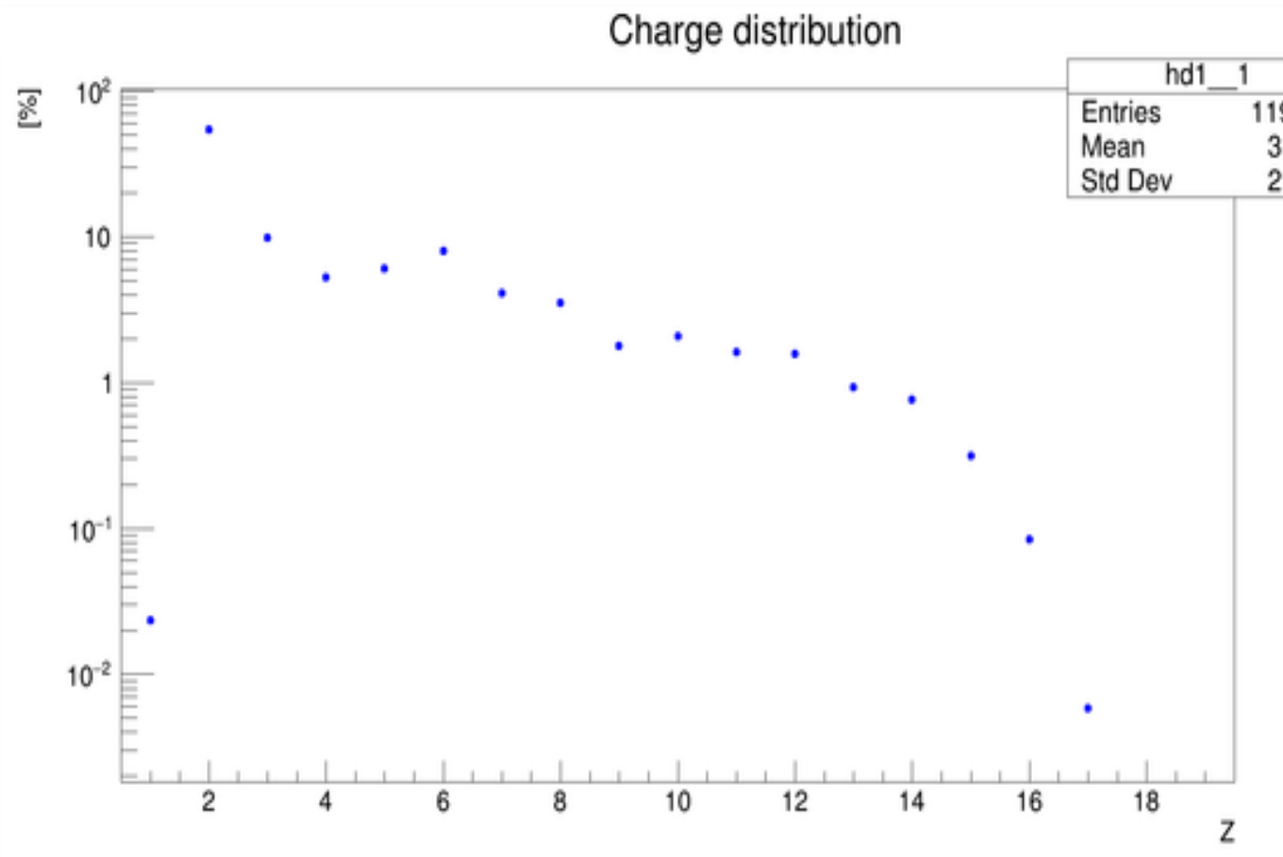

"neutron rich"
$^{124}$Sn+$^{64}$Ni
@ 20 AMeV

# Fit T5 DE-E identification

"isobaric"
$^{124}$Xe+$^{64}$Zn
@ 20 AMeV

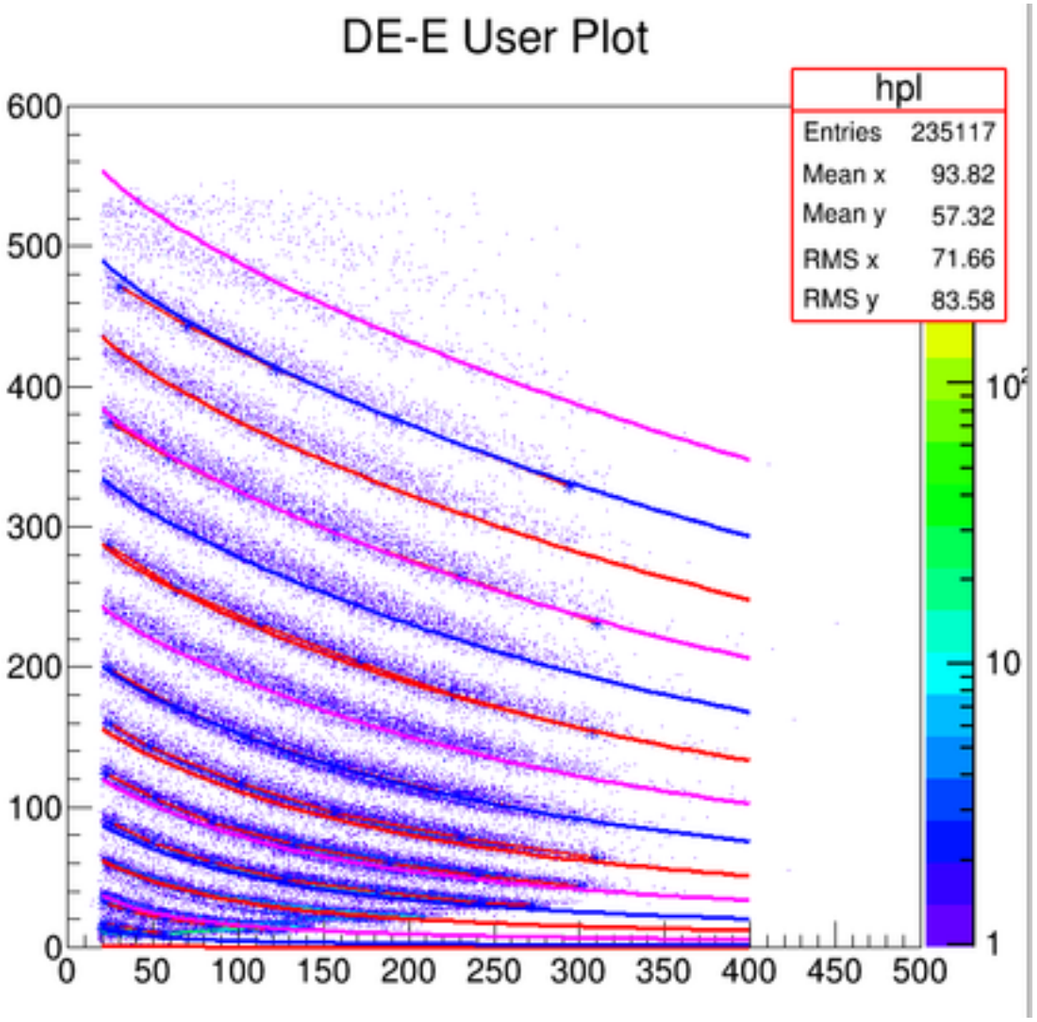


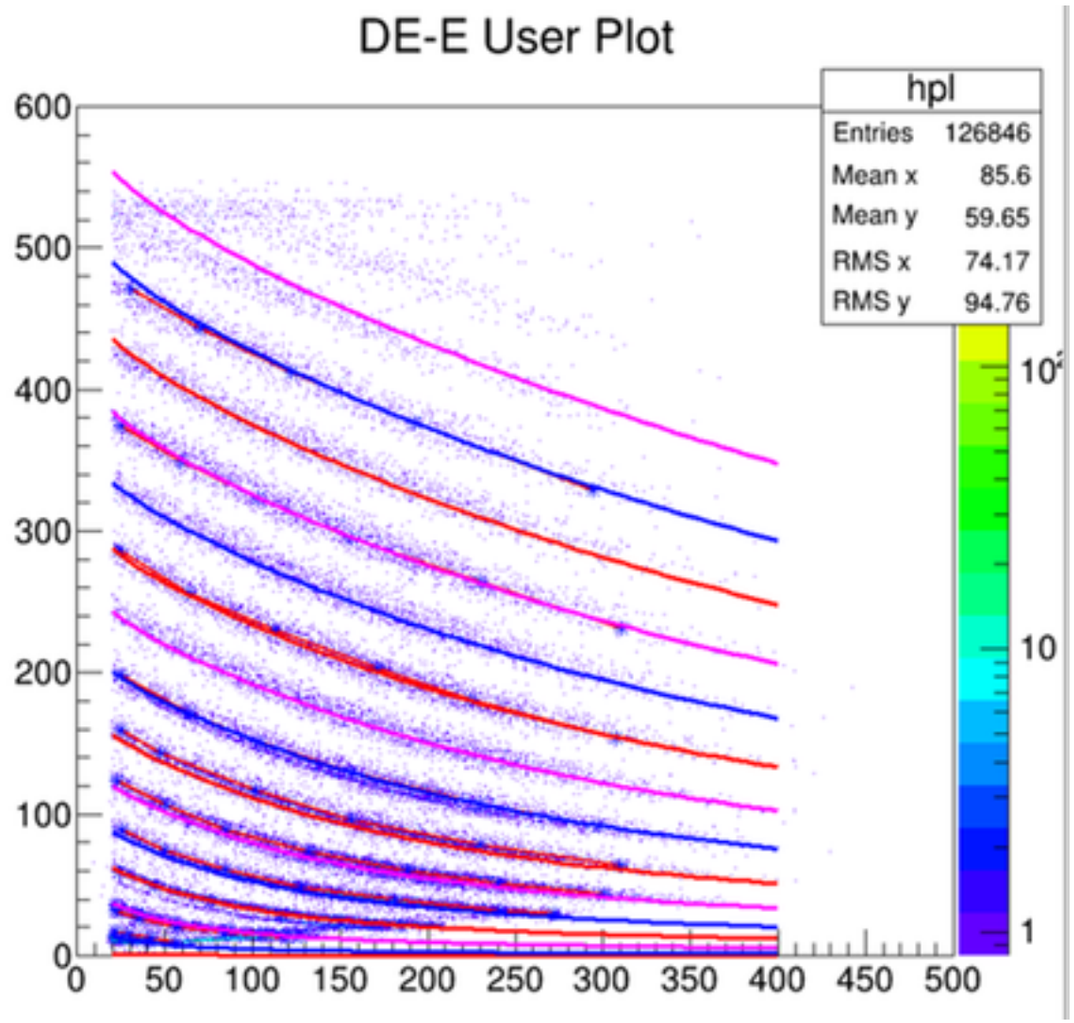

# Mass spectra: isotopic identification

"neutron rich" $^{124}Sn+^{64}Ni$ @ 20 AMeV

"isobaric" $^{124}Xe+^{64}Zn$ @ 20 AMeV

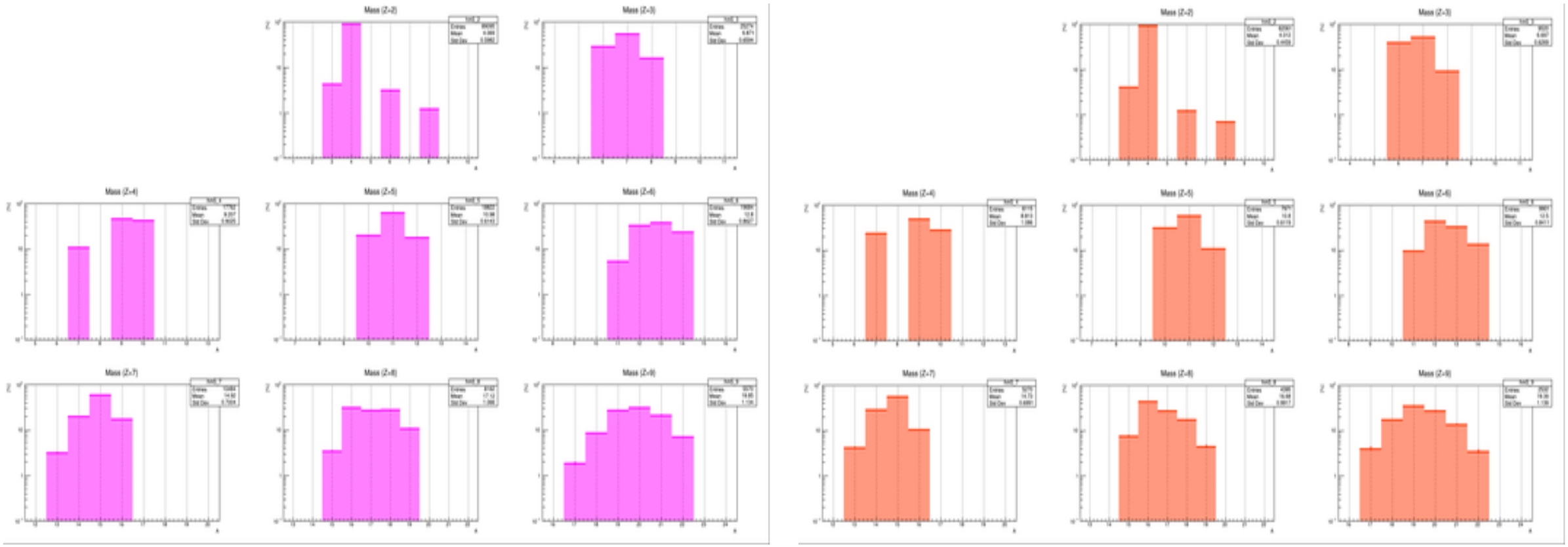


Part of Cristina Zagami's PhD work at UNICT

# Charge identification

"neutron rich"
$^{124}Sn+^{64}Ni$
@ 20 AMeV

"isobaric"
$^{124}Xe+^{64}Zn$
@ 20 AMeV

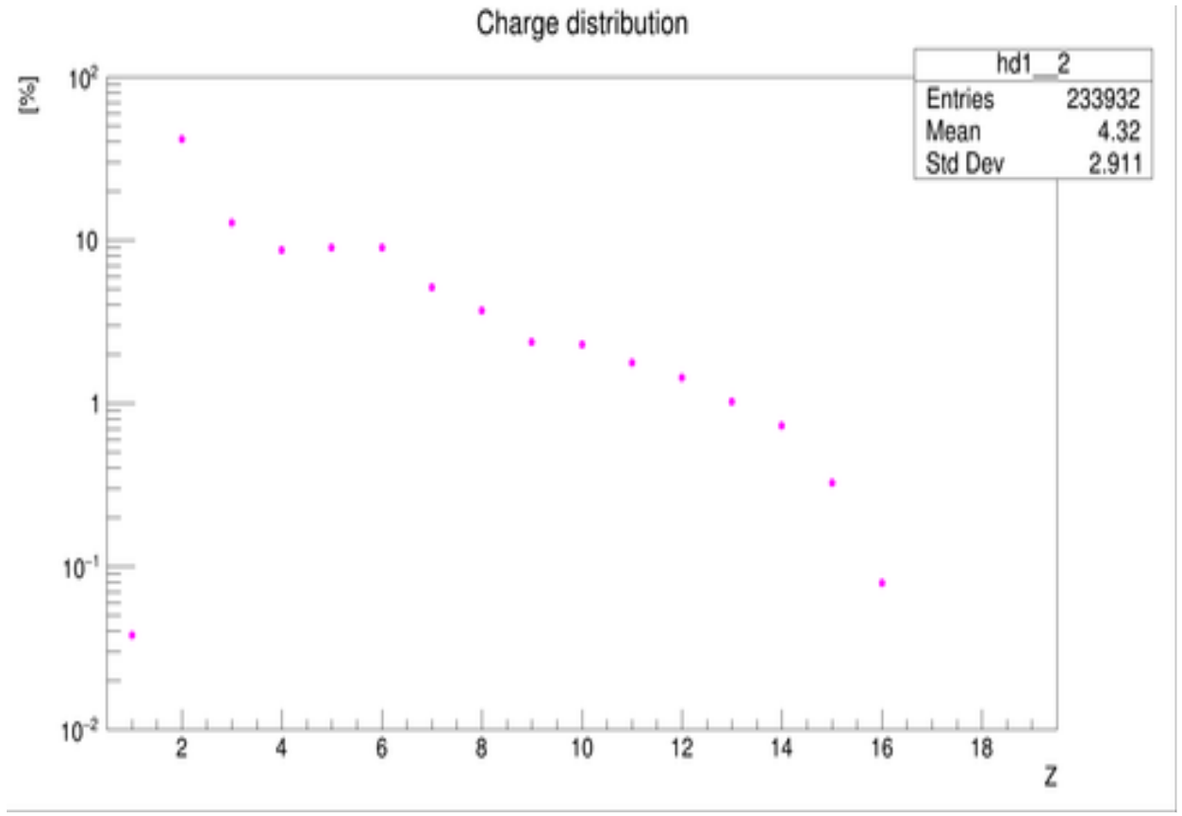


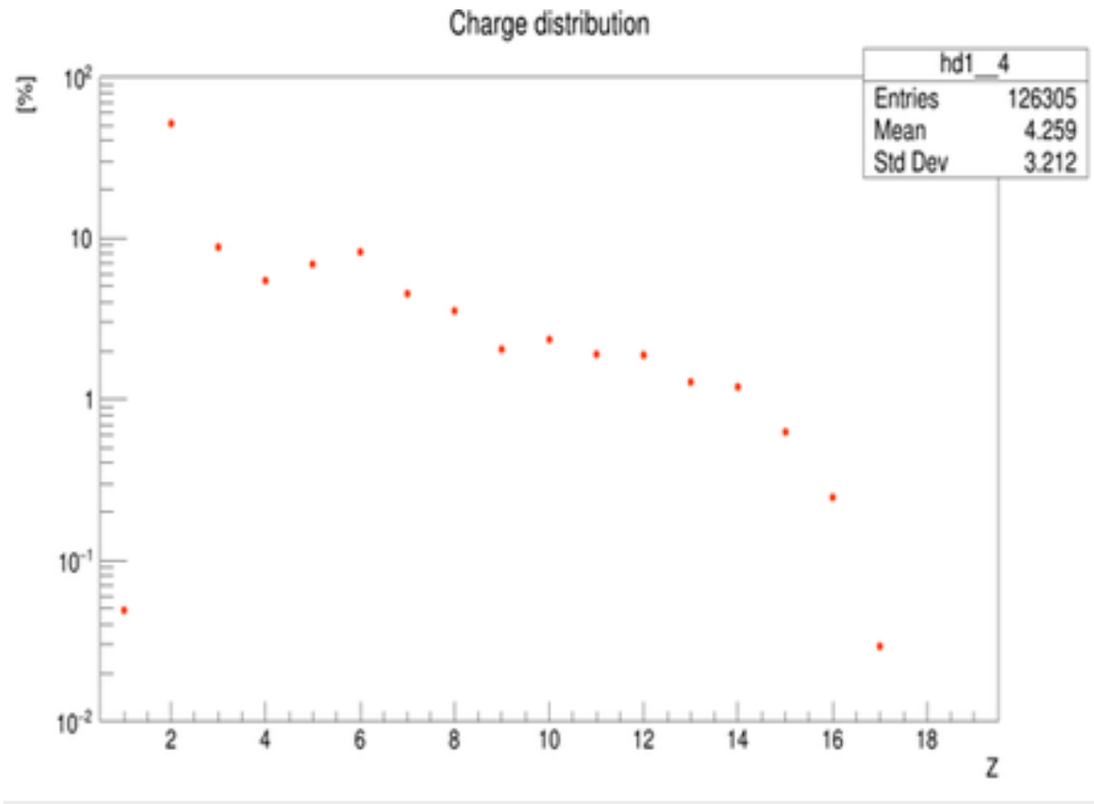


Part of Cristina Zagami's PhD work at UNICT

# Preliminary Comparisons

**$^{124}$Xe + $^{64}$Zn "Isobaric"**

**$^{112}$Sn + $^{58}$Ni "n-poor"**

**$^{124}$Sn + $^{64}$Ni "n-rich"**

Part of Cristina Zagami's PhD work at UNICT

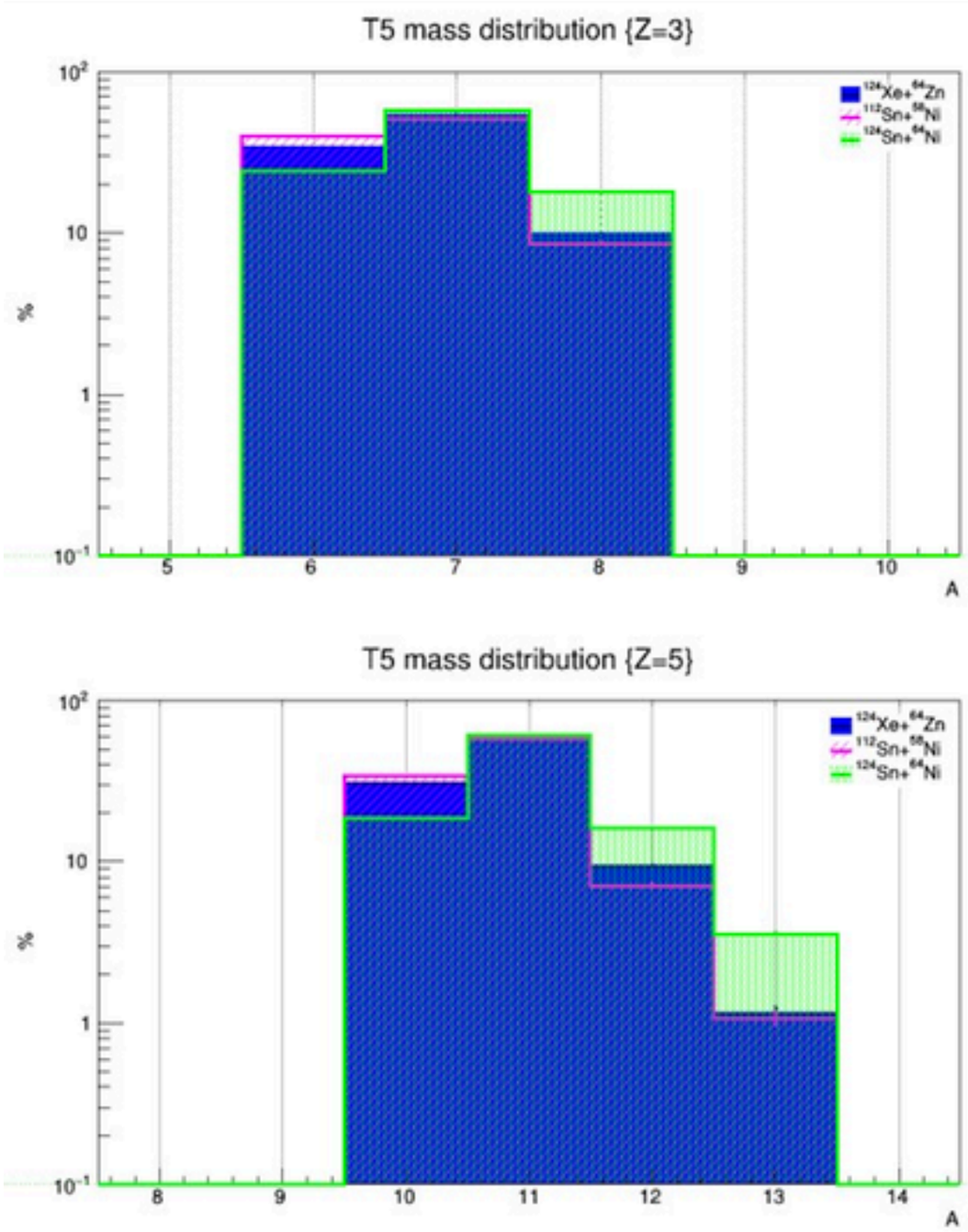

# First preliminary results of CHIMERA*

Binary events M=2 A>6

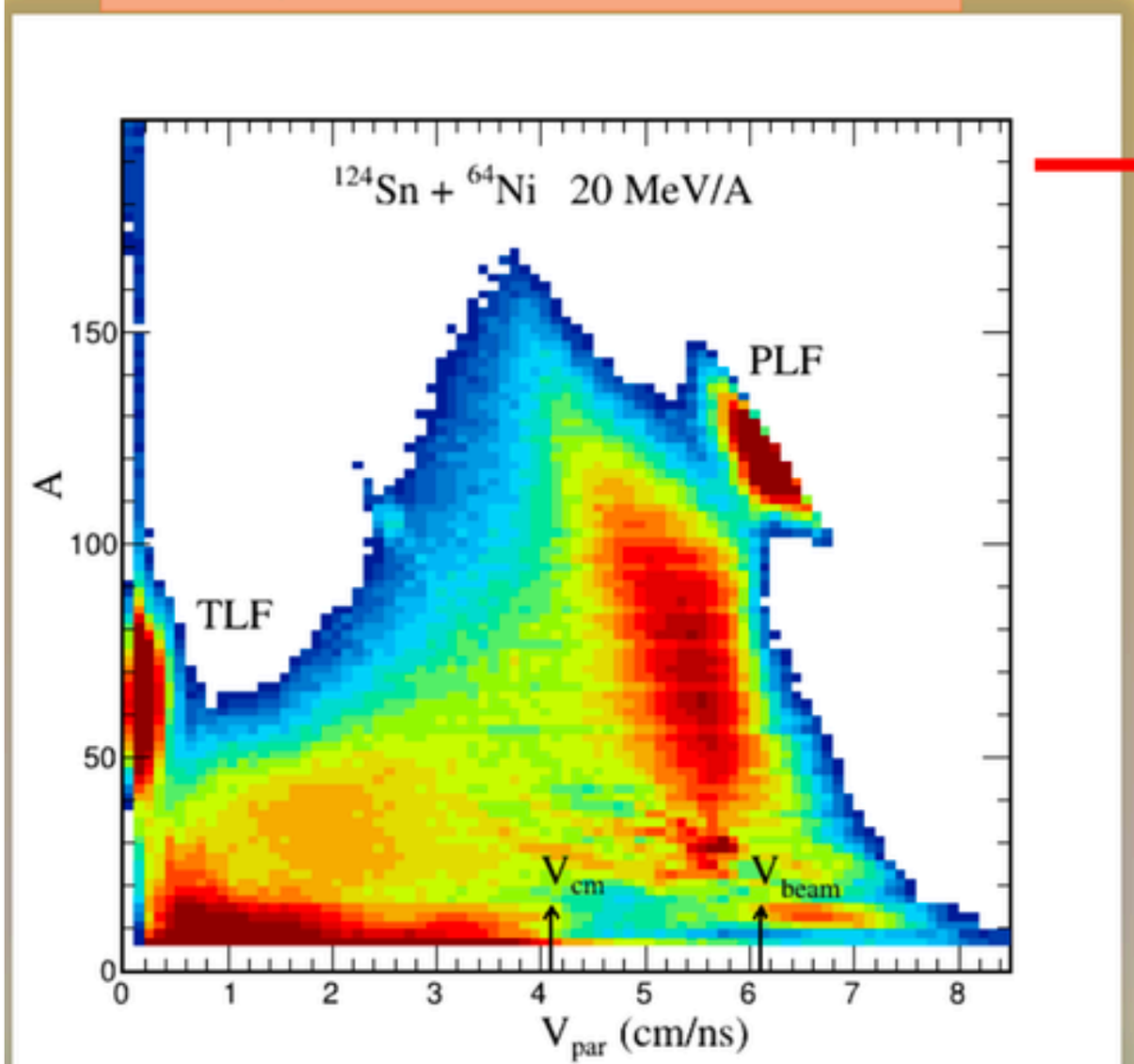


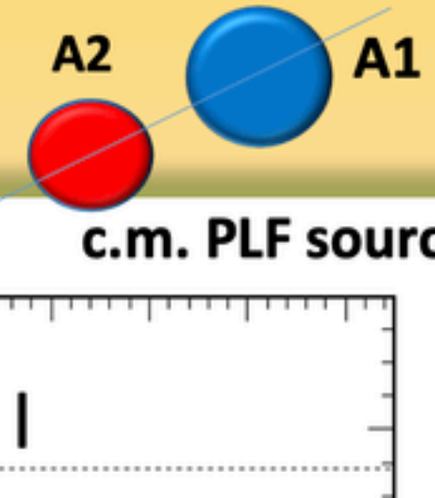


c.m. PLF source

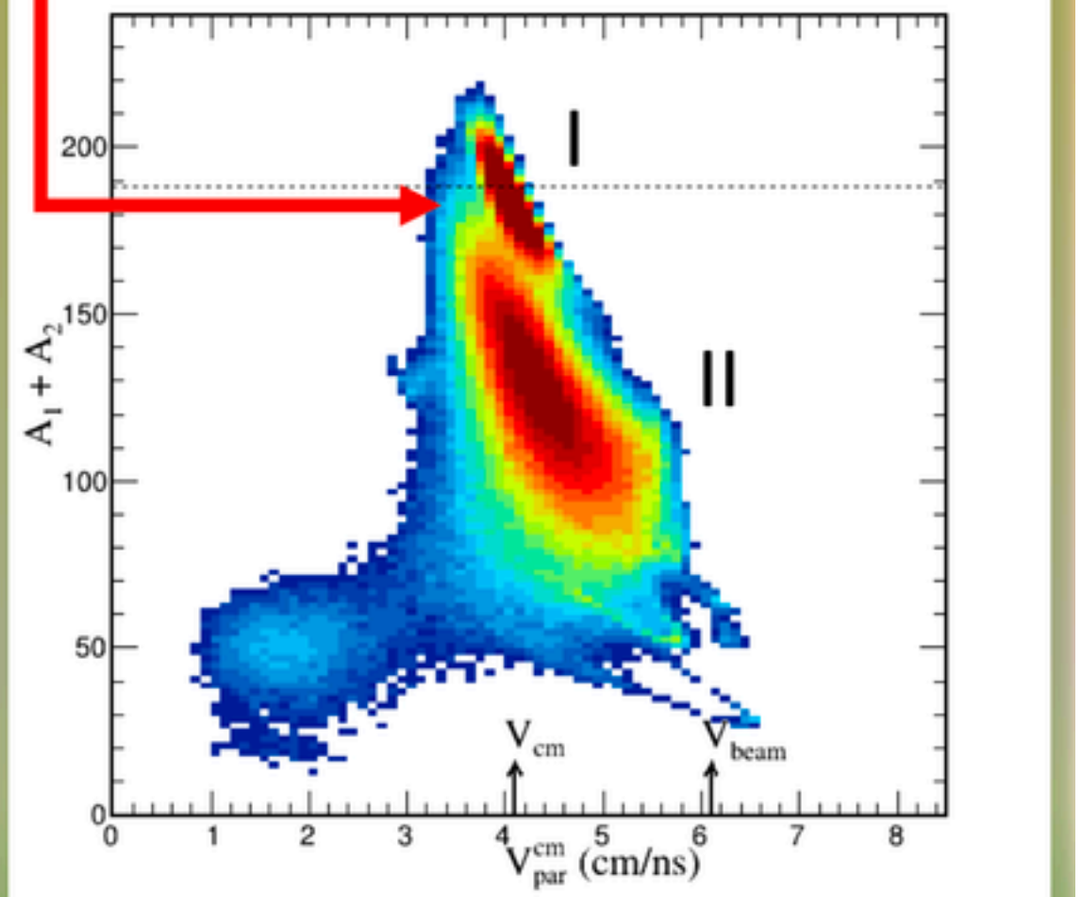


*CHIMERA data and FARCOS data are not yet merged

# First preliminary results of CHIMERA

## Total kinetic energy analysis

TKE vs. HF deflection angle

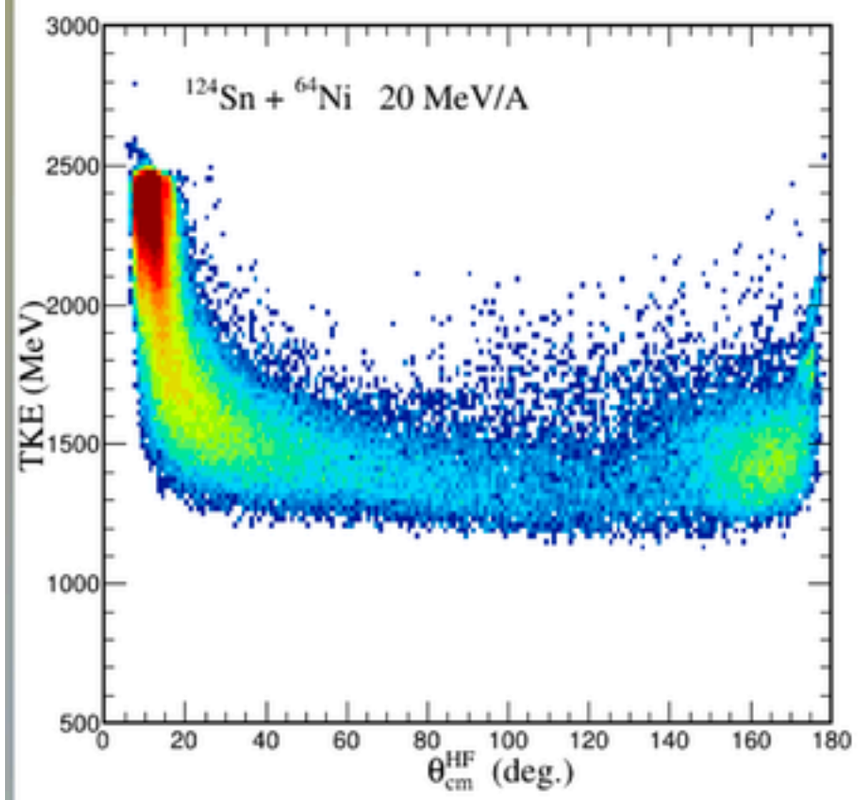


From QE scattering

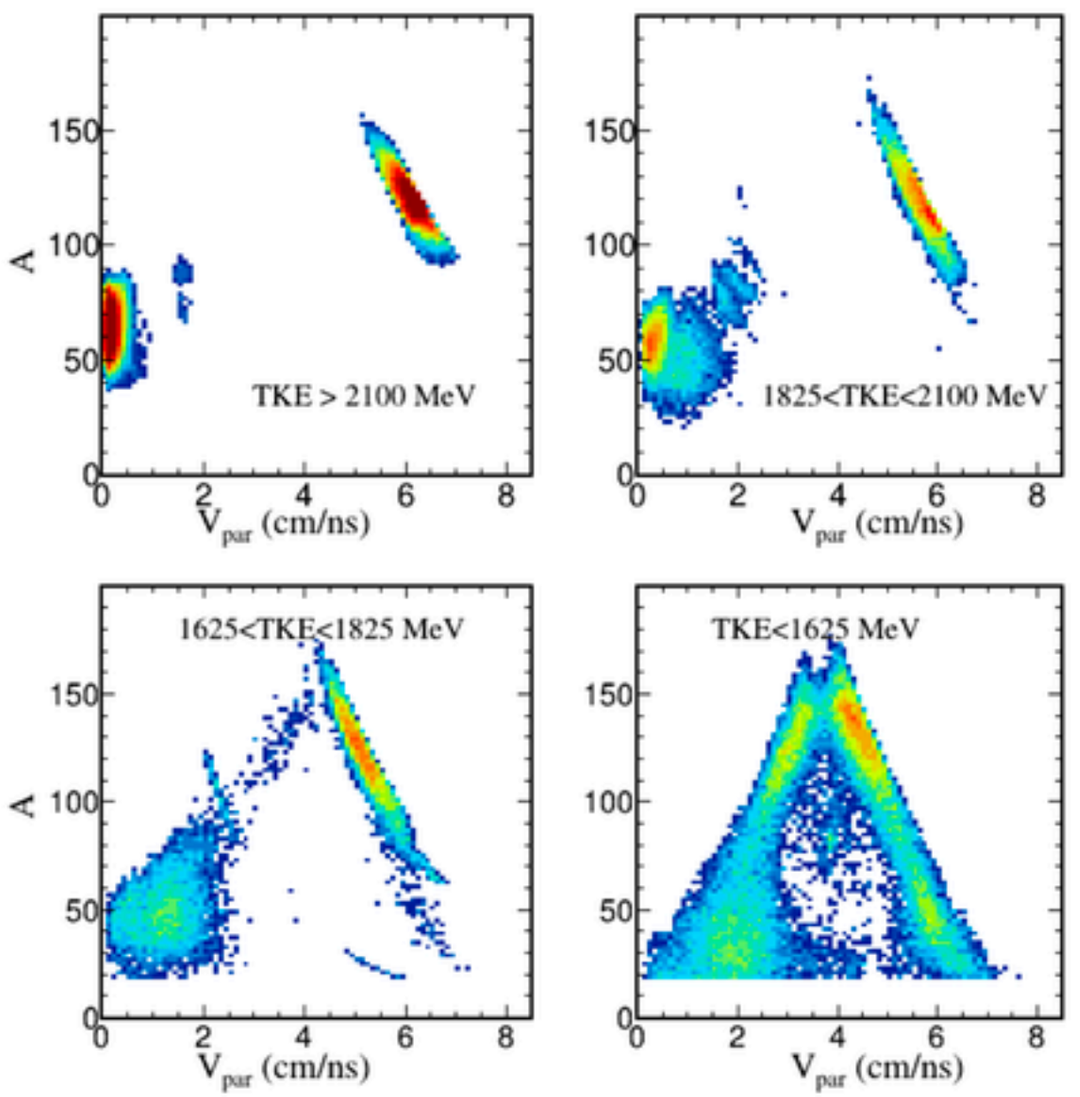


To Fusion-Fission reactions

# First preliminary results of CHIMERA

## PLF break-up

**$^{124}$Sn + $^{64}$Ni @20 MeV/A**

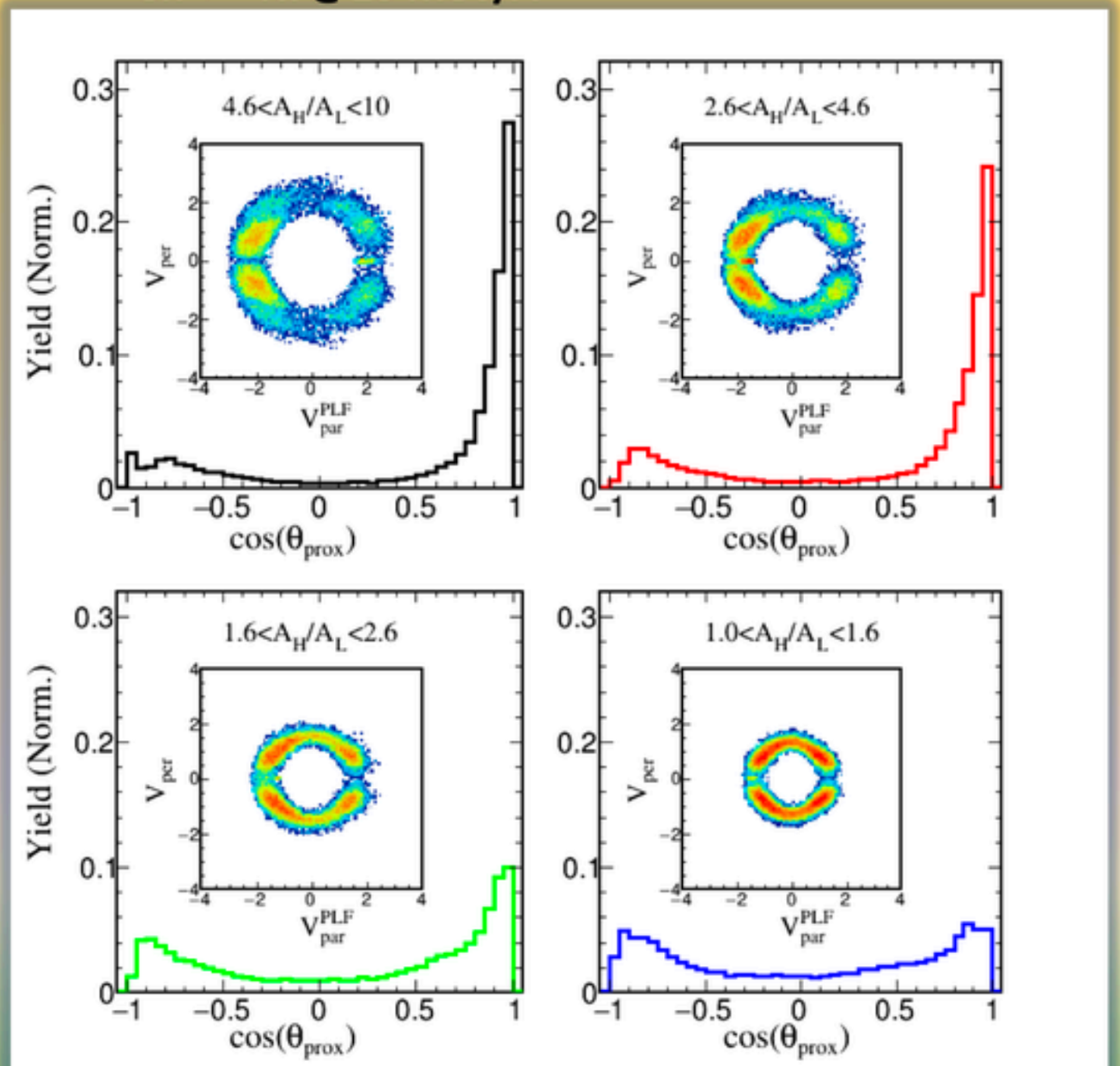


Several conditions to select «good» PLF break-up events. For example

1) 100<AH+AL<134
2) Vpar>2.15 cm/ns (TLF reject)
3) disentangle from fusion-fission reactions

etc, etc

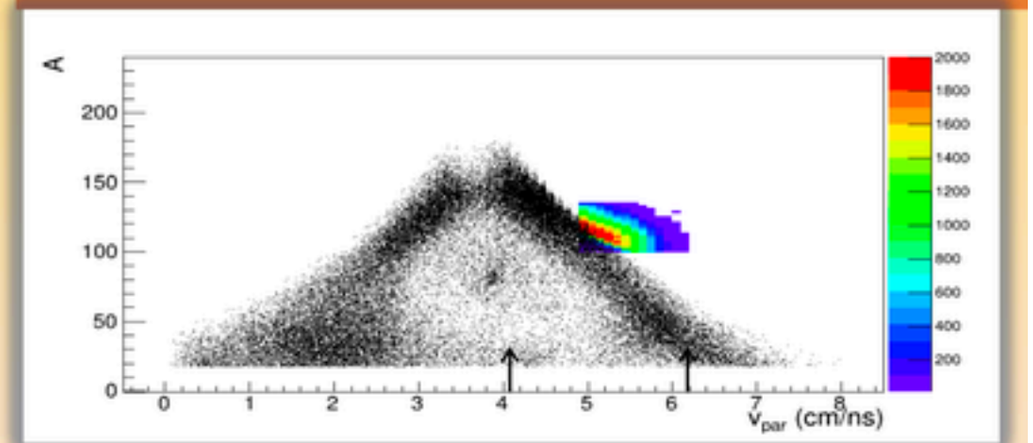


| | Dynamical emission (%) | |
|---|---|---|
| $A_H/A_L$ | $^{124}$Sn+$^{64}$Ni | $^{124}$Sn+$^{64}$Zn |
| 4.6–10 | 52 | 45 |
| 2.6–4.6 | 48 | 43 |
| 1.6–2.6 | 22 | 18 |
| 1.0–1.6 | 5 | 4 |

Very preliminary results but promising for next step data analysis

# New project:
# NArCoS (Neutron Array for Correlation Studies)
# IDEA

**To realize a prototype of detector able to detect at the same time charged particles and neutrons with high energy and angular resolution for reaction studies and applications**

- Candidate: The plastic scintillator EJ276-Green Type (ex EJ299-33) (3x3x3cm$^3$)
- 1 cluster: 4 consecutively cubes -> 3x3x12 cm$^3$
- Reading the light signal: Si-PM and digitalization
- Modular, reconfigurable (in mechanic and electronic)
- Discrimination of n/γ from PSD (but also light charged particles)
- Energy measurement from ToF ($\Delta t \leq 1$ ns with $L_{ToF} \approx 1 \div 1.5$m)
  TOF measured using the RF of the CS or with an ancillary MCP (low intensity exotic beams)

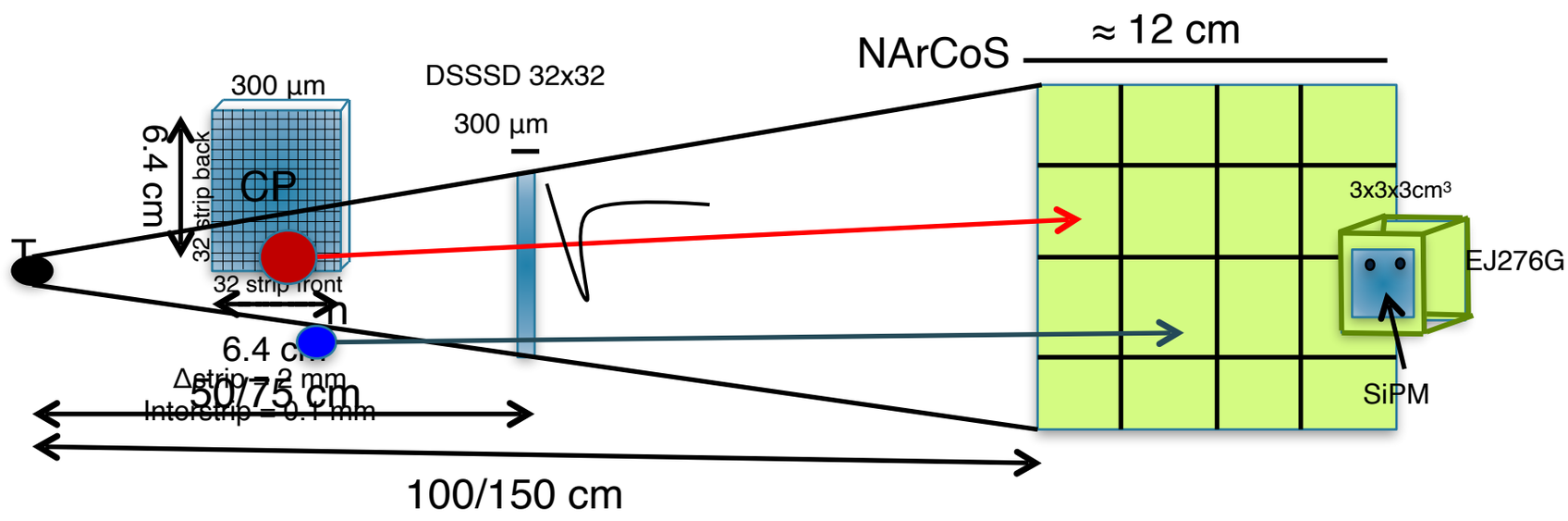

# NArCoS (Neutron Array for Correlation Studies)

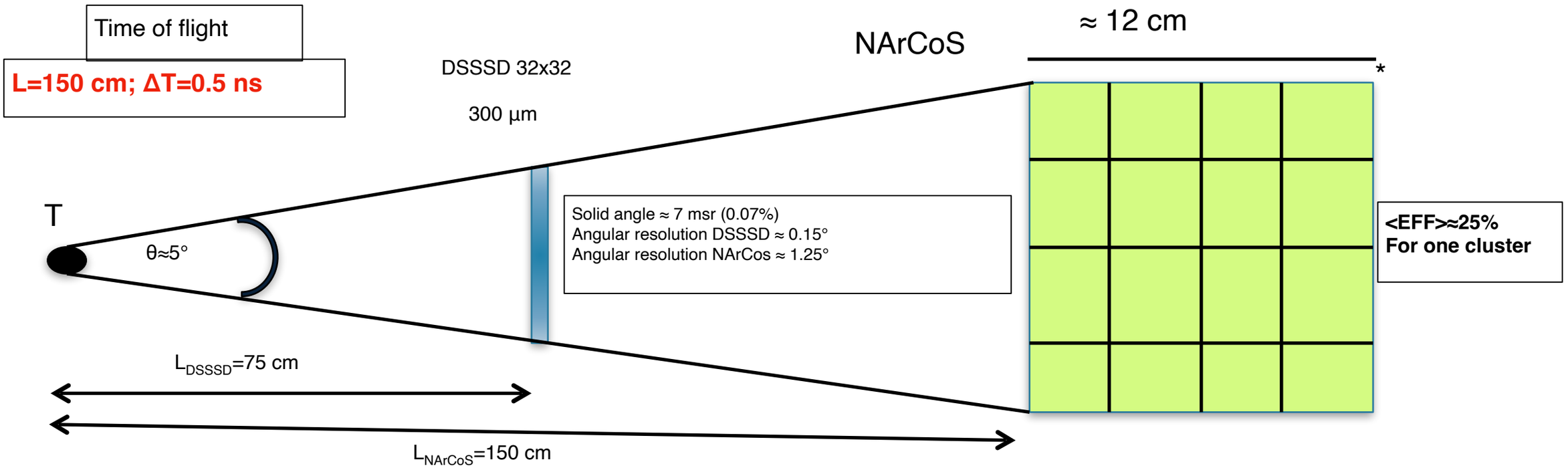


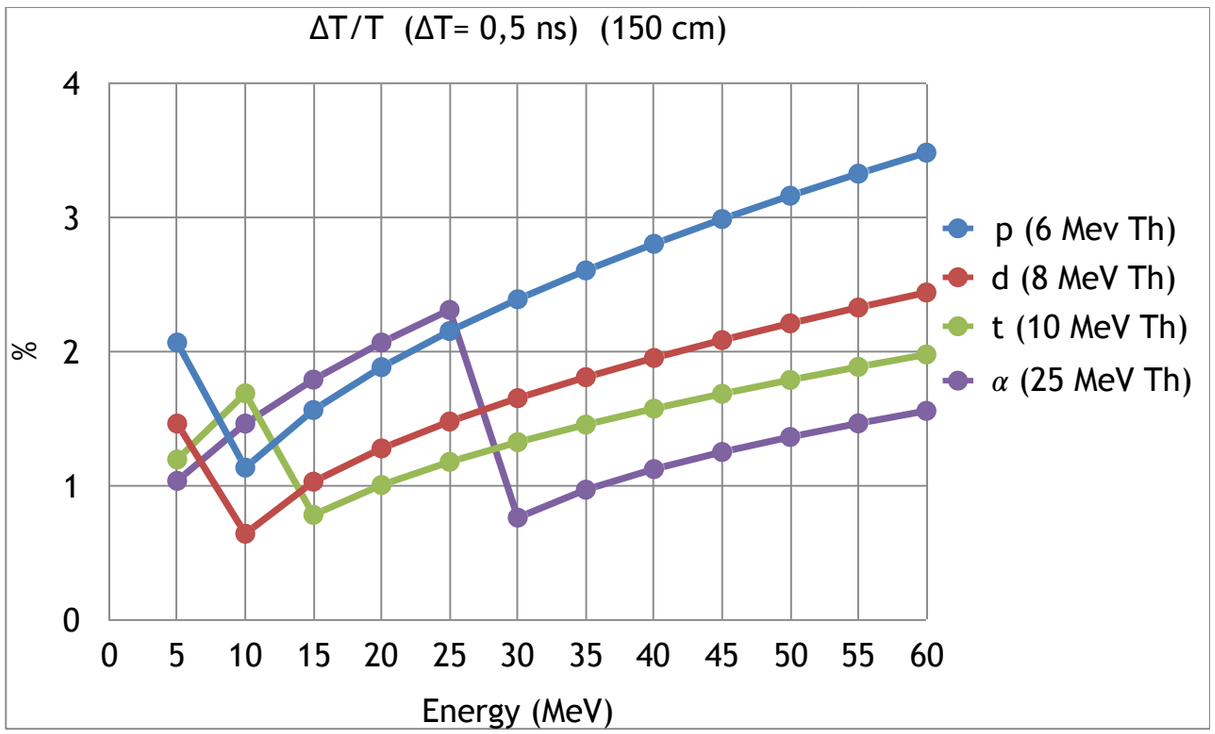


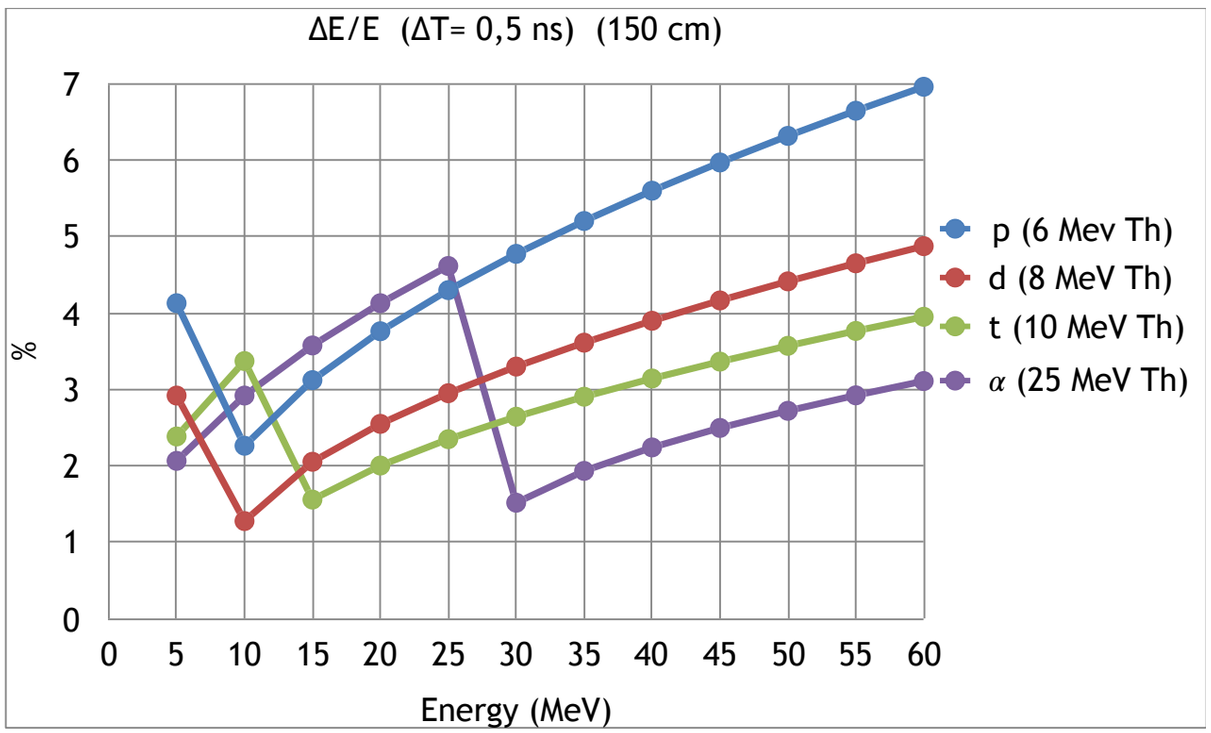

# NArCoS (Neutron Array for Correlation Studies)

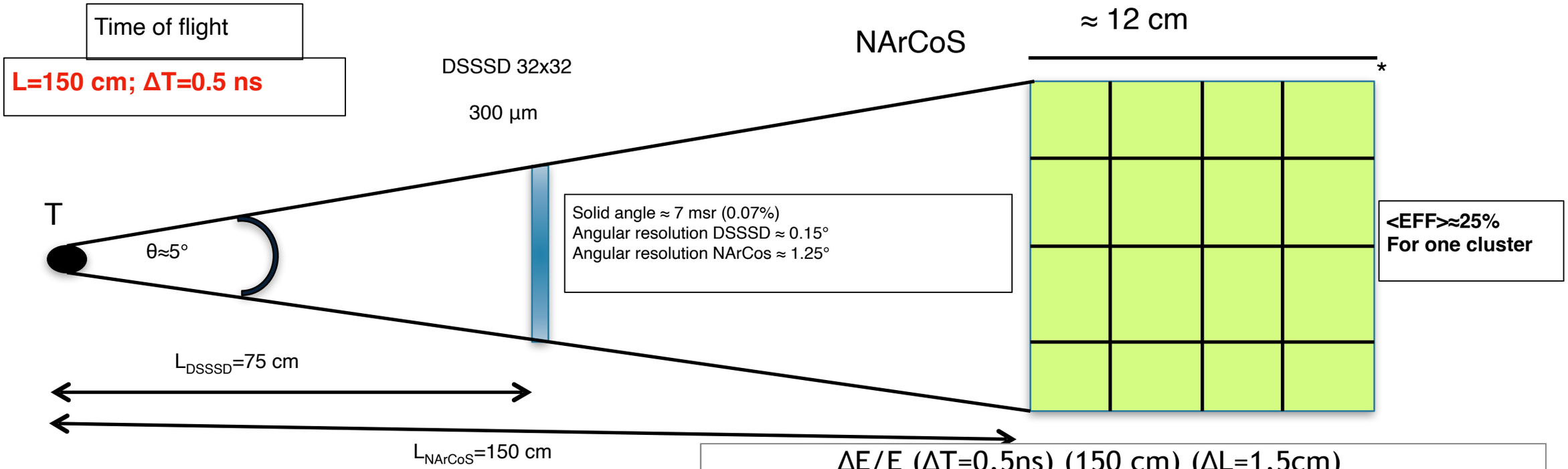


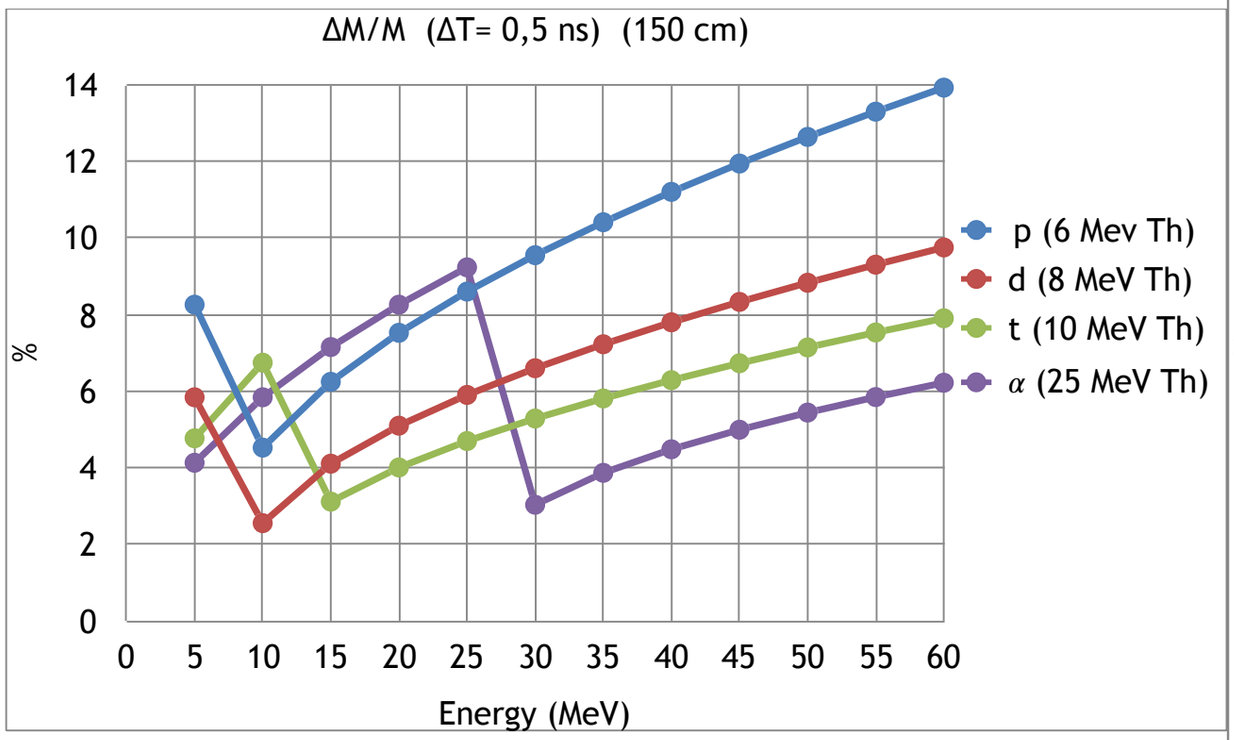


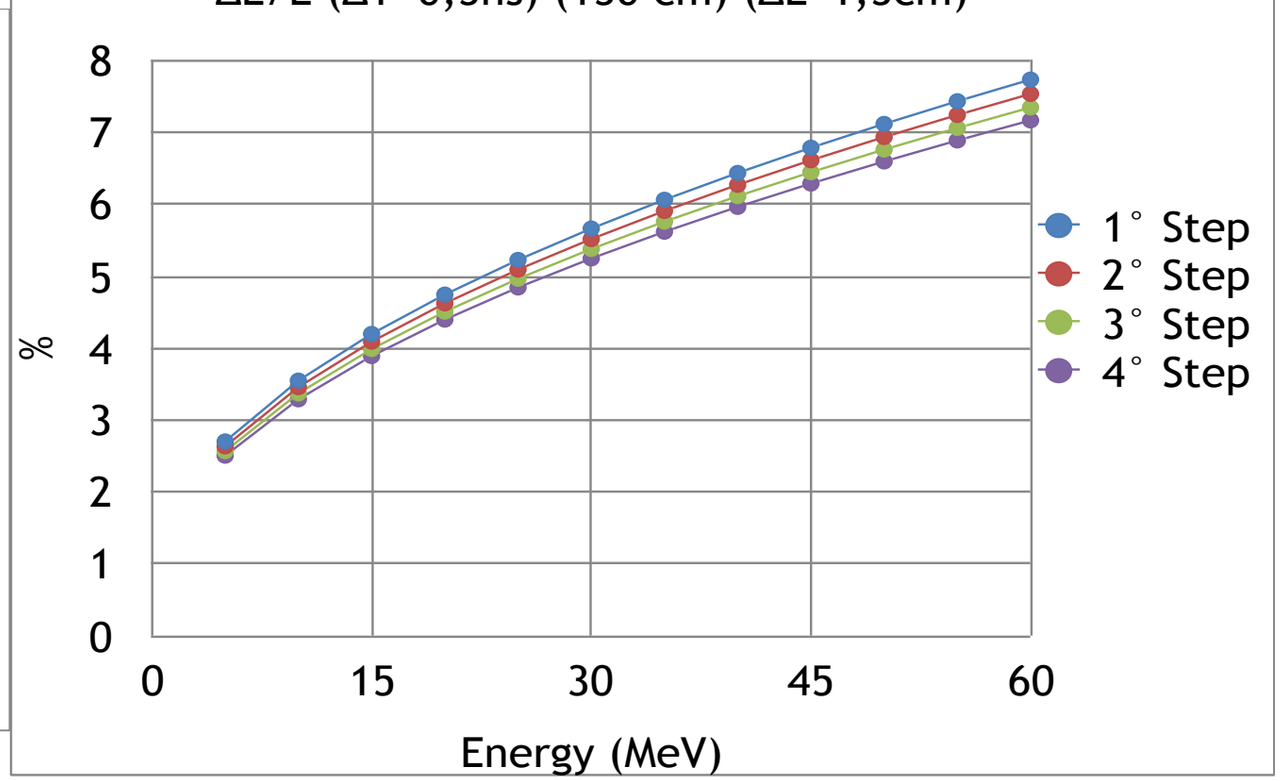

# What about the neutron detection efficiency?

## GEANT 4 simulation in order to estimate the neutron detection efficiency

**Mean value for one detection cell (3x3x3 cm$^3$) ≅ 9%**

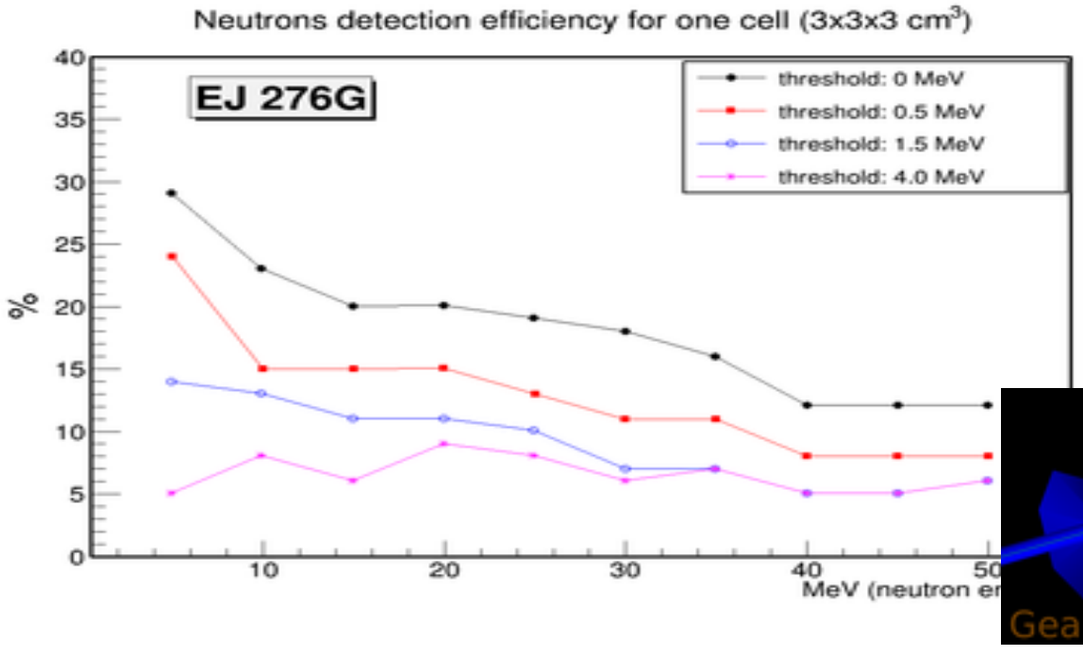


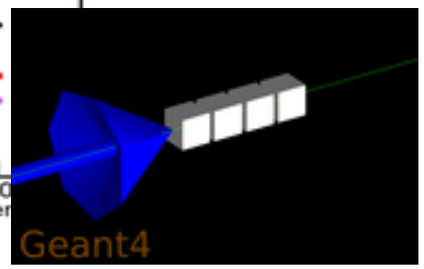


**Mean value for one detection cluster (3x3x12 cm$^3$) ≅ 25%**

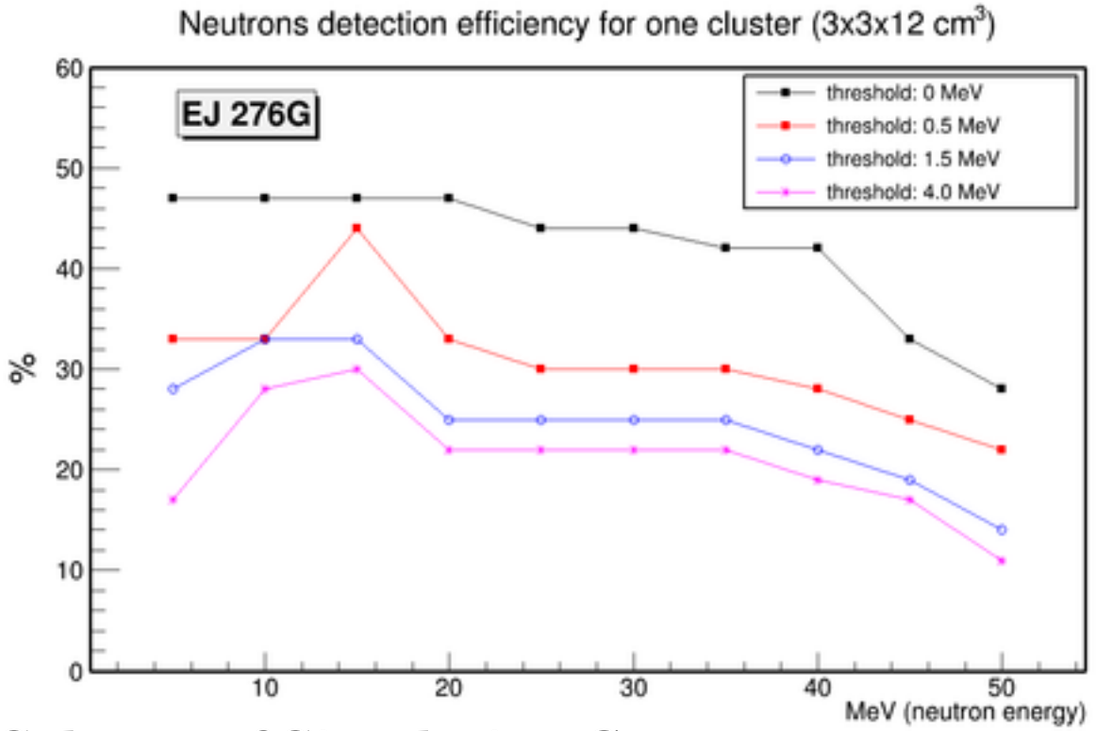


**Mean value for a 36-cell array (9x9x12 cm$^3$) ≅ 33%**

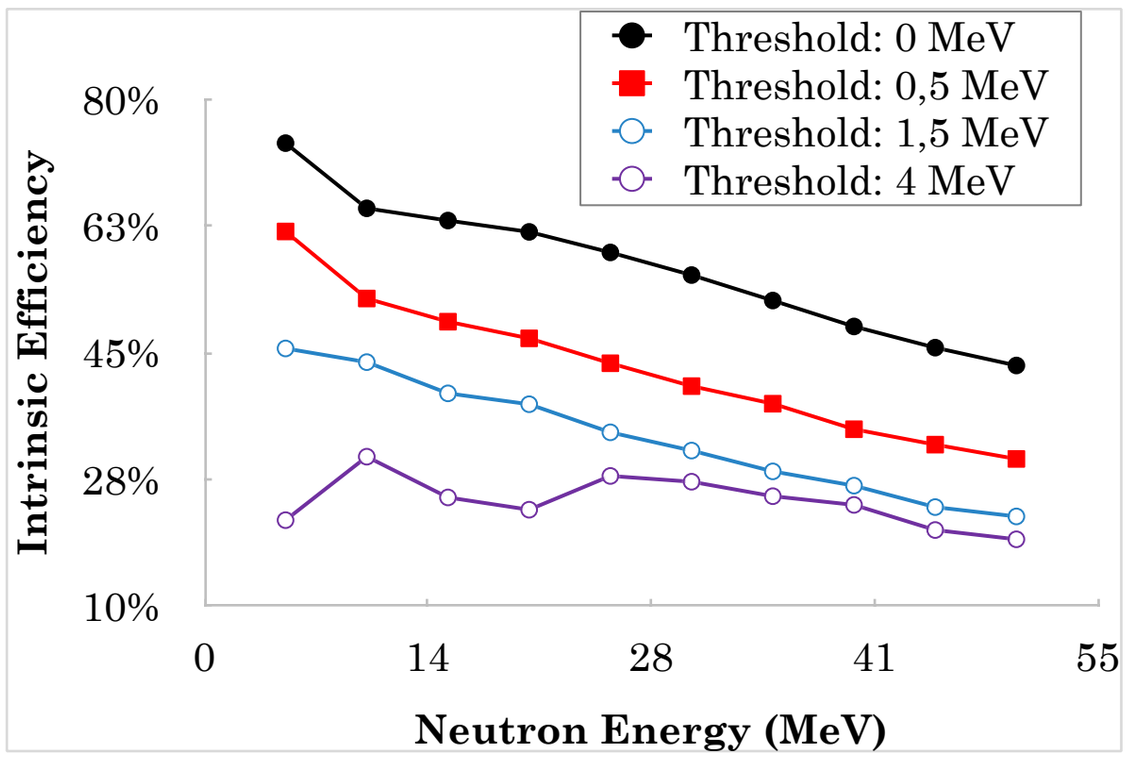


**Scheme of Simulation Geometry:**

36 (3 x 3 x 4) cell array

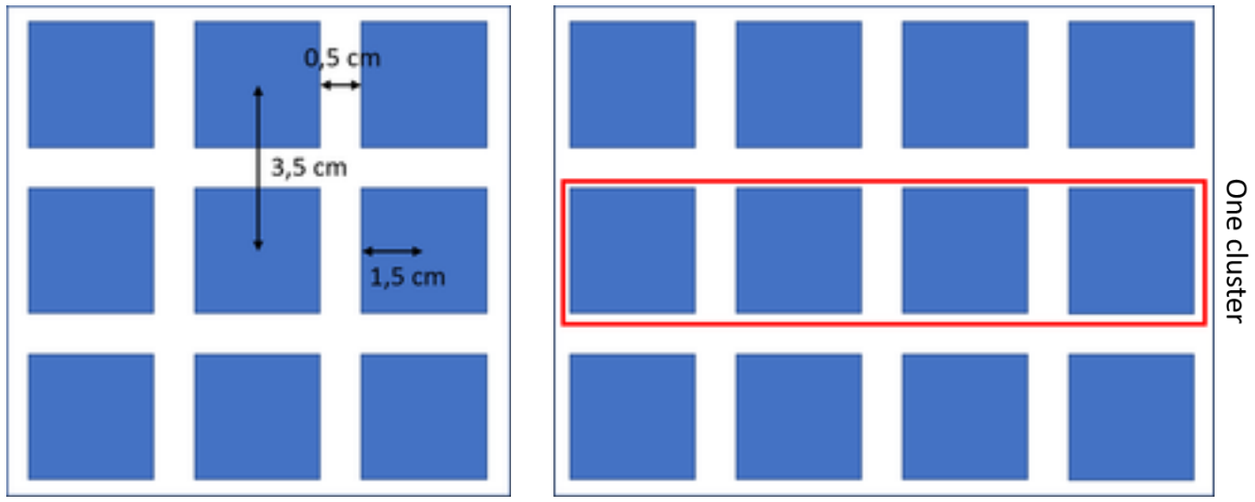

# Latest resuls: tests by using the SiPM (i-Spector CAEN)

**The test was done during the master thesis work of A. Simancas in Catania (EVP tutor)**

- **Detector Configurations:**
  - EJ-276G + PMT
  - EJ-276 + i-Spector
  - EJ-276G + i-Spector
- **Lab measurements with radioactive sources:**
  - Vacuum Chamber
  - Pb shield
  - Gamma sources: $^{133}$Ba, $^{137}$Cs, $^{60}$Co, $^{152}$Eu
  - Alpha source: $^{241}$Am
  - Digitizer from CAEN
- **Data analysis of heavy ion reactions:**
  - CHIMERA scattering chamber (LNS)
  - Detector at 11° in lab frame
  - Beam: $^{124}$Sn at 20 MeV/A (CHIFAR experiment)
  - Targets: $^{64}$Zn and $^{64}$Ni
  - GET digital electronics

E.V.Pagano, G. Politi, A. Simancas et al., in preparation

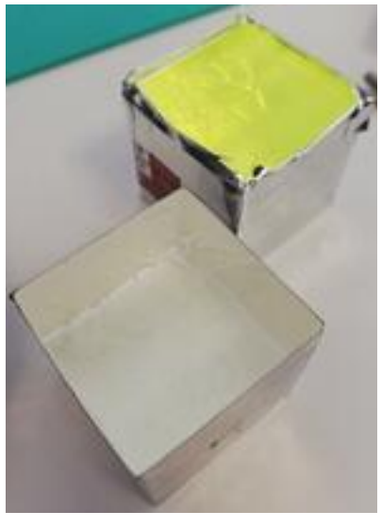

i-Spector from CAEN (3x3 cm SiPM and electronics)

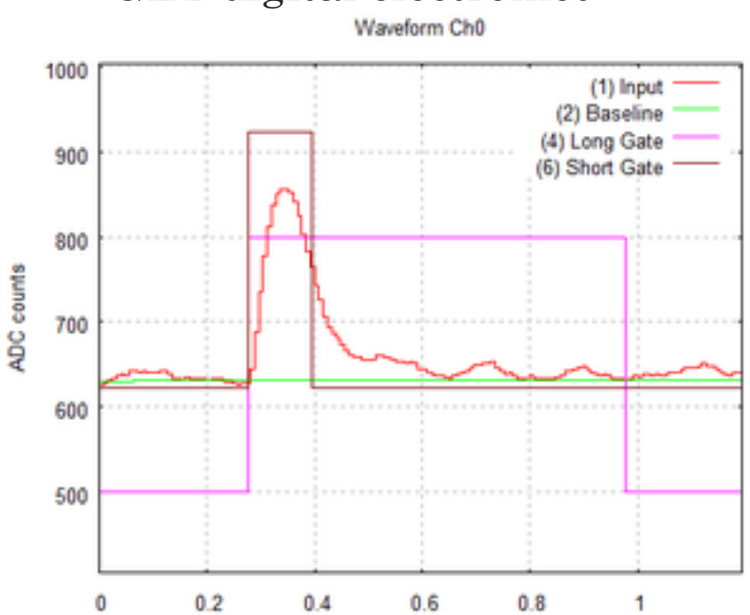


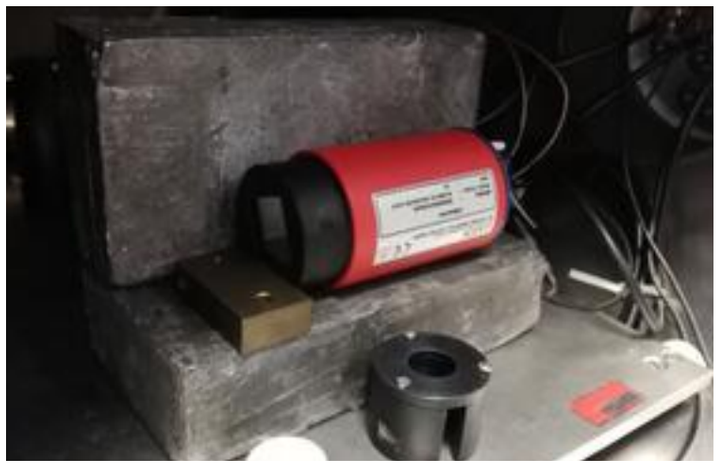

**Example of signal and integration windows**

# PSD studies using sources

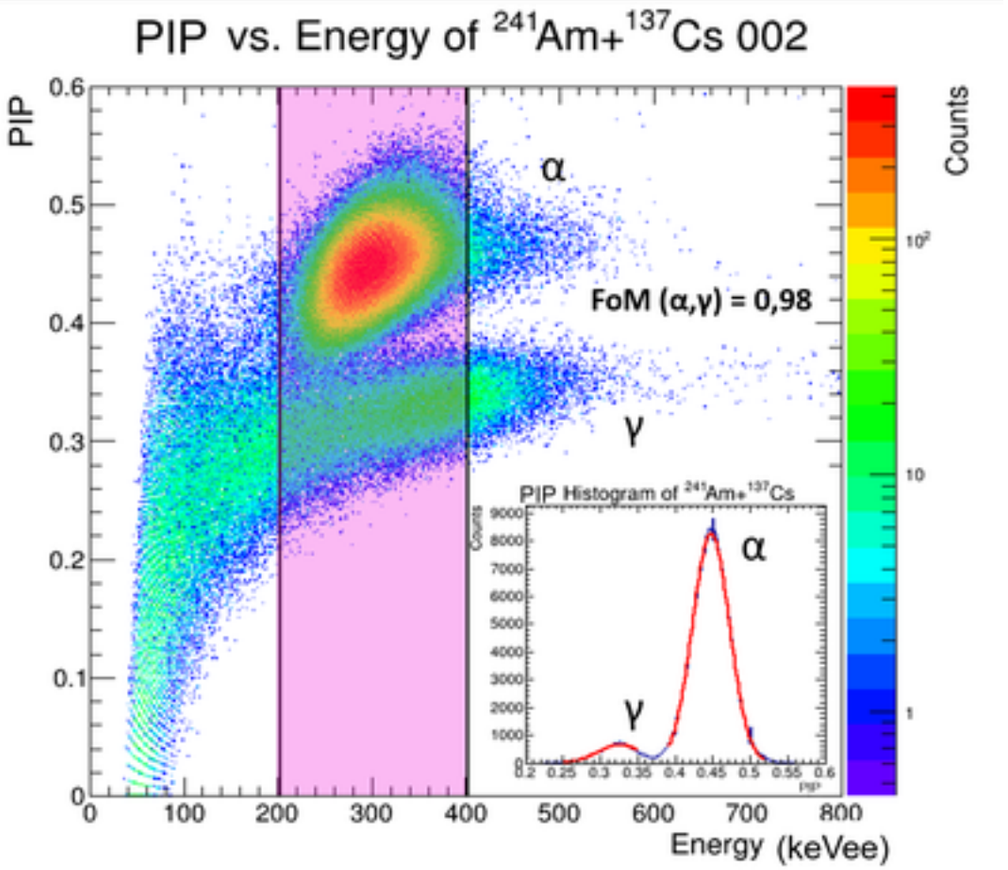


**EJ-276 + i-Spector**

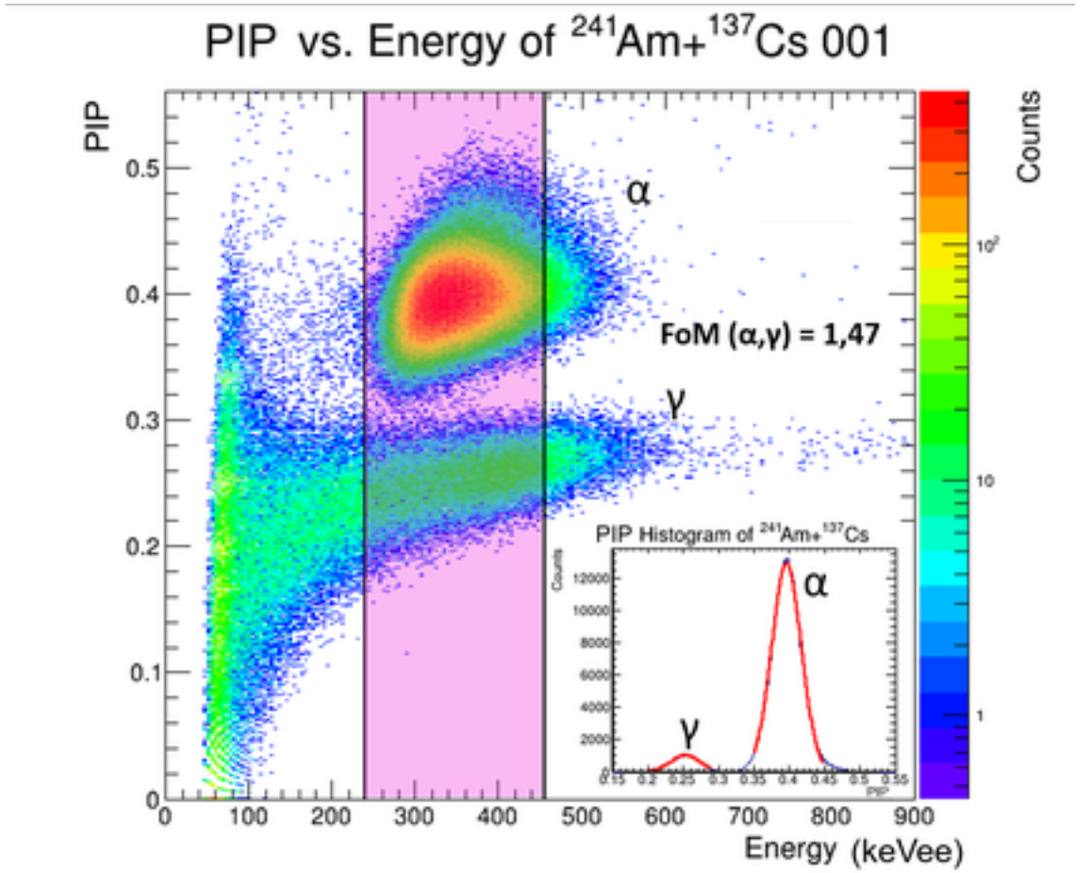


**EJ-276G + i-Spector**

| Detector | FoM |
|---|---|
| i-Spector + EJ-276 | 0.98 |
| i-Spector + EJ-276G | 1.47 |
| PMT + EJ-276G | 1.03 |

# PSD studies using beams

## CHIFAR exp @lns (spokesperson:EVP, E. De Filippo, P. Russotto)

**EJ-276 + i-Spector**

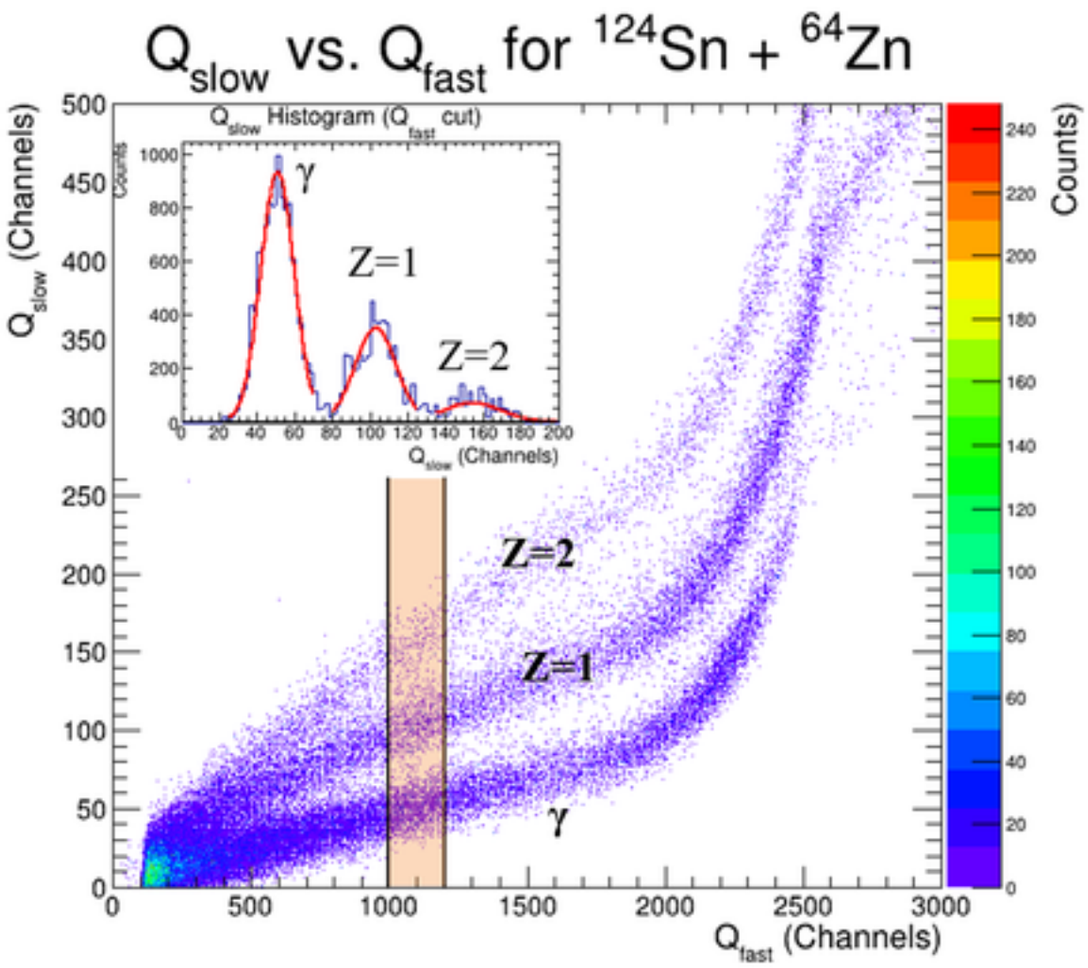


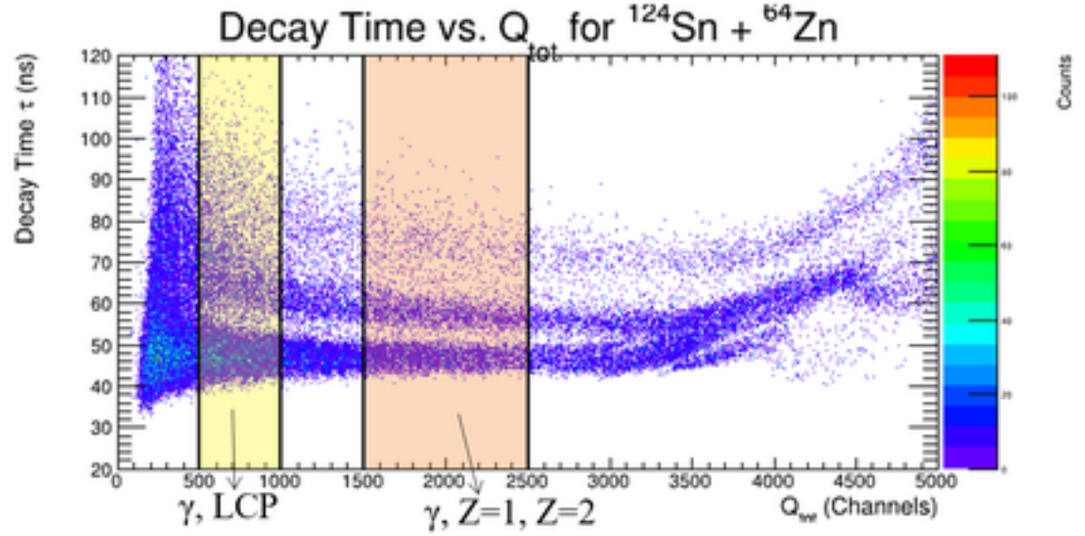


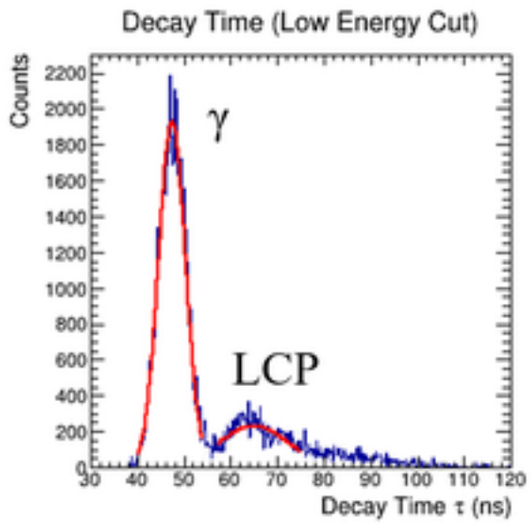


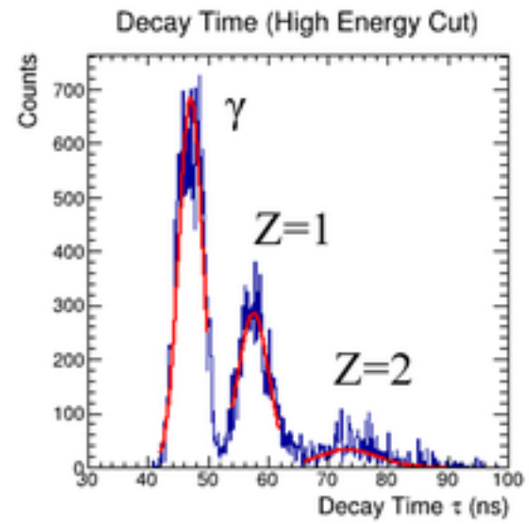


| PSD Method | FoM(γ, Z=1) | FoM(Z=1, Z=2) | FoM(γ, LCP) |
|---|---|---|---|
| Integration | 1.08 | 0.78 | - |
| Decay Time | 0.95 | 0.87 | 0.71 |

**LCP = Light Charged Particles**
**Neutrons included in Z=1**

For the “decay time” technique see: E. V. Pagano et al. NIM A 905 (2018) 47-52

# New opportunities at LNS

**FRAISE: a new FRAgment In-flight SEparator**
**Approved inside POTLNS PON** ≈20M€

## The idea in order to increase the beam intensity

### *A new extraction beam line for the INFN-LNS CS*

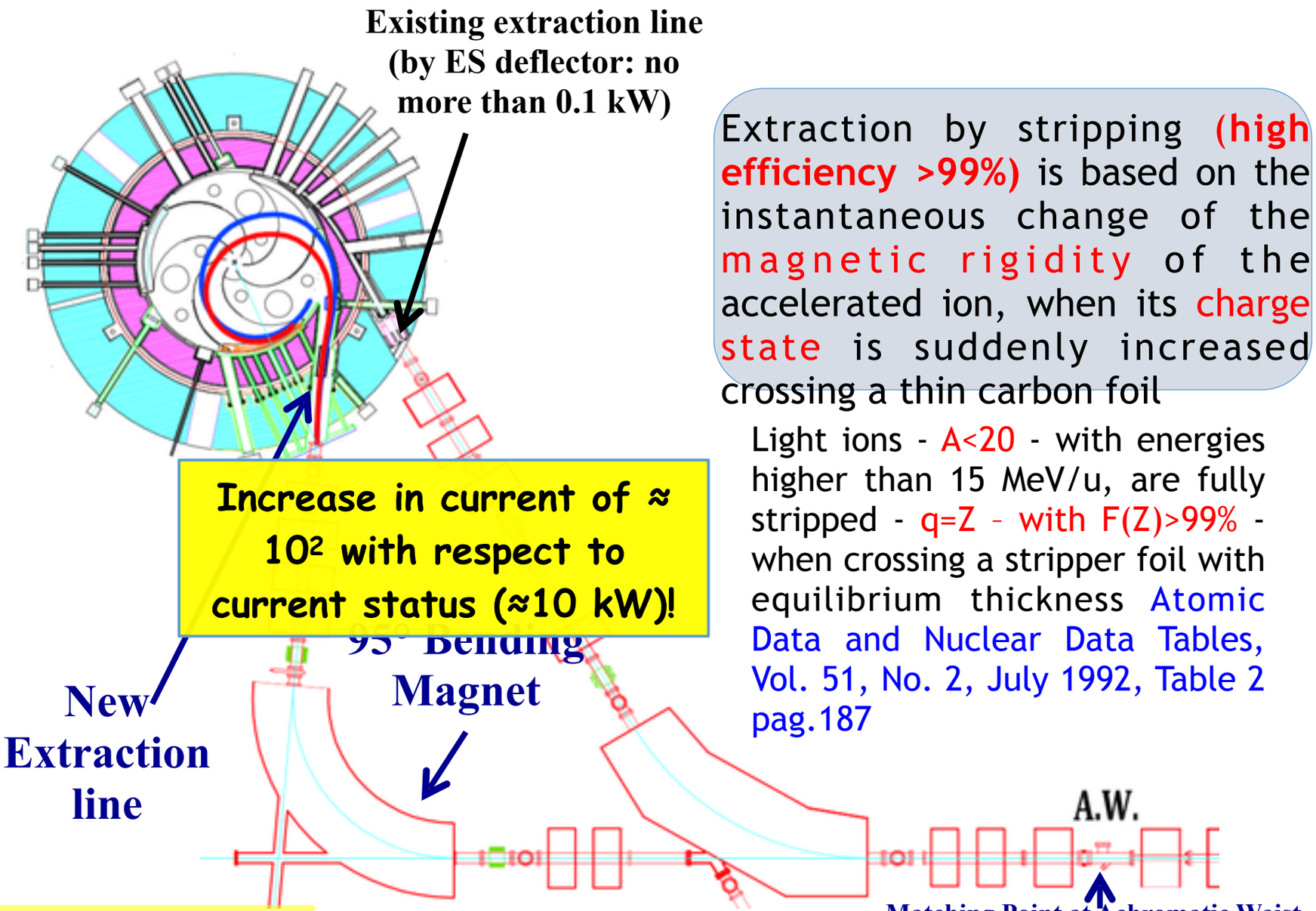


Courtesy by D. Rifuggiato
HIB@LNS 2015

Extraction by stripping **(high efficiency >99%)** is based on the instantaneous change of the magnetic rigidity of the accelerated ion, when its charge state is suddenly increased crossing a thin carbon foil

Light ions - A<20 - with energies higher than 15 MeV/u, are fully stripped - q=Z – with F(Z)>99% - when crossing a stripper foil with equilibrium thickness Atomic Data and Nuclear Data Tables, Vol. 51, No. 2, July 1992, Table 2 pag.187

# FRAISE: a new FRAgment In-flight SEparator
## Approved inside POTLNS PON

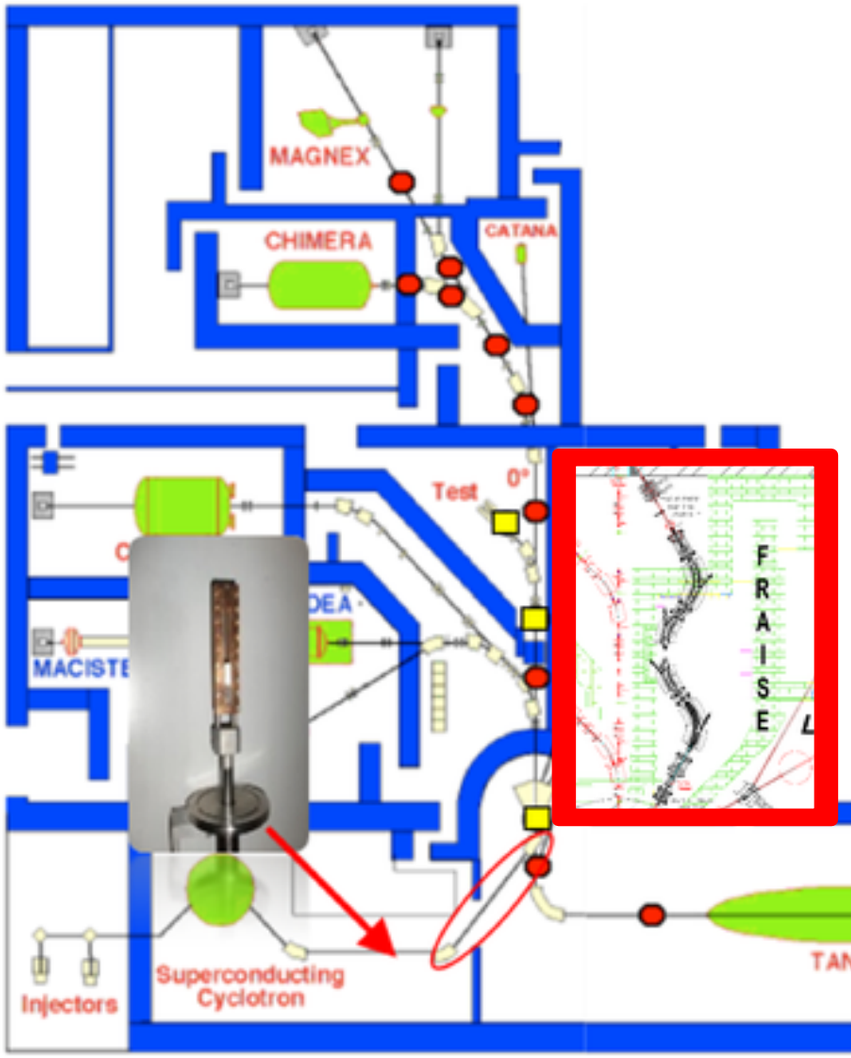


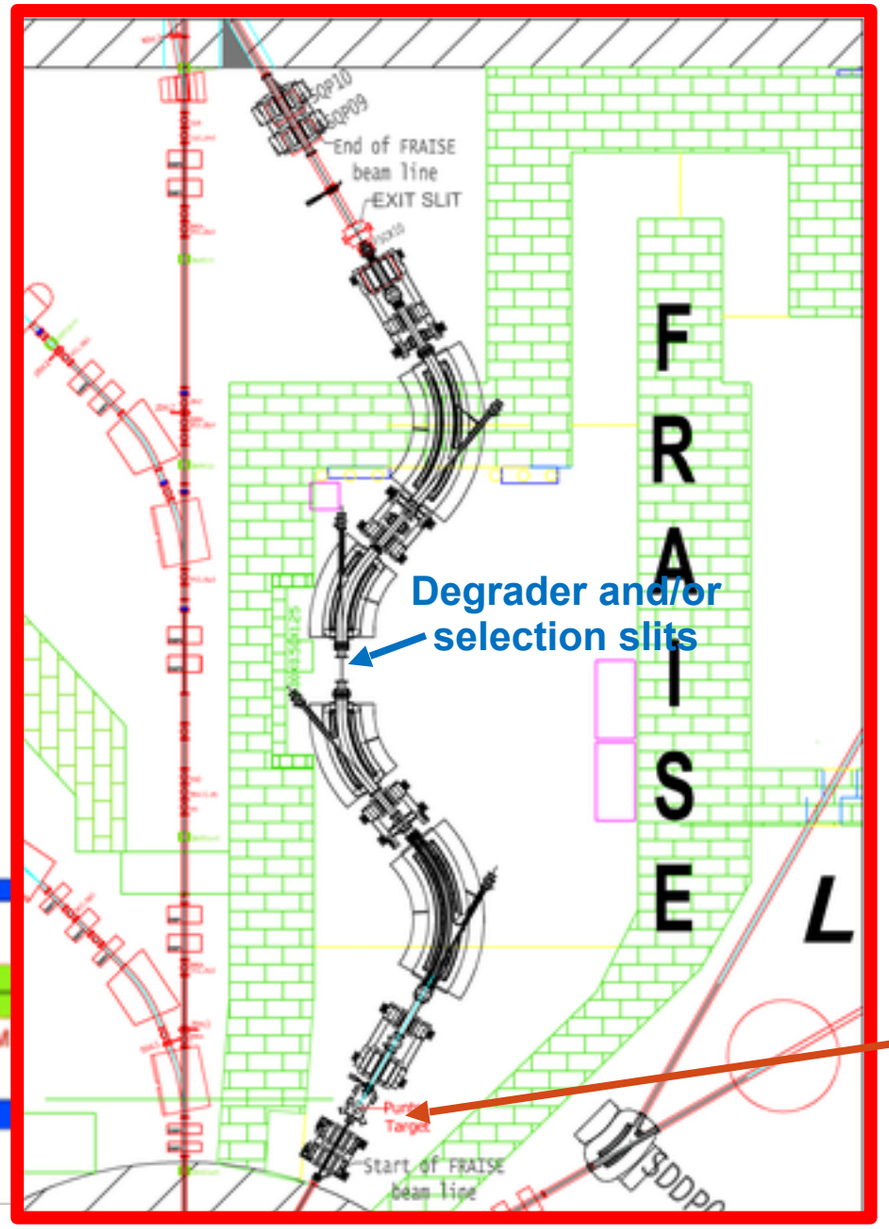


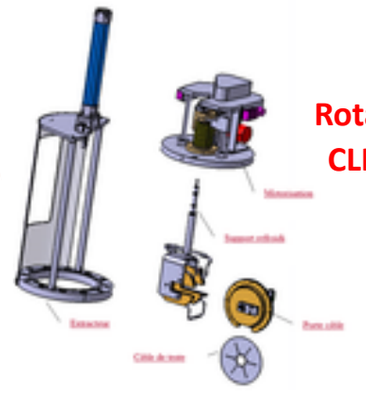

Rotating Target
CLIM (GANIL)

# FRAISE: a new FRAgment In-flight SEparator
## Approved inside POTLNS PON

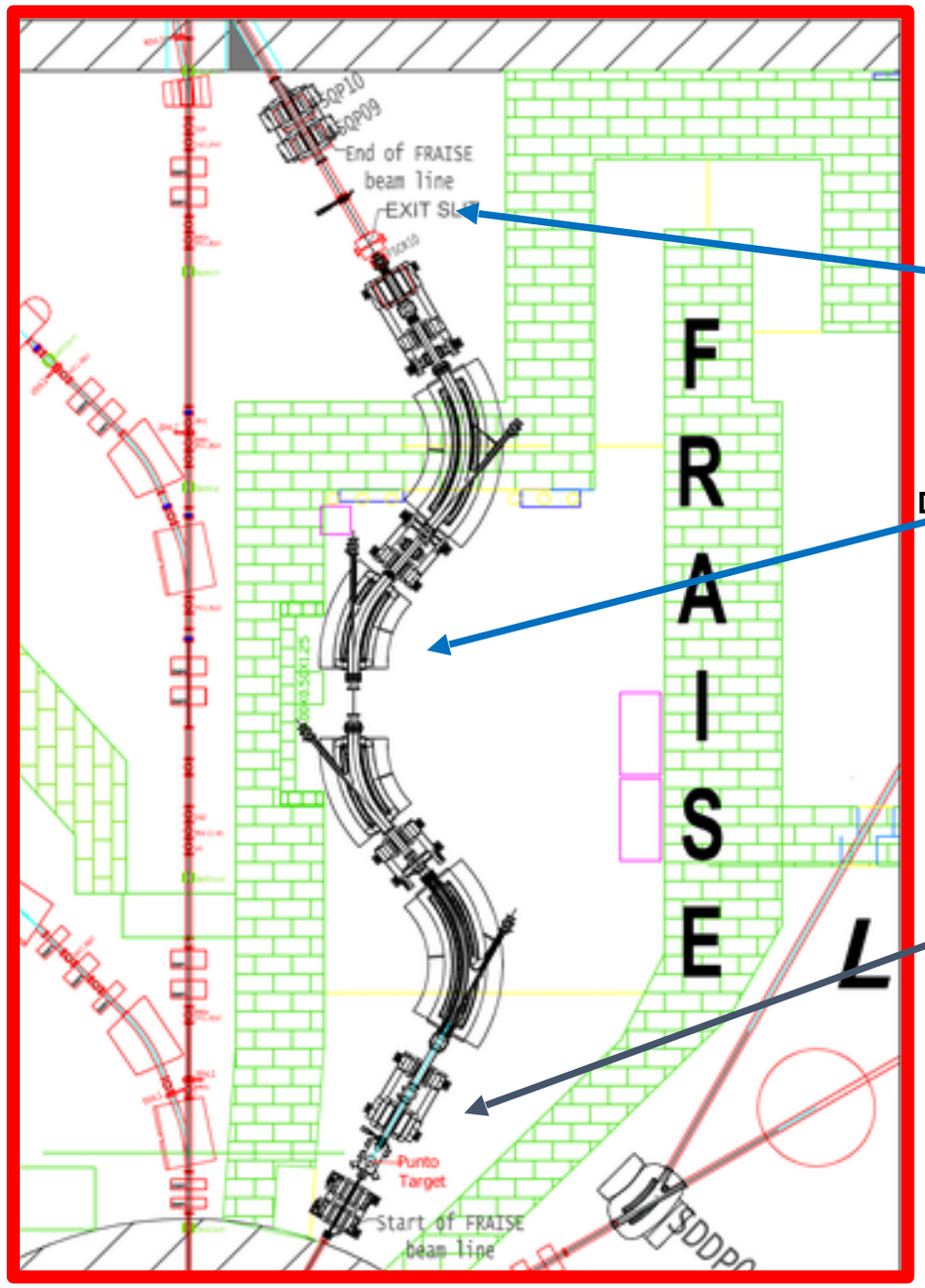


Main features:

- 4 dipoles and 6 quadrupoles, arranged in a symmetrical configuration
- maximum magnetic rigidity 3.2 *Tm*
- momentum acceptance ±1.2%
- solid angle acceptance ±2.5 *msr*,
- energy resolution 2500 for a beam spot size of 1 *mm*.

$$RP = \left|\frac{R_{16}}{2x_0 R_{11}}\right| = 2500 \quad \text{(beam spot } \pm 1 \text{ mm)}$$

- thanks to high energy dispersion value at the symmetry plane, it will allow to deliver stable beams with an energy spread of 0.1 %
- up to 2 kW as primary beam power

| Element | Name | Quantity | Features |
|---|---|---|---|
| Dipole | FSDP01,FSDP04 | 2 | R=2m $\alpha = 70°$, B=0.66-1.65 $T$ |
| Dipole | FSDP02,FSDP03 | 2 | R=2m $\alpha = 40°$, B=0.66-1.65 $T$ |
| Quadrupole | FSQP03,FSQP08 | 2 | $\phi$=104 mm Gmax=14.1 $T/m$ |
| Quadrupole | FSQP04-FSQP07 | 4 | $\phi$=132 mm Gmax=5.77 $T/m$ |
| Sexstupole | FSSP01,FSSP02 | 2 | $\phi$=130 mm Gmax=59.2 $T/m^2$ |

Table 1: FraISe magnetic transport elements features

# Some examples

*Courtesy P. Russotto*

## $^{12}C^{6+}$ @ 60 AMeV 2 kW on ≈2500 um $^{9}Be$

| | | | | | | | | | | | | | | | |
|---|---|---|---|---|---|---|---|---|---|---|---|---|---|---|---|
| | | | | $^{17}$Ne | $^{18}$Ne | $^{19}$Ne | $^{20}$Ne | $^{21}$Ne | $^{22}$Ne | $^{23}$Ne | $^{24}$Ne | $^{25}$Ne | $^{26}$Ne | $^{27}$Ne | $^{28}$Ne |
| | | | | | $^{17}$F | $^{18}$F | $^{19}$F | $^{20}$F | $^{21}$F | $^{22}$F | $^{23}$F | $^{24}$F | $^{25}$F | $^{26}$F | $^{27}$F |
| | | $^{13}$O | $^{14}$O | $^{15}$O | $^{16}$O | $^{17}$O | $^{18}$O | $^{19}$O | $^{20}$O | $^{21}$O | $^{22}$O | $^{23}$O | $^{24}$O | | |
| | | $^{12}$N | $^{13}$N | $^{14}$N | $^{15}$N | $^{16}$N | $^{17}$N | $^{18}$N | $^{19}$N | $^{20}$N | $^{21}$N | $^{22}$N | $^{23}$N | | |
| $^{9}$C 4.0E5 45 | $^{10}$C 1.2E7 43 | $^{11}$C 2.2E8 44 | $^{12}$C | $^{13}$C | $^{14}$C | $^{15}$C | $^{16}$C | $^{17}$C | $^{18}$C | $^{19}$C | $^{20}$C | | $^{22}$C | | |
| $^{8}$B 3.1E6 42 | | $^{10}$B | $^{11}$B | $^{12}$B | $^{13}$B | $^{14}$B | $^{15}$B | | $^{17}$B | | $^{19}$B | | | | |
| $^{7}$Be 1.5E7 43 | | $^{9}$Be | $^{10}$Be 1.6E7 50 | $^{11}$Be | $^{12}$Be | | $^{14}$Be | | | | | | | | |
| $^{6}$Li | $^{7}$Li | $^{8}$Li 4.2E6 50 | $^{9}$Li 8.9E5 51 | | $^{11}$Li | | | | | | | | | | |
| | $^{6}$He 2.1E6 51 | | $^{8}$He 1.8E4 51 | | | | | | | | | | | | |

**Expected yield (pps)**
**Energy after the exit slit (AMeV)**

# Some examples

*Courtesy P. Russotto*

## $^{12}C^{6+}$ @ 60 AMeV – $^{18}O^{8+}$ @ 70 AMeV 2 kW on ≈ 2500-1500

| | | | | | | | | | | |
|---|---|---|---|---|---|---|---|---|---|---|
| | | | | $^{17}$Ne | $^{18}$Ne | $^{19}$Ne | $^{20}$Ne | $^{21}$Ne | $^{22}$Ne | $^{23}$N |
| | | | | | $^{17}$F | $^{18}$F | $^{19}$F | $^{20}$F | $^{21}$F | 22 |
| | | $^{13}$O 7.2E4 54 | $^{14}$O 1.4E6 40 | $^{15}$O 2.8E7 54 | $^{16}$O | $^{17}$O | $^{18}$O | $^{19}$O 4.4E6 50 | $^{20}$O | 21 |
| | | $^{12}$N 1.2E6 49 | $^{13}$N 2.3E7 50 | $^{14}$N | $^{15}$N | $^{16}$N 6.9E8 53 | $^{17}$N 3.2E8 57 | $^{18}$N | $^{19}$N | 20 |
| $^{9}$C 4.0E5 45 | $^{10}$C 1.1E7 43 | $^{11}$C 2.2E8 44 | $^{12}$C | $^{13}$C | $^{14}$C 1.1E8 59 | $^{15}$C 4.0E7 59 | $^{16}$C 1.4E7 60 | $^{17}$C 1.2E5 58 | $^{18}$C 4.8E2 55 | 19 |
| $^{8}$B 3.1E6 42 | | $^{10}$B | $^{11}$B | $^{12}$B 2.6E7 57 | $^{13}$B 7.5E6 58 | $^{14}$B 1.4E6 60 | $^{15}$B 2.6E5 51 | | $^{17}$B | |
| $^{7}$Be 1.5E7 43 | | $^{9}$Be | $^{10}$Be 1.6E7 50 | $^{11}$Be 1.5E6 58 | $^{12}$Be 2.8E5 60 | | $^{14}$Be 3.0E3 63 | | | |
| $^{6}$Li | $^{7}$Li | $^{8}$Li 4.2E6 50 | $^{9}$Li 8.9E5 51 | | $^{11}$Li 3.3E3 60 | | | | | |
| | $^{6}$He 2.1E6 51 | | $^{8}$He 1.8E4 51 | | | | | | | |

**Notes:**

- **$^{13}$C will allow: $^{12}$B 1.2E8 pps**
- **$^{16}$O will allow: $^{15}$O 2.7E8 pps, $^{14}$O 1.3E7 pps, $^{13}$O 4.2E5 pps**
- **Primary beams at lower energy (≈30 AMeV) and thinner target will give about yield lower by ≈ 1 order of magnitude and final energies of 15-25 AMeV**

**Expected yield (pps)**
**Energy after the exit slit (AMeV)**

## Some examples

### $^{12}C^{6+}$ @ 60 AMeV - $^{18}O^{8+}$ @ 70 AMeV - $^{20}Ne^{10+}$ 2 kW @ 70 AMeV on 2500-1500-1250 um $^{9}Be$ target

| | | | | | | | | | | | | | | | |
|---|---|---|---|---|---|---|---|---|---|---|---|---|---|---|---|
| | | | | $^{17}$Ne 8.7E5 53 | $^{18}$Ne 3.1E7 51 | $^{19}$Ne 6.0E8 52 | $^{20}$Ne | $^{21}$Ne | $^{22}$Ne | $^{23}$Ne | $^{24}$Ne | $^{25}$Ne | $^{26}$Ne | $^{27}$Ne | $^{28}$Ne |
| | | | | | $^{17}$F 1.7E8 50 | $^{18}$F | $^{19}$F | $^{20}$F 9.5E6 55 | $^{21}$F | $^{22}$F | $^{23}$F | $^{24}$F | $^{25}$F | $^{26}$F | $^{27}$F |
| | | $^{13}$O 7.2E4 54 | $^{14}$O 1.4E6 40 | $^{15}$O 2.8E7 54 | $^{16}$O | $^{17}$O | $^{18}$O | $^{19}$O 2.3E6 39 | $^{20}$O | $^{21}$O | $^{22}$O | $^{23}$O | $^{24}$O | | |
| | | $^{12}$N 1.2E6 49 | $^{13}$N 2.3E7 50 | $^{14}$N | $^{15}$N | $^{16}$N 6.9E8 53 | $^{17}$N 3.2E8 57 | $^{18}$N 3.7E6 57 | $^{19}$N | $^{20}$N | $^{21}$N | $^{22}$N | $^{23}$N | | |
| $^{9}$C 4.0E5 45 | $^{10}$C 1.1E7 43 | $^{11}$C 2.2E8 44 | $^{12}$C | $^{13}$C | $^{14}$C 1.1E8 59 | $^{15}$C 4.0E7 59 | $^{16}$C 1.4E7 60 | $^{17}$C 1.2E5 58 | $^{18}$C 4.8E2 55 | $^{19}$C | $^{20}$C | | $^{22}$C | | |
| $^{8}$B 3.1E6 42 | | $^{10}$B | $^{11}$B | $^{12}$B 2.6E7 57 | $^{13}$B 7.5E6 58 | $^{14}$B 1.4E6 60 | $^{15}$B 2.6E5 51 | | $^{17}$B | | $^{19}$B | | | | |
| $^{7}$Be 1.5E7 43 | | $^{9}$Be | $^{10}$Be 1.6E7 50 | $^{11}$Be 1.5E6 58 | $^{12}$Be 2.8E5 60 | | $^{14}$Be 3.0E3 63 | | | | | | | | |
| $^{6}$Li | $^{7}$Li | $^{8}$Li 4.2E6 50 | $^{9}$Li 8.9E5 51 | | $^{11}$Li 3.3E3 60 | | | | | | | | | | |
| | $^{6}$He 2.1E6 51 | | $^{8}$He 1.8E4 51 | | | | | | | | | | | | |

**Expected yield (pps)**
**Energy after the exit slit (AMeV)**

*Courtesy P. Russotto*

# FRAISE: a new FRAgment In-flight SEparator
## Approved inside POTLNS PON

**For our physical case**

Isospin degree of freedom affect the enrichment of the dynamical components with respect of the statistical one in the IMF production

**FRAISE beams**

$^{68}$Ni from a primary of $^{70}$Zn around 25 AMeV
minimum intensity ≈ $10^6$
$^{56}$Ni from a primary of $^{58}$Ni around 25 AMeV
minimum intensity ≈ $10^6$

**Future Reactions with FRAISE beams ?**

CHIMERA
$^{68}$Ni + $^{124}$Sn N/Z = 1.46 Neutron rich
$^{56}$Ni + $^{112}$Sn N/Z = 1.15 Neutron poor

**Future Reactions with stable beams ?**

CHIMERA
$^{96}$Zr + $^{96}$Zr N/Z = 1.40 Neutron rich
$^{96}$Ru + $^{96}$Ru N/Z = 1.18 Neutron poor

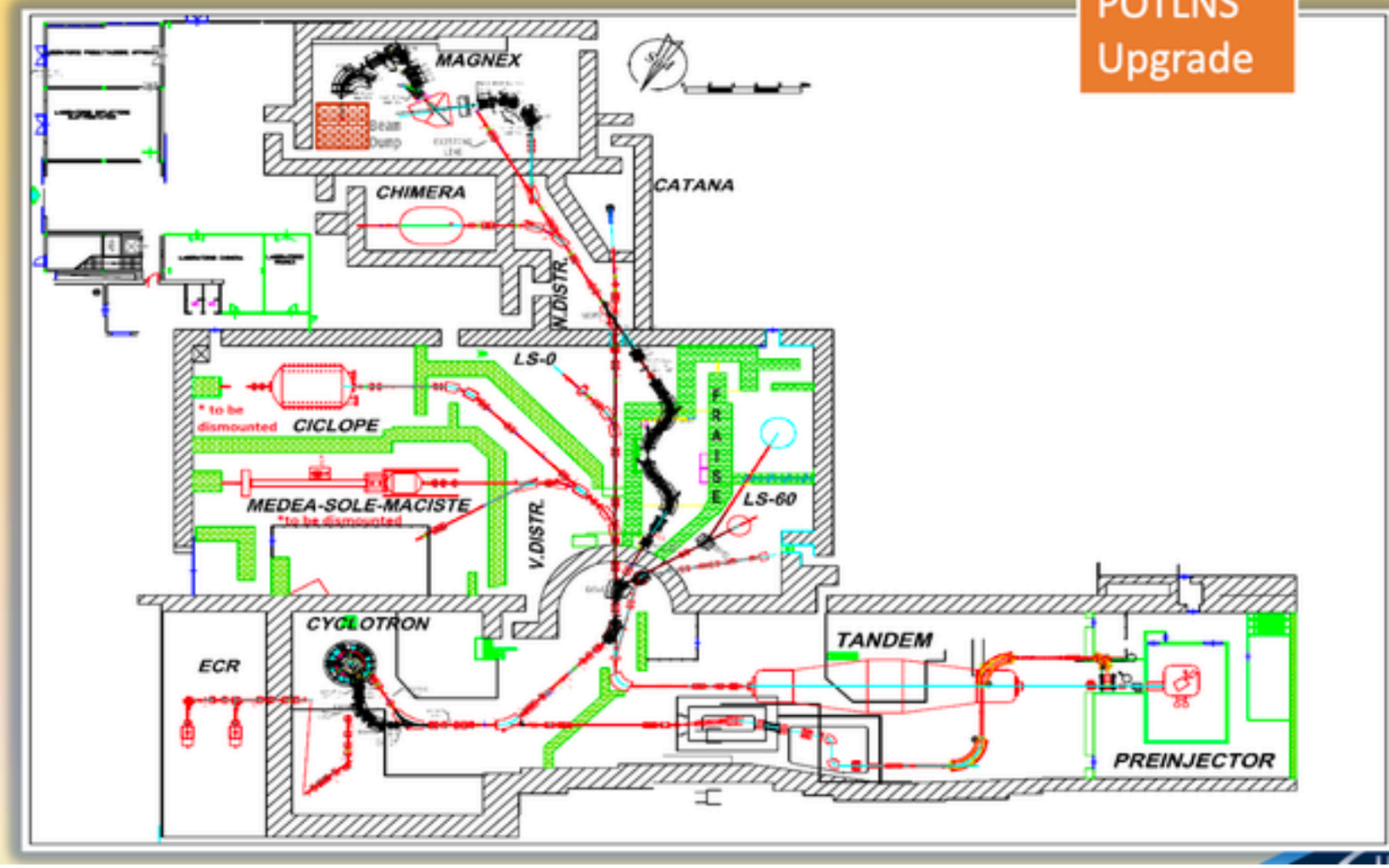

# Bibliography

## NArCoS


1) “Pulse shape discrimination of plastic scintillator EJ 299-33 in with radioactive source”
Pagano E. V., et al., NUCLEAR INSTRUMENTS & METHODS IN PHYSICS RESEARCH SECTION A, ACCELERATORS, SPECTROMETERS, DETECTORS AND ASSOCIATED EQUIPMENT, Vol. 889, (2018) 83-88.
DOI: 10.1016/j.nima.2018.02.010

2)”Measurement of pulse shape discrimination with EJ 299-33 plasticscintillator using heavy ion reaction”
Pagano E. V., et al.,NUCLEAR INSTRUMENTS & METHODS IN PHYSICS RESEARCH SECTION A,ACCELERATORS, SPECTROMETERS, DETECTORS AND ASSOCIATEDEQUIPMENT, A905(2018) 47-52
DOI: https://doi.org/10.1016/j.nima.2018.07.03

3)”The NArCoS project”
Pagano E. V., et al.,IL NUOVO CIMENTO 41 C (2018) 181
DOI 10.1393/ncc/i2018-18181-

4)”The NArCoS Project: the latest results”
Pagano E. V., et al.,Proc. 13th Int. Conf. on Nucleus-Nucleus CollisionsJPS Conf. Proc. 32, 010096 (2020)
DOI: https://doi.org/10.7566/JPSCP.32.010096

5)”NArCoS project for nuclear physics and applications”
Pagano E. V., et al.,IL NUOVO CIMENTO 43 C (2020) 12,
DOI 10.1393/ncc/i2020 20012-9

6)”The NArCoS Project: efficiency estimation and the cross talk problem studied through Monte Carlo simulations”
Pagano E. V., et al.,J. Phys.: Conf. Ser. 1643 (2020) 012037
doi:10.1088/1742-6596/1643/1/012037

7)”Recent results on the construction of a new correlator for neutrons and charged particles and for FARCOS”
Pagano E. V., et al.,IL NUOVO CIMENTO 45 C (2022) 64,
DOI 10.1393/ncc/i2022-22064-1

8)”NArCoS: The new hodoscope for neutrons and charged particles”
Pagano E. V. et al., Front. Phys. 10:1051058
DOI:10.3389/fphy.2022.1051058


## FRAISE


[1] Russotto P. et al., Jour. of Phys. Conf. Ser., 1014 (2018) 012016

[2] Russo A.D. et al., NIM B, 463 (2020) 418.

[3] Martorana N.S., Il Nuovo Cimento 44 C (2021) 1.


## FARCOS


1) “Status and perspective of FARCOS: A new correlator array for nuclear reaction studies.
Pagano E.V. et al, EPJ Web of Conferences (2016) 117:10008. doi:10.1051/epjconf/201611710008

2) Campaign of measurements to probe the good performance of the new array FARCOS for spectroscopy and correlations.2
Acosta L. et al., J Phys Conf Ser (2016) 730:012001. doi:10.1088/1742- 6596/730/1/012001

# Conclusions

The study of the Reaction mechanism is a very active area in HIC. The dependence of the dynamical emission of the reaction on the Isospin degree of freedom tell us a lot about the EoS of nuclear matter and the property of the in medium interaction with implications not only for nuclear structure e reaction mechanism but also for the study of cosmic objet like neutron stars.
In the next future new facility for RIBs will allow to perform new experiments using intense radioactive beams. Using this beams and in particular with the n-rich ones a large amount of neutron production is expected in the HIC. For this reason, new projects, for the construction of new neutron detectors performing high energy and angular resolution are ongoing

# Thanks for the attentions